

7-3-2018

Integrated Reservoir-Wellbore Nodal Analysis Workflow For Worst-Case Discharge Modeling

Florencia Anahi Vasquez Cordoba

Louisiana State University and Agricultural and Mechanical College

Follow this and additional works at: https://digitalcommons.lsu.edu/gradschool_theses



Part of the [Other Engineering Commons](#)

Recommended Citation

Vasquez Cordoba, Florencia Anahi, "Integrated Reservoir-Wellbore Nodal Analysis Workflow For Worst-Case Discharge Modeling" (2018). *LSU Master's Theses*. 4762.

https://digitalcommons.lsu.edu/gradschool_theses/4762

This Thesis is brought to you for free and open access by the Graduate School at LSU Digital Commons. It has been accepted for inclusion in LSU Master's Theses by an authorized graduate school editor of LSU Digital Commons. For more information, please contact gradetd@lsu.edu.

INTEGRATED RESERVOIR – WELLBORE NODAL ANALYSIS WORKFLOW FOR WORST-CASE DISCHARGE MODELING

A Thesis

Submitted to the Graduate Faculty of the
Louisiana State University and
Agricultural and Mechanical College
in partial fulfillment of the
requirements for the degree of
Master of Science

in

The Department of Petroleum Engineering

by

Florencia Anahi Vasquez Cordoba
B.S., Universidad Catolica de Salta, Argentina, 2014
August 2018

ACKNOWLEDGMENTS

I owe a debt of gratitude to my advisor Dr. Ipsita Gupta, who provided me guidance and invaluable support during my time here in the United States. I am also grateful to my committee members, Dr. Mileva Radonjic, Dr. Mauricio Almeida, and Dr. Paulo Waltrich for their suggestions and feedback in their review of this thesis, their time amidst busy schedules, but above all for their support – emotional and professional. Without them, it would have been very difficult for me to stay motivated. Dr. Seung Kam provided feedback on the proposal.

I would like to thank Petroleum Experts – engineering software development, for license donation.

I would like to take this occasion to thank Fulbright Commission for the opportunity to study abroad and enrich my knowledge in Petroleum Engineering, and in meeting different people from across the world in a foreign nation – it has helped me grow as a person.

Thanks also to fellow student and good friend Hope Asala for his help in general, and to my lab mates German, Makua and Sulav. My fellow graduate students – I have learnt so much from you. Denis – you are in my heart, and I will always remember your unconditional support and help.

Last but not the least – this work is dedicated to my parents.

TABLE OF CONTENTS

ACKNOWLEDGMENTS.....	ii
LIST OF TABLES.....	v
LIST OF FIGURES.....	vi
LIST OF SYMBOLS	ix
ABSTRACT	xii
CHAPTER 1. INTRODUCTION.....	1
CHAPTER 2. LITERATURE REVIEW	2
2.1 Definitions	2
2.2 Historic Events	2
2.3 Oil Spill Risk.....	11
2.4 Oil Spill Response Plan (OSRP).....	14
2.5 Gulf of Mexico (GoM) Geologic Sequences	15
2.6 Conventional Nodal Analysis	19
2.7 Flow Correlations for Different Flow Regimes.....	22
2.8 Two-Phase Flow Regimes	23
2.9 Flow correlations.....	24
CHAPTER 3. RESEARCH GOALS	26
CHAPTER 4. METHODOLOGY	27
4.1 Governing Equations	29
CHAPTER 5. RESULTS – DEVELOPED WORKFLOW USING PRODUCTION MODELING TOOLS	33
5.1 Basis of Workflow	33
CHAPTER 6. RESULTS - WORKFLOW VALIDATION WITH RESERVOIR SIMULATION	37
6.1 Base Case	37
6.2 Sensitivities.....	58
CHAPTER 7. CONCLUSIONS AND RECOMMENDATIONS	89
REFERENCES.....	91
APPENDIX A. ROCK COMPRESSIBILITY AND AQUIFER INFLUX.....	95
APPENDIX B. WORKFLOW ADOPTED IN INTEGRATED PRODUCTION MODELING SOFTWARE.....	98

VITA	103
------------	-----

LIST OF TABLES

Table 1. Top 5 U.S. offshore well blowouts since 1969, ordered by volume.	13
Table 2. Errors for BaseCase Model (OWWO Scenario) for Hagedorn and Brown Correlation.	40
Table 3. Scenarios represented.	59
Table 4. Comparative results between OWWO, OGWO and OWWG.	60
Table 5. Errors for water sands at top and bottom of open-hole sections in variation for base-case model.	72
Table 6. Cumulative Oil, Water and Gas Productions for Different Compressibility Scenarios.	83

LIST OF FIGURES

Figure 1. Deepwater Horizon rig.	4
Figure 2. Left, Deepwater Horizon BOP. Right, 3-D model of Deepwater Horizon BOP.....	5
Figure 3. Flow through the seal assembly.....	7
Figure 4. Flow up the production casing.....	8
Figure 5. Damaged riser at the Macondo well.....	10
Figure 6. Figure showing classification of risks	12
Figure 7. Stacked GoM geologic sequence against a fault.	17
Figure 8. Stacked GoM gas reservoirs against a possible salt-dome.....	18
Figure 9. Well deliverability: Combination of IPR and VFP.....	20
Figure 10. Gas-liquid flow regimes in vertical pipes	24
Figure 11. Figure showing typical wellbore configuration for 8.5" and 12" wellbores with stacked reservoir/non-reservoir rocks	28
Figure 12. Example of a wellbore open to four sands.	38
Figure 13. Cumulative Oil Production for GAP and Reveal Base Case Model (OWWO Scenario) – Hagedorn Brown	41
Figure 14. Cumulative Water Production for GAP and Reveal Base Case Model (OWWO Scenario) - Hagedorn Brown	42
Figure 15. Cumulative Gas Production for GAP and Reveal Base Case Model (OWWO Scenario) - Hagedorn Brown	43
Figure 16. Average Oil Production for GAP Base Case Model (OWWO Scenario) - Hagedorn Brown	45
Figure 17. Reservoir simulation model for base case (OWWO scenario).	46
Figure 18. Cumulative Oil Production for GAP and Reveal Base Case Model (OWWO Scenario) – Duns and Ros Correlation	48
Figure 19. Cumulative Water Production for GAP and Reveal Base Case Model (OWWO Scenario) – Duns and Ros Correlation	49

Figure 20. Cumulative Gas Production for GAP and Reveal Base Case Model (OWWO Scenario) – Duns and Ros Correlation	50
Figure 21. Cumulative Oil Production for GAP and Reveal Base Case Model (OWWO Scenario) – Beggs and Brill Correlation.....	51
Figure 22. Cumulative Water Production for GAP and Reveal Base Case Model (OWWO Scenario) – Beggs and Brill Correlation.....	52
Figure 23. Cumulative Gas Production for GAP and Reveal Base Case Model (OWWO Scenario) – Beggs and Brill Correlation.....	53
Figure 24. Cumulative Oil Production for GAP and Reveal Base Case Model (OWWO Scenario) – Mukherjee Brill Correlation	54
Figure 25. Cumulative Water Production for GAP and Reveal Base Case Model (OWWO Scenario) – Mukherjee Brill Correlation	55
Figure 26. Cumulative Gas Production for GAP and Reveal Base Case Model (OWWO Scenario) – Mukherjee Brill Correlation	56
Figure 27. Reservoir pressure for base case.	57
Figure 28. Oil, water, oil, water (OWOW) sands.	61
Figure 29. Water, oil, water, oil (WOWO) sands.	62
Figure 30. Oil, gas, water, oil (OGWO) sands.....	63
Figure 31. Oil, water, water, gas (OWWG) sands.	64
Figure 32. Water and gas bearing sand.	65
Figure 33. Nine oil layer sands.....	67
Figure 34. Reservoir pressure for nine layers case.....	68
Figure 35. Comparison of cumulative oil production for different stacking patterns of oil, water and gas reservoirs.....	69
Figure 36. Comparison of cumulative water production for different stacking patterns of oil, water and gas reservoirs.....	70
Figure 37. Comparison of cumulative gas production for different stacking patterns of oil, water and gas reservoirs.....	71
Figure 38. Oil, water, oil sands. Bottom water is disabled.....	73

Figure 39. Scenario with water sand at the base.	74
Figure 40. Oil, water, oil. Water sand at top disabled.	75
Figure 41. Scenario with water sand at the top.	76
Figure 42. Reservoir pressure for scenario with water sand at the top.....	77
Figure 43. Cumulative oil and water production when water bearing sand (OWWO).....	79
Figure 44. Cumulative gas production when water bearing sand (OWWO).	80
Figure 45. WCD cumulative oil volumes for different compressibility when only oil sands are considered.	82
Figure 46. Cumulative oil production, rock compressibility comparison.	84
Figure 47. Cumulative water production, rock compressibility comparison.	85
Figure 48. Cumulative gas production, rock compressibility comparison.	86
Figure 49. Cumulative oil production; comparison between deviated well and vertical well.	88
Figure 50. Example of a wellbore open to four sands.	100

LIST OF SYMBOLS

A = pipe cross-sectional area, L^2 .

A_c = cross-sectional area of the formation.

A' = laminar-flow coefficient, $\text{psia}/\text{STB}/\text{day}$.

a_{j-1} = water influx rate, barrels per dimensionless time unit for the j th interval.

B_g = gas formation volume factor, bbl/SCF .

B_g = gas formation volume factor at initial reservoir pressure, bbl/SCF .

B_o = oil formation volume factor, bbl/STB .

B_{oi} = oil formation volume factor at initial reservoir pressure, bbl/STB .

B_w = water formation volume factor, bbl/STB .

B_1 = constant of proportionality.

B' = turbulence coefficient, $\text{psia}/(\text{STB}/\text{day})^2$.

C' = flow coefficient, $\text{STB}/\text{day}/\text{psia}^{2n}$.

c_f = compressibility of the formation, psi^{-1} .

c_{fa} = compressibility of the aquifer formation, psi^{-1} .

c_t = total compressibility coefficient, psi^{-1} .

c_p = pore compressibility coefficient, psi^{-1} .

c_w = compressibility of the water, psi^{-1} .

d = pipe diameter, L .

e = intrinsic specific energy, L^2/t^2 .

F_E = Sukarno and Wisnogroho flow efficiency, dimensionless.

g = acceleration of gravity, L/t^2 .

g_c = gravitational conversion factor.

G_i = cumulative gas injection, SCF.

h = specific enthalpy, L^2/t^2 .

J = mechanical equivalent of heat.

k = permeability of the formation, md.

k_a = permeability of the aquifer, md.

L = pipe length.

m = ratio of initial reservoir free gas volume to initial reservoir oil volume.

N = initial volume of oil in reservoir, STB.

N_p = cumulative produced oil, STB.

$\Delta P(t_{Dj})$ = total pressure drop, psi.

$P(t_D)$ = dimensionless pressure.

$P'(t_D)$ = dimensionless pressure derivative.

r_e = radius of the reservoir, ft.

R_p = cumulative produced gas-oil ratio, SCF/STB.

R_s = solution gas-oil ratio at current reservoir pressure, SCF/STB.

R_{si} = solution gas-oil ratio at initial reservoir pressure, SCF/STB.

p = pressure, m/Lt^2 .

P_{wf} = flowing wellbore pressure, psi.

P_R = average reservoir pressure, psi.

P_b = bubble point pressure, psi.

q_o = oil production rate, bbl/day.

$q_{o,max}$ = maximum oil production rate, bbl/day.

Q_f = heat flux, m/t^3 .

Q = flow rate of the formation, bbl/day.

s = skin factor, dimensionless.

S_{wc} = connate water saturation.

t = time.

t_{Dj} = dimensionless time at the end of the j th interval.

U = specific internal energy, L^2/t^2 .

V = velocity, L/t .

V_p = pore volume.

W_e = water influx, bbl.

W_i = cumulative water injection, STB.

W_p = cumulative produced water, STB.

x = length of the formation.

μ = viscosity of the fluid, cp.

μ_w = viscosity of water in the aquifer, cp.

ϕ = porosity.

θ = inclination angle from horizontal.

ρ = density, m/L^3 .

ϕ_a = porosity of the aquifer.

τ = shear stress, m/Lt^2 .

ABSTRACT

According to the Bureau of Ocean Energy Management (BOEM), worst-case discharge (WCD) is the single highest possible daily flow rate of liquid hydrocarbon during an uncontrolled wellbore flow event [49]. The main objective of this research is to develop a workflow to calculate worst case discharge (WCD) volumes for a drilling scenario using an integrated reservoir-nodal analyses approach. Using robust integrated production modeling (IPM) tools, a nodal analysis workflow is developed to compute WCD volumes and rates that operators can use easily if they have IPM, or adapt to using a different software (including excel) in absence of IPM. A secondary objective of this research is to test different geologic sequencing patterns (sand/shale and reservoir-non reservoir sequences as in Gulf of Mexico) as well as reservoir parameters like rock compressibility and aquifer presence to assess impact on WCD rates and cumulative volumes. The integrated reservoir-nodal analysis workflow is validated using reservoir simulation of the same scenarios.

CHAPTER 1. INTRODUCTION

In the face of the BP-Macondo blowout in the Gulf of Mexico in 2010, the US government revamped rules and regulations related to these kind of situations in order to be proactive in taking preventive measures for the future. The Bureau of Safety and Environmental Enforcement's (BSEE) Oil Spill Preparedness Division (OSPD) is responsible for the development and management of the regulations in the case of an accidental oil discharge. If any spill occurs, it is mandatory for operators to submit an Oil Spill Response Plan (OSRP) explaining the procedures in place so as to respond to the unexpected oil spill, especially in regards to the worst-case scenario or maximum potential discharge [8].

This research is focused on developing a reservoir-coupled nodal analysis workflow that can be used to compute worst case discharge (WCD) volumes and rates for offshore wells as in Gulf of Mexico (GoM). This workflow is developed using available production modeling tools for a loss of control situation during drilling. Using various sensitivity studies, the correlation between certain parameters and WCD volumes and rates are also demonstrated through this research. The uniqueness of the workflow developed through this research is that it goes beyond steady-state nodal analysis and wellbore models for computing potential blowout discharge rates, but is simpler to build and use than full-scale reservoir simulation models. Following the publication of the thesis, this workflow can be used by both operators and regulatory sectors to compute WCD rates, and or adapted to simpler spreadsheet-like tools such as MS Excel.

CHAPTER 2. LITERATURE REVIEW

2.1 Definitions

According to the Bureau of Ocean and Energy Management (BOEM), worst-case discharge (WCD) can be defined as the single highest daily flow rate of liquid hydrocarbon during an uncontrolled wellbore flow event [49]. A blowout is an uncontrolled flow of fluids from the well [47]. However, in this study, blowout refers to a loss of well control in which there is a release of oil to the environment.

An oil spill is defined as an event in which oil is discharged by accident or with intent during a short time of period [18]. In general, blowout accidents discharge small amount of oil into the environment. Operators take those accidents under control or the well is sealed by bridging over, which is a natural process of sealing [8]. Large-scale oil spills are unusual events, and there have been only two major offshore spills in the U.S. waters: the Santa Barbara Channel Alpha Well 21 Platform “A” blowout in 1969 and the Gulf of Mexico Deepwater Horizon MC252 blowout in 2010 [49].

2.2 Historic Events

In January 1969, the United States Geological Survey (USGS) had approved five development wells in the Santa Barbara Channel, California [3]. 28 days after the year started, an uncontrolled flow of oil occurred during drilling operations on ocean Union Oil’s Platform A-21 situated in Santa Barbara coast. The well was drilled 3,479 feet from the platform crossing three faults [3]; subsequently the oil flowed through fissures in oil-bearing sands to the sea floor [22]. The main reason for that catastrophic accident was the pressure increase caused by the extraction of a pipe while drilling. An emergency attempt sealed the well while the pressure built up and started to fragment the upper part

of the casing, but doing this resulted in an accelerated pressure increase in the wellbore which resulted in loss of control [11].

The next eleven days consisted of desperate attempts to contain the spill including capping the well [11]. The amount of thick, crude oil that spilled into the Santa Barbara Channel for ten days was estimated to be 3.25 million U.S. gallons (77380 barrels) [29]. This catastrophic event made the regulatory agencies to rethink their approach and improve the regulations in order to be more preventative.

On 20 April 2010, a drilling rig explosion caused a catastrophic oil spill in the Gulf of Mexico waters that killed 11 (eleven) people and injured 17 others [35]. The blowout occurred in the Macondo well – which was situated in the Mississippi Canyon Block 252 (MC252). The fire on the rig was fed by hydrocarbons from the well, and it lasted for 36 hours until the rig became submerged [6]. The blowout of the Macondo oil well lasted 87 days –from 20 April to 15 July 2010-, and the spill discharged an estimated 4.9 million barrels of oil into the Gulf of Mexico [37]. It was the largest oil spill in the United States history. In addition to loss of life, the tragedy caused substantial economic and environmental damage to the U.S. Gulf Coast [28].

The Deepwater Horizon (Figure 1) was a semi-submersible MODU. A MODU is a mobile offshore drilling unit, which can be moved from a site to another with self-power. It was owned by Transocean, but BP leased it for a period of three years, which later was extended [4].

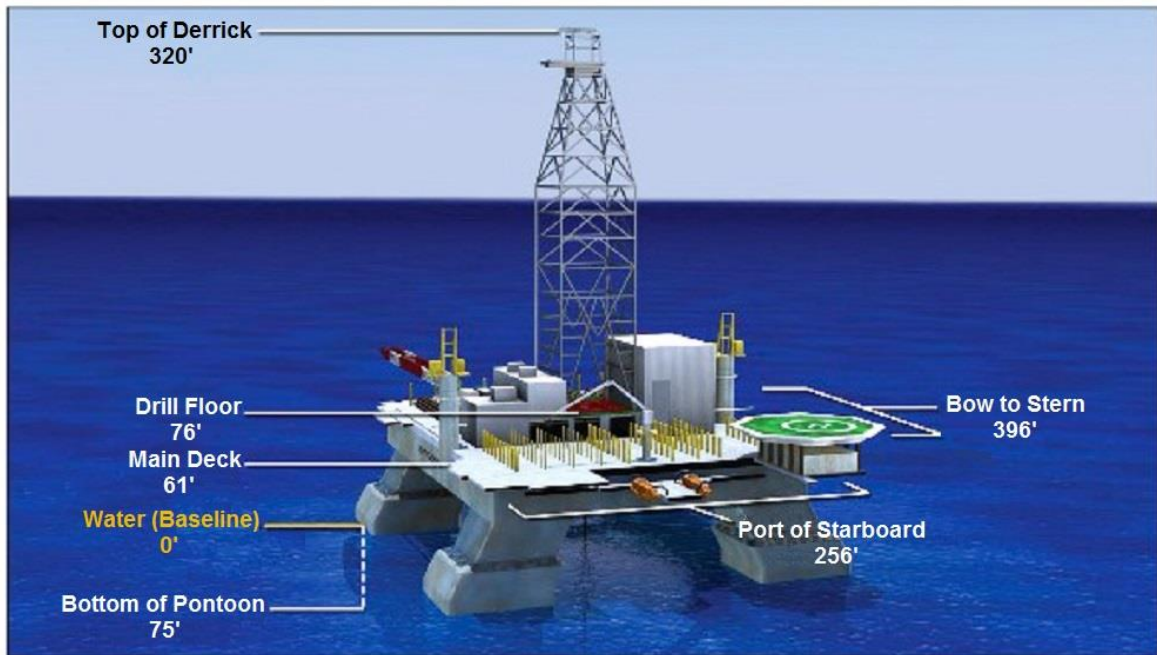
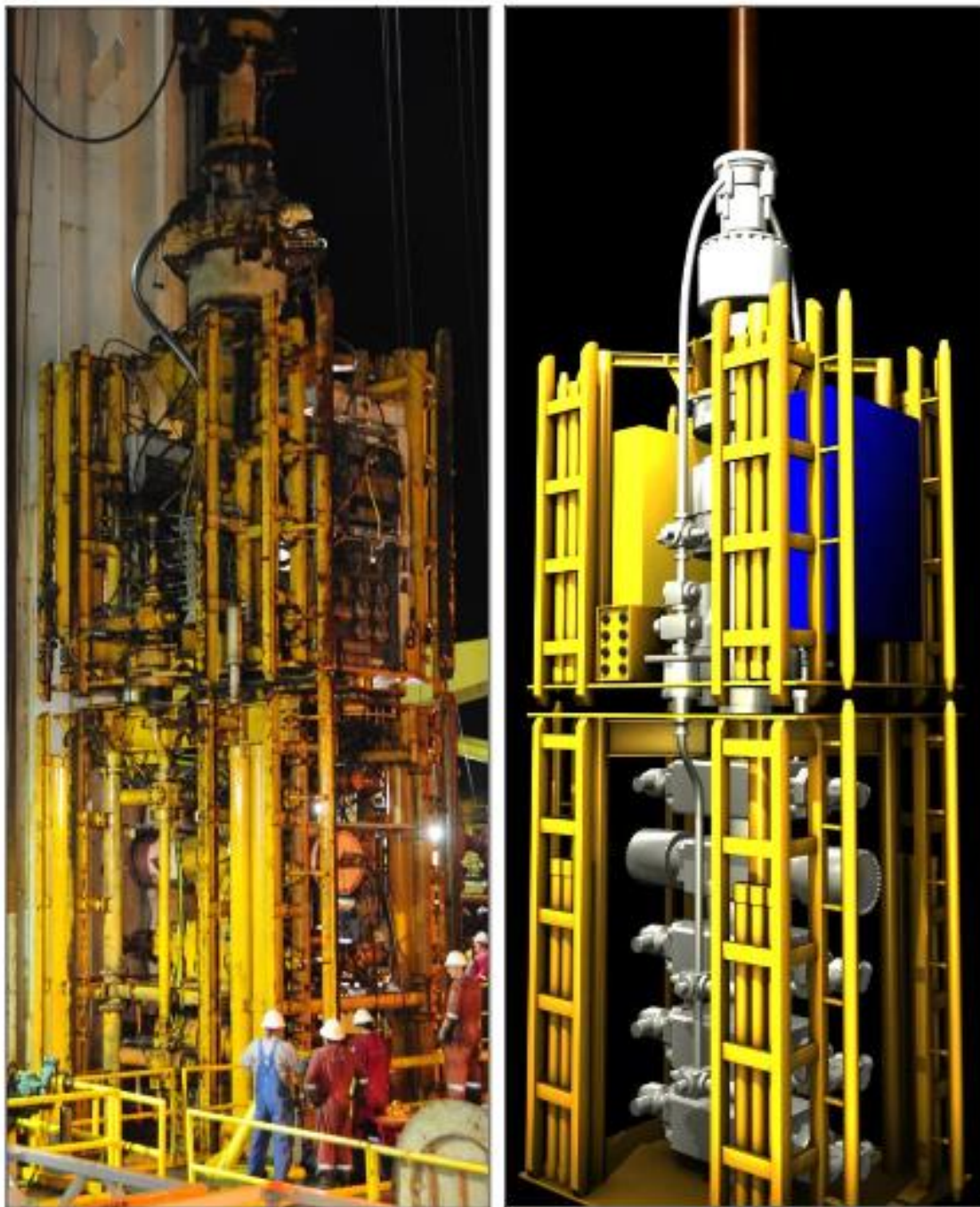


Figure 1. Deepwater Horizon rig [4].

The main reason/cause of Macondo blowout was that the cement did not isolate the hydrocarbons from the formation. The negative pressure test showed a cement failure, the results were misinterpreted. The rig crew recognized hydrocarbons coming to the surface just one hour before the blowout, but it was too late for activating the blowout preventer (BOP) [4].



U.S. Coast Guard photo/
Petty Officer 1st Class Thomas M. Blue

TrialGraphix

Figure 2. Left, Deepwater Horizon BOP. Right, 3-D model of Deepwater Horizon BOP. [4].

In context of this research, as well as for mitigation efforts, the critical question was: which possible flow paths did the hydrocarbons follow? The annular cement did not

seal off the pay zones, and because of that the hydrocarbons flowed into the wellbore. Once in the wellbore, for hydrocarbons to reach the surface there were two possible paths [4]:

- 1) Flow through the seal assembly (Figure 3): The seal assembly belongs to the wellhead, and its main function is to seal the interface between the casing hanger for the production casing and the inside of the wellhead. Between the casing hanger and the annulus there are small flow passages that allow the crew to circulate drilling fluids through the annulus. Those passages are sealed off by a lockdown sleeve once drilling fluids are not needed any longer. For hydrocarbons to flow throughout the seal assembly and reach the surface, a leak through the flow passages must have occurred or the lockdown sleeve had not been set at the time of the blowout.
- 2) Flow up the production casing (Figure 4): For hydrocarbons to travel through the production casing, either the cement in the shoe track failed, or an opening in the casing –like a hole or a leak– allowed the hydrocarbons to flow. According to the Chief Counsel’s report, the hydrocarbons reached the surface due to the failure of the shoe track cement. However, the annulus could have also served as a pathway for the fluids to the surface.

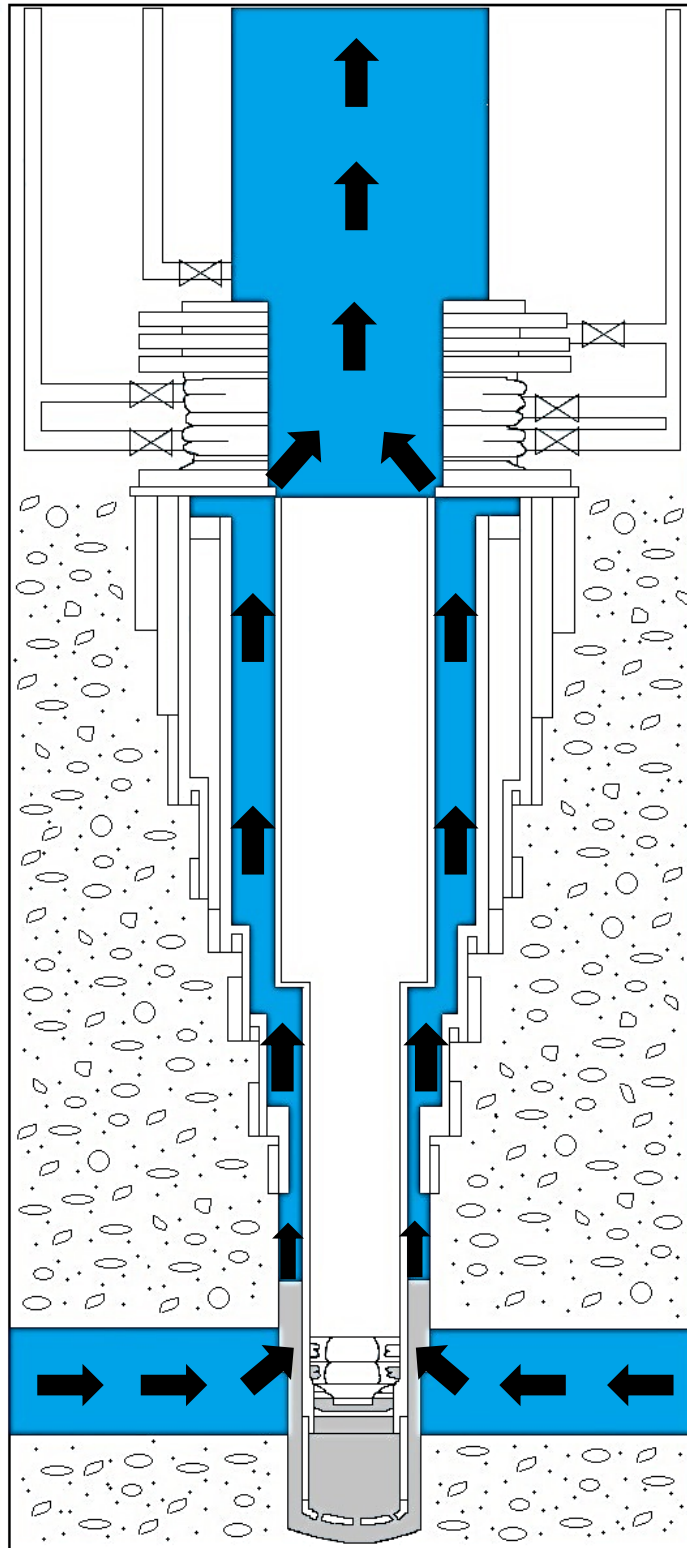


Figure 3. Flow through the seal assembly. [4]

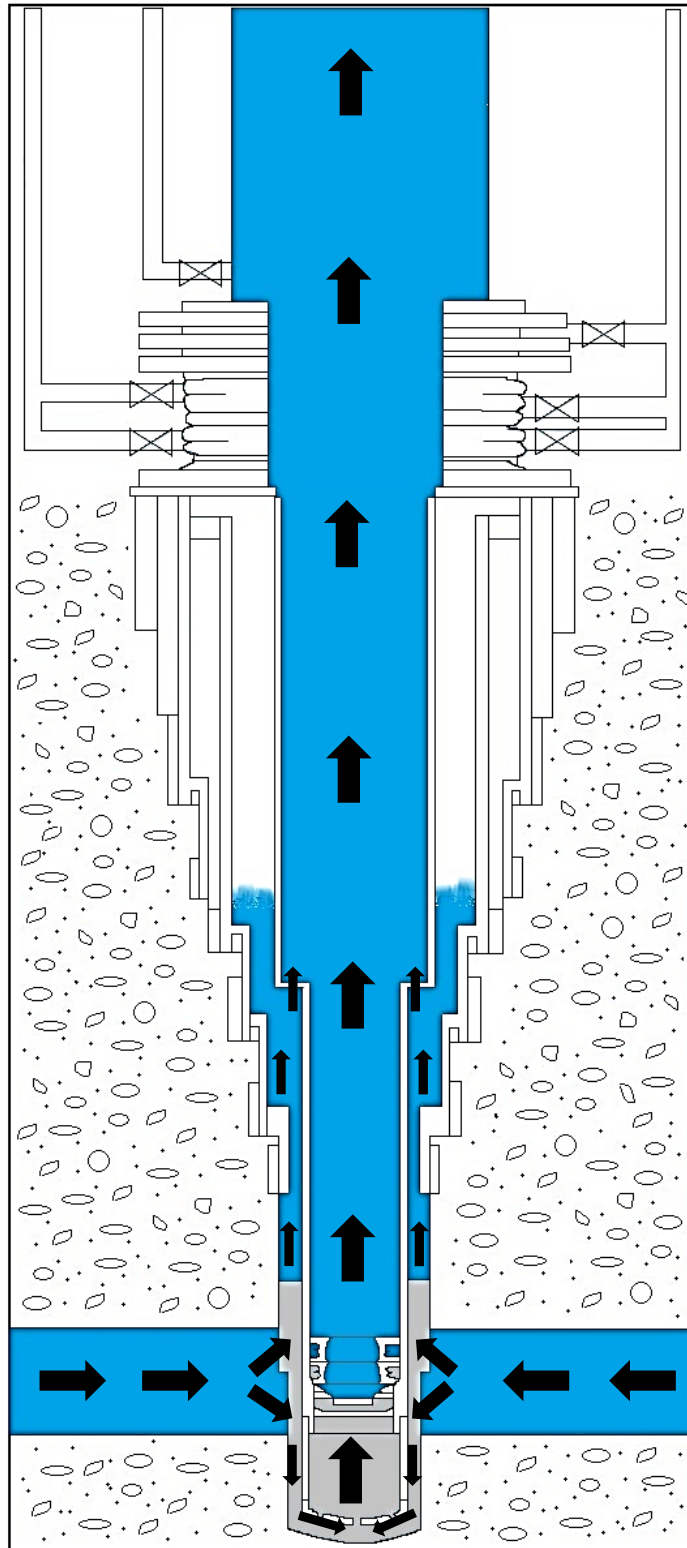


Figure 4. Flow up the production casing. [4]

One relevant information in Macondo is the negative pressure test that was performed. This test showed for a three-hour period the lack of integrity in the well and that the cement had failed to isolate the pay zone. However, the results were misinterpreted. Finally, a decision was made to continue to temporary abandonment so that another rig (less expensive) could move to Macondo complete the well construction process at a later time [4]. For a negative pressure test to be successful, for a period of time, there should not be any increase in the pressure inside the well and there should not exist flow from the well. During the three negative pressure tests conducted at Macondo, the pressure increased from 0 to 1,400 psi [4].

Once the hydrocarbons flowed into the wellbore, they moved up hole. As the hydrocarbons were released from the kink into the riser, the remotely operated vehicles (ROVs) intervened with the blowout preventer, but that failed to seal the well. Even worse, the flow was diverted to the mud gas separator, which was not designed to handle that situation, so it increased the risk of explosion of the rig [4].

Finally, the problem of attempting to contain the blowout and associated spill was solved by blocking the damaged zone of the drill pipe and capping it to channel the flow [36].

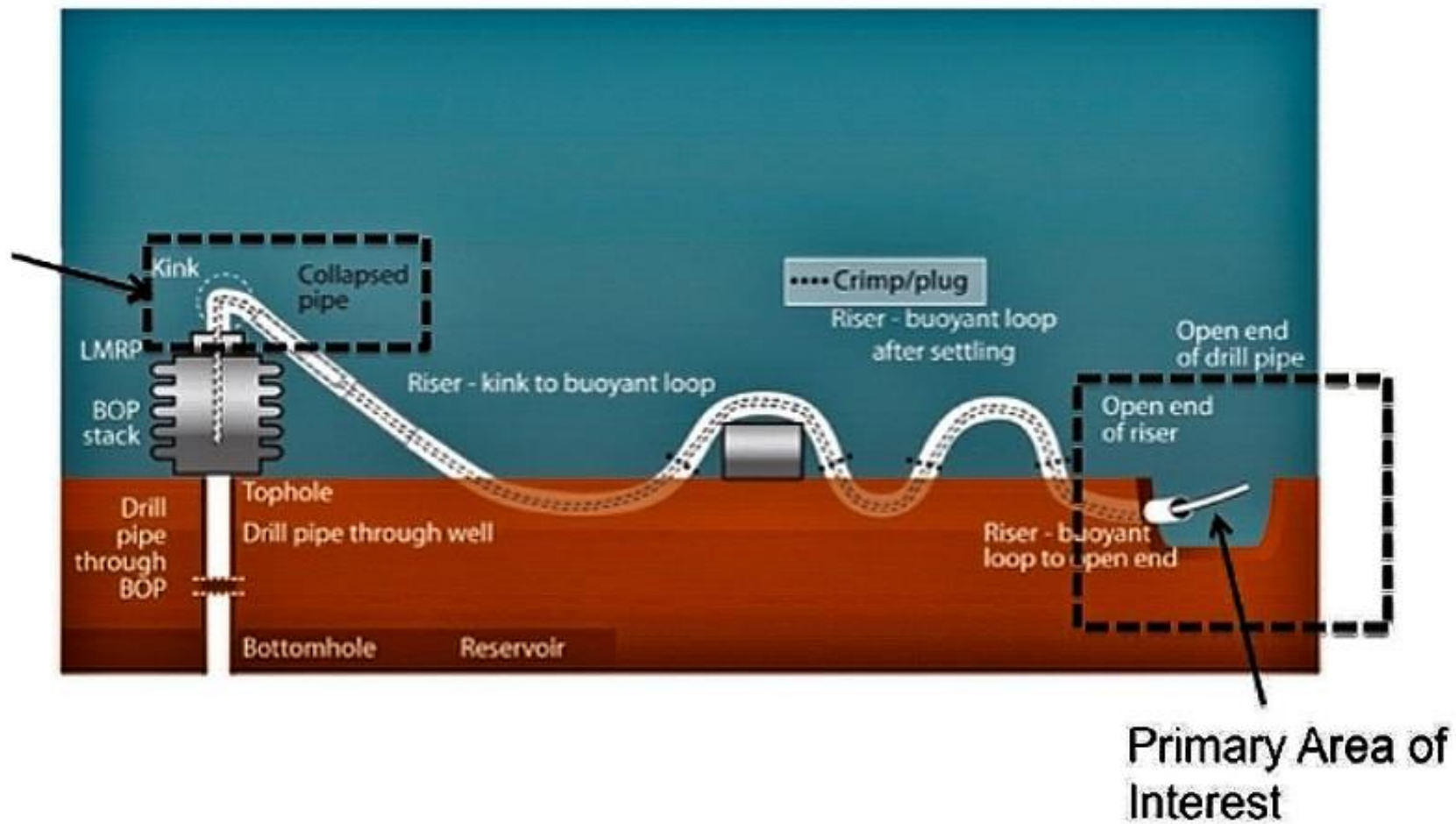


Figure 5. Damaged riser at the Macondo well. [36]

2.3 Oil Spill Risk

Definition of risks can vary, and risk can be quantified differently depending on the perspective. One definition of risk is a situation or event in which something of human value has been put at stake and where the outcome is uncertain [30], while Sandman defines risk as $\text{Risk} = \text{Hazard} * \text{Outrage}$, assuming that risk is related to a combination of hazards –like mortality– and outrage factors –like voluntariness– [12].

In effect, risk is a broad concept, and it can be interpreted differently. However, from a fundamental perspective, effectively addressing and handling risk involves understanding the relationship between the possibility and uncertainty of an event occurring. Usually, risk can be illustrated in a risk matrix as shown in Figure 6.

In order to relate the amount of an oil spill to its potential impact, it is important to classify a spill by its spill volume. U.S. crude oil production in the Federal Gulf of Mexico (GOM) increased from 44,000 barrels per day b/d in 2009 to 1.6 million b/d in 2016, and it is expected to continue increasing during 2018, based on information provided by the U.S. Energy Information Administration. BOEM refers to a “large” spill as one of 1,000 bbl or more, and as “small” spill to one that discharges less than 1,000 bbl [31]. Although each spill is unique, the impact from an oil spill is influenced by factors such as response effort, specifications of the well, oceanographic conditions, and atmospheric conditions [9]. Predicting the oil spilled volume will thus be a necessary plan and an effective response to minimize the potential negative consequences can be developed.

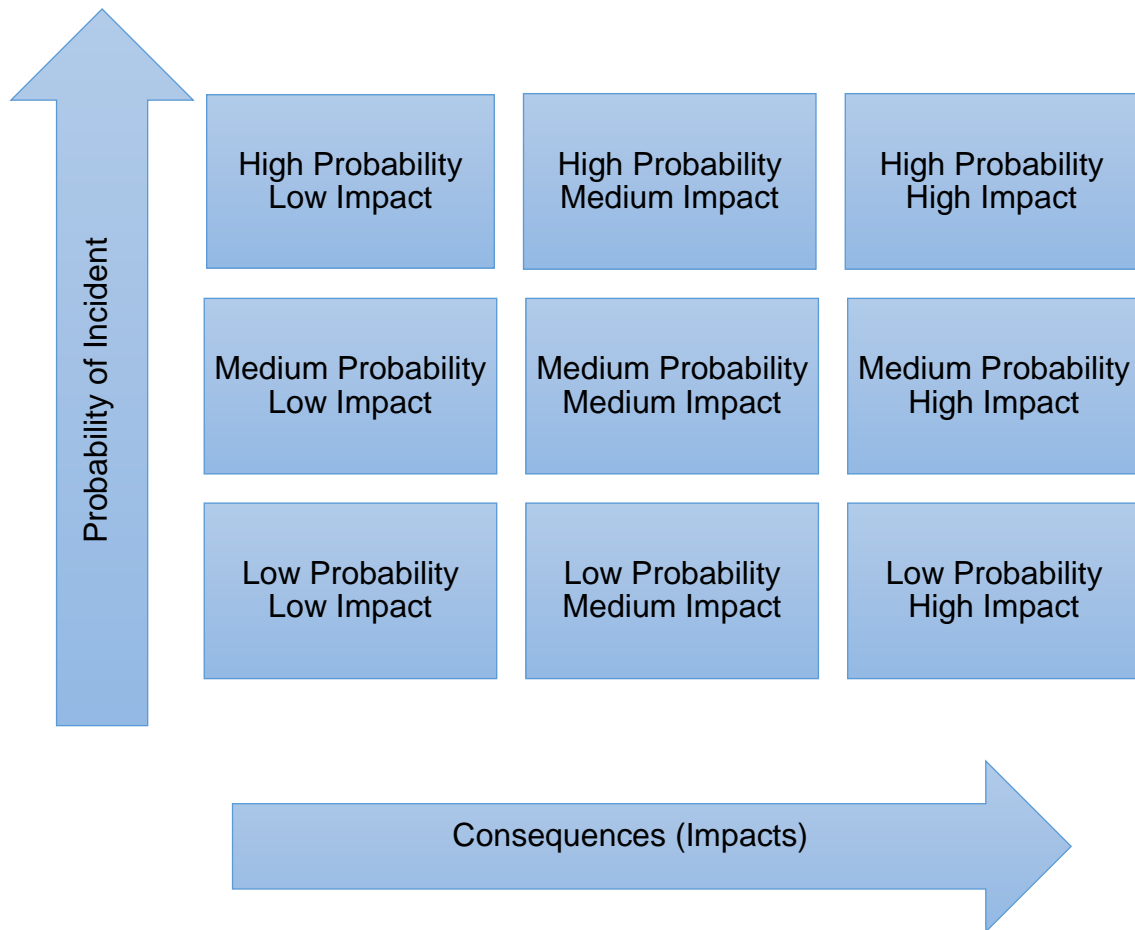


Figure 6. Figure showing classification of risks. [20]

Because of the increase in offshore resources, it is very important to analyze the developing risks of well kicks and blowouts. The basic operating risks are: having mud weight less than the formation pore pressure; a failure to keep the hole full while tripping; cleaning with a swab while tripping; lost circulation; and the mud being cut by gas, water or oil [25].

Recognition of potential risk is the best way to manage accidental oil spills because it is preventative in nature. If a kick is at risk of occurring, some warning signals generally show up in advance. Examples of red flags would be drilling rate suddenly increases, fluid

volume at the surface increases, pump pressure decreases; drill pipe weight decreases; observation of gas, oil, or water cut mud [25].

One important question is how much is the time needed to kill the well. The time that it takes to kill an uncontrolled well with a relief well or capping the well is the most influential factor in this inquiry. Table 1 shows the 5 (five) major oil spills in USA waters [8] and their durations.

Considering shallow water to those with depths less than 500 ft and deepwater with depths of 500 ft and deeper, and taking into account Table 1 and historical data, drilling a relief well for shallow water should take approximately 60 (sixty) days and in deep waters the relief well time estimate should be 90 days for offshore GoM.

Table 1. Top 5 U.S. offshore well blowouts since 1969, ordered by volume. [8]

Well	Date	Location	Barrels spilled	Duration (days)
Deepwater Horizon MC252	4/20/2010	GOM	4,200,000	84
Alpha Well 21 Platform A	1/28/1969	Pacific	80,000-100,000	11
Main Pass Block 41 (MP-41C)	2/10/1970	GOM	65,000	21 ¹
ST-26B	12/1/1970	GOM	53,000	137 ²
Greenhill Timbalier Bay 251	9/29/1992	GOM	11,500	17 ³

¹ EPA United States Environmental Protection Agency.

² 11 out of 22 producing wells were involved according to EPA United States Environmental Protection Agency.

³ IncidentNews website.

2.4 Oil Spill Response Plan (OSRP)

There are four regions in United States in which an offshore blowout could occur: Pacific, Alaska, Gulf of Mexico and Atlantic. Each region is responsible for their decisions and WCD verification. This paper is focused on Gulf of Mexico scenarios.

Federal Water Pollution Control Act and the Oil Pollution Act of 1990 requires the operators to submit an Oil Spill Response Plan (OSRP) including WCD calculations before drilling any well in GoM and an estimate of the maximum possible discharge (WCD) should a blowout occur.

WCD calculated volumes have to be submitted by operators, and they have to provide information in pursuance to NTL 2015-N01, which requires information for exploration plans, development operations coordination documents for WCD and blowout scenarios [50].

The required OSRP is based on the Code of Federal Regulations (CFR), for instance:

- 30 CFR 550.219: Information about potential oil spills in Exploration Plan (EP);
- 30 CFR 550.250: Information about potential oil spills in Contents of Development and Production Plans (DPP) and Development Operations Coordination Documents (DOCD);
- 30 CFR 254.26: Information that must be included in WCD scenario and the ability to contain it.
- 30 CFR 254.47: Methods for WCD calculations.
- 30 CFR 550.213: Indicate the information that must be included in the EP.

- 30 CFR 550.243: Indicate the information that must be provided in the DPP and DOCD.

The last two CFR, 550.213 and 550.243, should describe a potential blowout event, and explain what to expect. Expected flow rate, total volume discharged, and length of a potential blowout have to be included [50].

OSRP requires explaining the probabilities of intervention from the surface, and also the possibilities of drilling a relief well and the time that it would take to complete it. It is necessary, also, to describe the assumptions used in calculations of PVT data, reservoir characteristics and fluid characteristics. If analog reservoir data is used, the assumptions should be described and the chosen analog reservoirs should be justified.

Per requirements of the OSRP, a WCD estimate is mandatory, and recent reports have predictions of up to 476,000 barrels per day (bbl/d) [8]. Some of the most common problems in calculations and assumptions in OSRP, according to BOEM, are inconsistent data, insufficient data, analogs are listed but not linked to reservoir parameters, and the borehole data need to be submitted to BSEE.

2.5 Gulf of Mexico (GoM) Geologic Sequences

Gulf of Mexico is a basin between the North American plate and the Yucatan block. According to the morphology of GoM, it initiated during Middle Jurassic, and the depositional history is primarily dominated by middle-late Jurassic, early Cretaceous, late Cretaceous and Cenozoic sequences [24].

In the Gulf of Mexico (GoM), the primarily sedimentary rocks are siliciclastics with some carbonates occurring in certain areas. The siliciclastics are typical sand-shale sequences juxtaposed on top of each other (stacked sequences). There is significant

occurrence of salt in this sedimentary basin [54]. Figure 7 (from Brown, 2010) shows a seismic image of a stacked geologic sequence against an interpreted fault (black dashed line). One of the formations shows polarity reversal marked by blue over red (highlight in yellow). The same formation continues as red over blue due to phase change from water (aquifer). The remaining formations in that sequence are water bearing sands/shales.

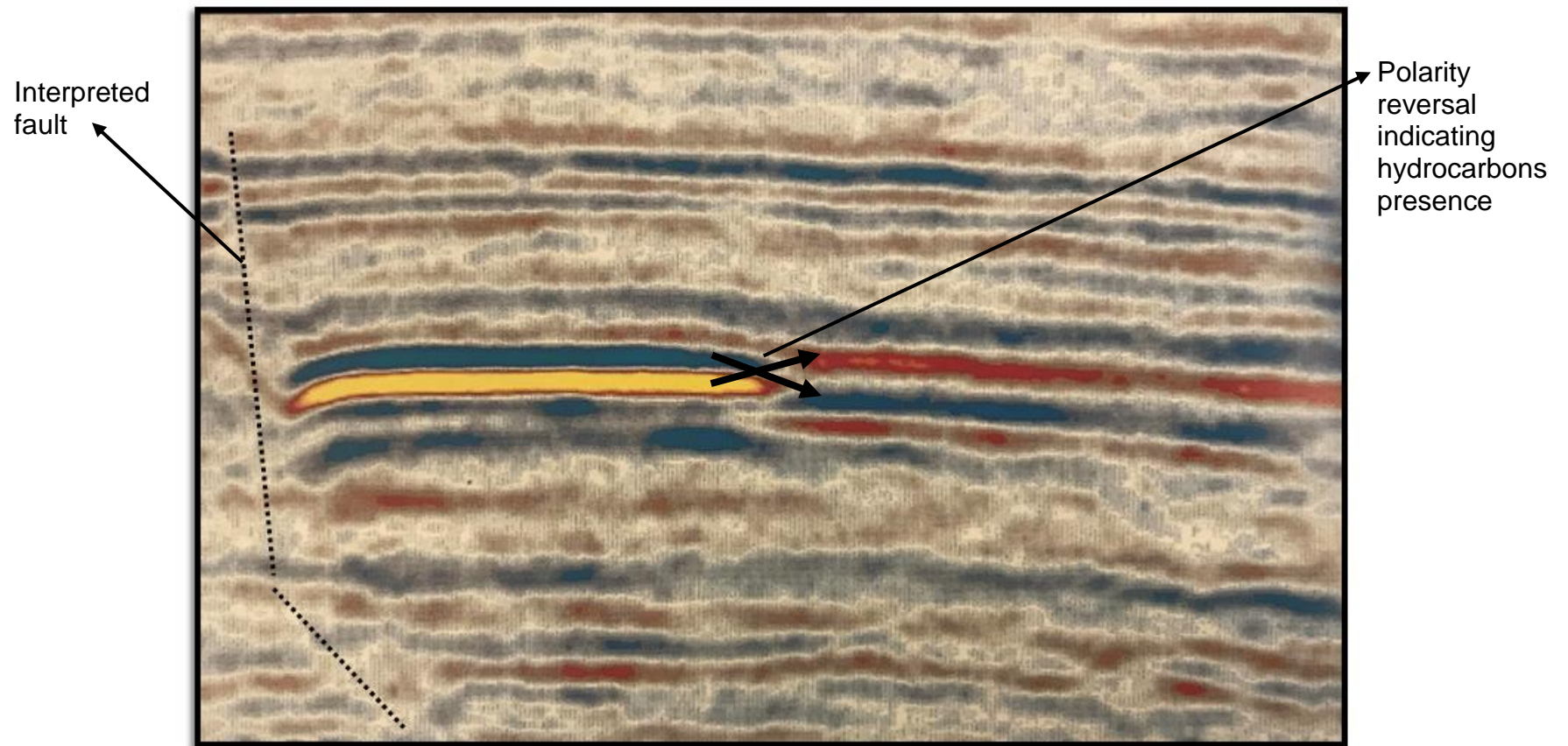


Figure 7. Stacked GoM geologic sequence against a fault [7].

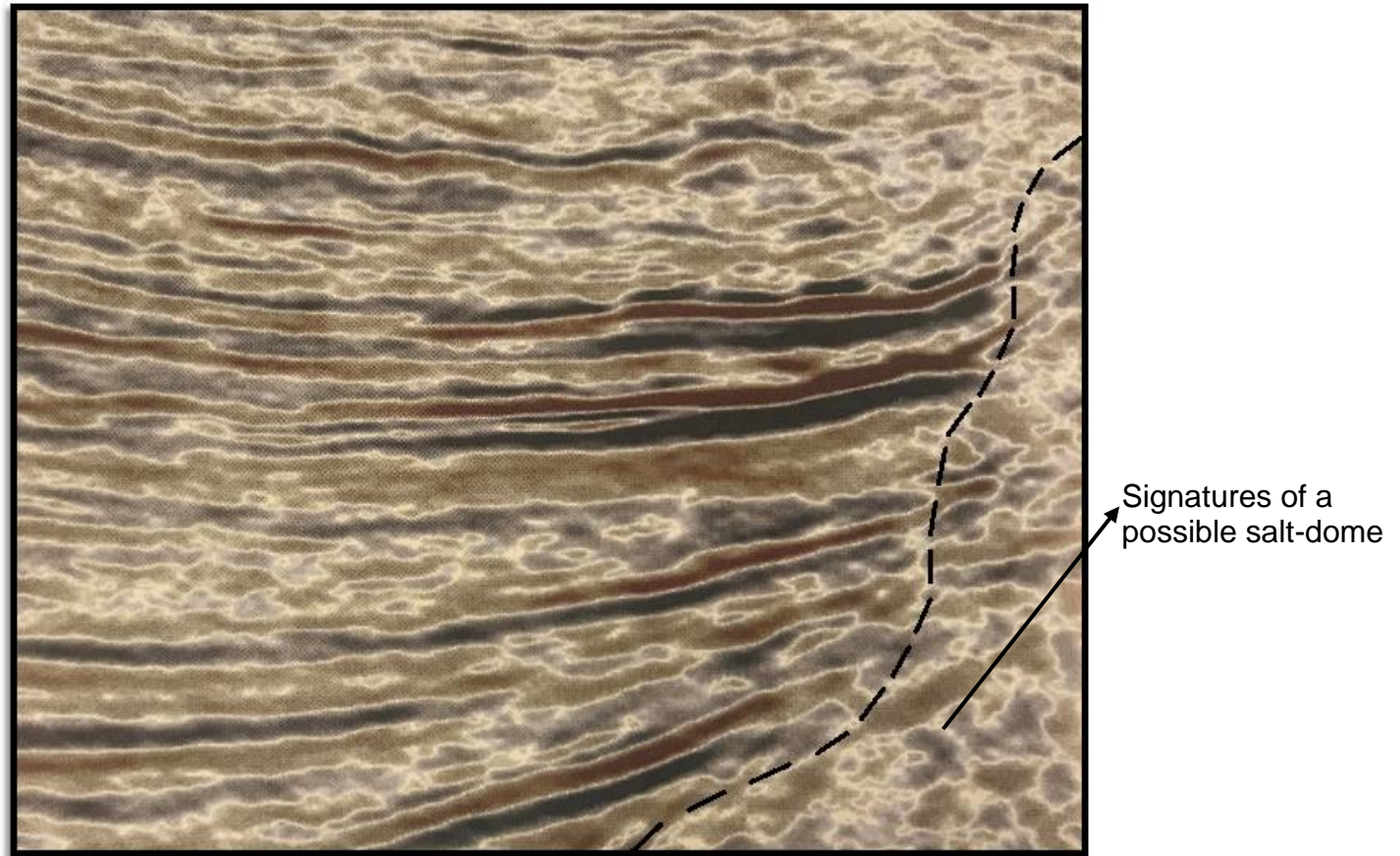


Figure 8. Stacked GoM gas reservoirs against a possible salt-dome [7].

Gulf of Mexico reservoirs pressures may range from surface conditions to tens of thousands of psi (especially deepwater reservoirs) [33], and formation temperatures can be often up to 250-300 °F [21].

2.6 Conventional Nodal Analysis

Nodal analysis is a well-established production modeling procedure whereby the entire wellbore flow system is discretized into multiple elements (or nodes) of which fluid properties are evaluated locally. Fluid properties change with temperature and pressure, and thus the necessity to estimate them at different temperatures and pressures along the wellbore. The fundamental outcome of a nodal analysis is an “operating point” which is a pressure and temperature at which flow occurs from the well. The nodal analysis procedure in Petroleum Engineering is based on the principle of pressure continuity, which states that there is only one pressure value at a given node [26]. The entire wellbore system is broken down into upstream and downstream components. The upstream component gives the reservoir performance, also known as an inflow performance relationship (IPR). The IPR is mostly estimated through Darcy’s Law or a modified version of it, or through numerical methods. The downstream component gives the well deliverability, also called the tubing performance curve/rate (TPR) or the vertical lift profile (VLP) [26]. The VLPs use empirical models to estimate fluid flow regimes, pressure gradients and liquid hold-up.

Calculation of well flow rate usually begins with an inflow/outflow assessment.

Inflow Performance is the flow from the reservoir to the well, while Inflow Performance Relationship (IPR) is the plot of producing rate versus bottomhole flowing pressure. The Vertical Lift Performance Relationship (VLP) describes the bottomhole

pressure as a function of flow rate. The main difference between both curves is that IPR represents what the reservoir can deliver to the bottomhole, while the VLP represents what the well can deliver to the surface [17].

In production, usually, the IPR curve is plotted in the “Flowing Bottom Hole Pressure, p_{wf} ” versus “Flow Rate, q ” plot. Then, the VLP curve is plotted in the same graph, showing an intersection (solution/operational point), which provides the expected production rate and the bottomhole flowing pressure, for a given operating condition

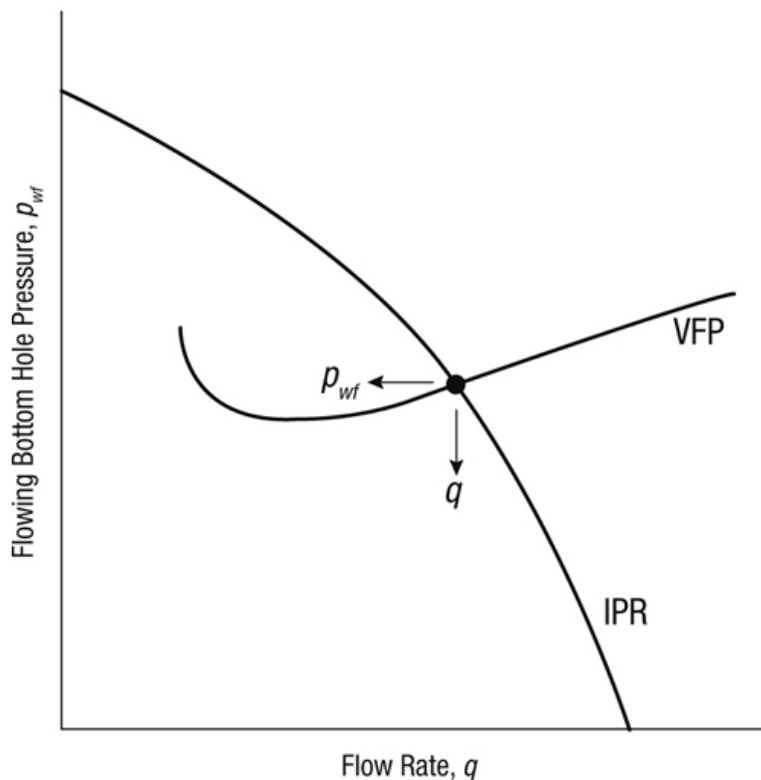


Figure 9. Well deliverability: Combination of IPR and VFP. [17]

In using a nodal analysis approach for WCD calculations/modeling, we predominantly follow the conventional nodal analysis method but because we have stacked sand/shale sequences in Gulf of Mexico, for each WCD model we have multiple IPRs and only one VLP curve.

Depending on the available information and the type of sensitivities as well as fluid type and formation type, there are various inflow options available. One item in common between most of the inflow performance models is that average reservoir pressure and reservoir temperature are needed data, along with other reservoir parameters as described below. All of the correlations are based on the fundamental equation of Darcy's law. Some of the most common correlations available for inflow performance relationships for estimating the pressure/production behavior during two-phase flow are [23]:

- Vogel: it is an empirical IPR for solution-gas drive reservoirs with two-phase flow (oil and gas) [23]. Vogel developed one of the earliest IPRs and it is based on numerical simulation results. It is based on a wide range of rock and fluid properties [53].

$$\frac{q_o}{q_{o,max}} = 1 - 0.2 \frac{P_{wf}}{P_R} - 0.8 \left(\frac{P_{wf}}{P_R} \right)^2 \quad [51]$$

- Fetkovich: in order to estimate the productivity, Fetkovich proposed the isochronal testing of oil wells [23]. The range of permeability used in this experiment were from 6 md to more than 1000 md [19]. The data needed for this correlation are reservoir permeability, formation thickness, drainage area, DIETZ shape factor, wellbore radius and relative permeability of oil [36]. For predicting performance, the following equation is the most suitable:

$$q_o = C'(P_R^2 - P_{wf}^2)^n \quad [23]$$

- Jones, Blount and Glaze: it is a modified equation of Darcy's law for gas, and it allows laminar and turbulent flow pressure drops. The data needed for this correlation are reservoir permeability, formation thickness, drainage area, DIETZ shape factor, wellbore radius and perforated interval [44].

$$\frac{P_R - P_{wf}}{q_o} = A' + B' q_o \quad [32]$$

The coefficient A is the laminar-flow coefficient and B is the turbulent coefficient [23].

- Klins and Majcher: the bubble point pressure is incorporated, based on Vogel's work [23].

$$\frac{q_o}{q_{o,max}} = 1 - 0.295 \frac{P_{wf}}{P_R} - 0.705 \left(\frac{P_{wf}}{P_R} \right)^{d'} \quad [34]$$

Where,

$$d' = \left(0.28 + 0.72 \frac{P_R}{P_b} \right) (1.235 + 0.001 P_b)$$

- Sukarno and Wisnagroho: this correlation introduces the flow-efficiency variation caused by rate-dependent skin as bottomhole pressure changes [23].

$$\frac{q_{o,actual}}{q_{o,max,r=0}} = F_E \left[1 - 0.1489 \frac{P_{wf}}{P_R} - 0.4416 \left(\frac{P_{wf}}{P_R} \right)^2 - 0.4093 \left(\frac{P_{wf}}{P_R} \right)^3 \right] \quad [23]$$

Where,

$$F_E = a_0 + a_1 \left(\frac{P_{wf}}{P_R} \right) + a_2 \left(\frac{P_{wf}}{P_R} \right)^2 + a_3 \left(\frac{P_{wf}}{P_R} \right)^3$$

And

$$a_R = b_0 + b_1 S + b_2 S^2 + b_3 S^3$$

2.7 Flow Correlations for Different Flow Regimes

Numerous pipe flow correlations are used in the industry and they are available in most nodal analysis software packages [49]. Each of these flow correlations have an applicable range depending on different aspects such as diameter of tube, oil gravity, and gas liquid ratio [14].

The main reasons for using multiphase flow correlations are predicting liquid holdup and pressure gradient [44], and in WCD calculations, they have been used to predict pressure and temperature changes in wellbore [52]. Flow regimes identification, which are essential as part of the multiphase flow analysis, rely on a particular flow correlation.

2.8 Two-Phase Flow Regimes

Flow regime or flow pattern is basically a qualitative description of the manner in which the two phases are distributed in the well pipe. There are four kinds of flow regimes [17], as shown in figure 10:

- Bubble flow: The bubbles of gas are dispersed in an uninterrupted liquid phase.
- Slug flow: With a high gas rate, the bubbles merge into greater bubbles that eventually fill almost the whole pipe cross section. Slugs of liquid that contain smaller bubbles of gas is between the large gas bubbles.
- Churn flow: As gas rate increases even further, the larger gas bubbles present instability and they start collapsing. Therefore, with both phases dispersed, this flow regime can be consider as chaotic.
- Annular flow: At a very high gas rate, gas becomes the continuous phase. Gas itself flows in the core of the pipe, while liquid flows in a homogenous thin film on the pipe wall.

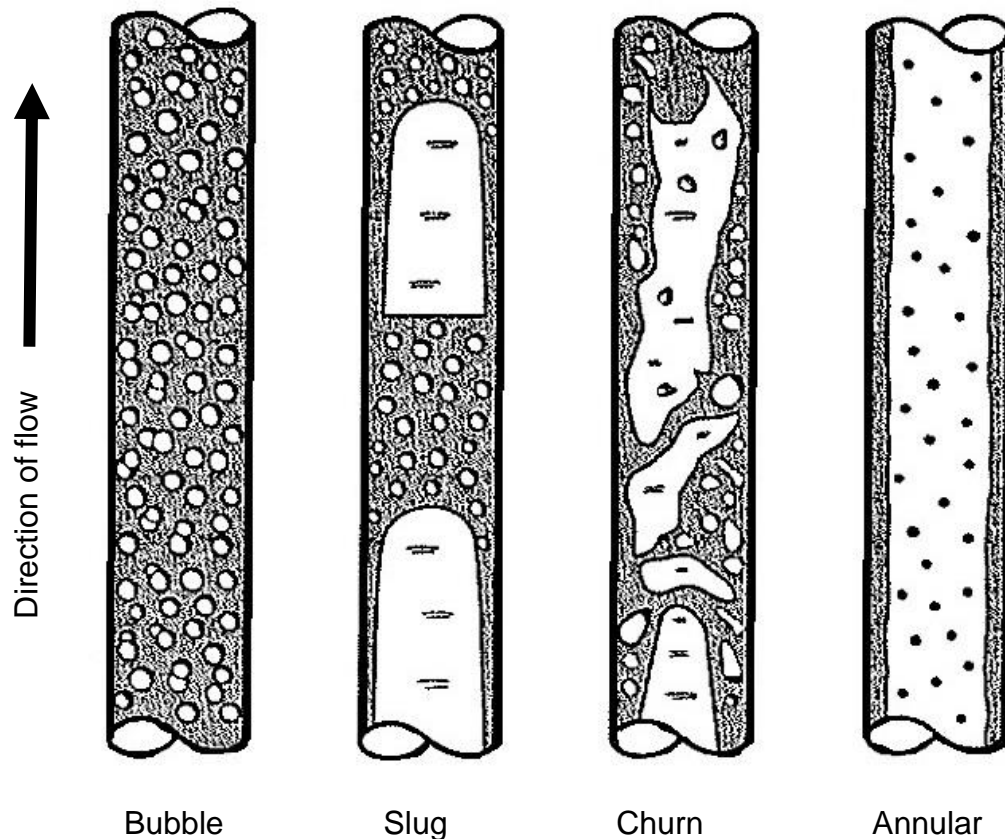


Figure 10. Gas-liquid flow regimes in vertical pipes [48].

2.9 Flow correlations

- **Hagedorn & Brown Correlation:** It is an experimental study developed in a 1,500 ft. experimental well. The tubing diameters ranging from 1-1.5 inches. Five types of fluids were used: water and four kind of oil with viscosities oscillating between 10-110 cp (at 80°F) [27]. At moderate to high production rates in oil wells, this correlation works fine for slug flow. However, it is not recommendable to use this correlation for condensates and when the main flow regime is mist flow [44].
- **Duns and Ros Correlation:** It is developed for a vertical flow of gas and liquid mixtures in wells. Its intention is to be applicable over the full range of field conditions: tubing and annular flow for a wide range of oil and gas mixtures with

varying water cuts. This correlation works fine in mist flow case, and it has been optimized for use with condensates [16].

- Orkiszewski Correlation: This method is an extension of the work done by Griffith and Wallis, with a precision of about 10%. It is restricted to vertical pipes and two-phase pressure drop [41]. This correlation is acceptable in the following flow regimes: bubble, slug, transition, and annular mist [14]. However, instability is caused since its formulations present a discontinuity at velocity equal to 10 ft/s in calculation [44].
- Beggs and Brill Correlation: This correlation is applicable in pipelines for hilly terrain and tubing strings for inclined wells. The fluids used in the experiment were air and water [5]. It generally over-predicts pressure drops in vertical and deviated trajectory [44].
- Mukherjee and Brill Correlation: It is applicable in two-phase inclined flow. The average prediction relative error is 35%. This correlation is acceptable in the following flow regimes: bubble, slug, and annular [38].

CHAPTER 3. RESEARCH GOALS

The goals of this research are threefold: the first goal is to develop a workflow to calculate worst-case discharge volumes (in a drilling scenario) using an improved nodal analysis method; the second goal is to perform sensitivity studies on the rock compressibility and aquifer presence to assess their impact on the inflow-performance and WCD rates; the third goal is to validate the results from models built with the workflow built through this research using accepted reservoir simulation tools.

For the most part, reservoir simulations are validated with analytical solutions. Here, we are validating an improved nodal analysis workflow with reservoir simulation results. The greatest advantage of this workflow is that it serves as an efficient tool that is simpler, quicker and validated for computing any and all of GoM's future well's WCD volumes and rates.

For certain special scenarios, the improved nodal methodology, however, may not prove to be ideal. Nonetheless, the proposed workflow and the modeling results help identify scenarios where reservoir simulation may actually be a better tool than nodal solutions.

The uniqueness of the workflow developed through this research is that it goes beyond steady-state nodal analysis and wellbore models for computing potential blowout rates, but is simpler to build and use than full-scale reservoir simulation models. Additionally, the workflow can be adapted in simple software/research codes like MS Excel and MATLAB, although in this research we use the Integrated Production Modeling (IPM) tool from Petroleum Experts [45].

CHAPTER 4. METHODOLOGY

The fundamental methodology used in this research is of nodal analysis (for developing the primary WCD calculation workflow) coupled with multiple IPRs/reservoirs. The new workflow is validated using accepted reservoir simulation methods, which are for example GEMINI [15] and REVEAL [44], and results are compared with the reservoir-coupled nodal analysis workflow and reservoir simulation models.

Adapting from the SPE 2015 report on estimating WCD rates, this research incorporates multiple stacked reservoirs and non-reservoirs as in the GoM stacked patterns (Figures 7 and 8), and couples them with an open-hole section (as in a during-drilling scenario). The wellbore is set-up according to the designed well-schematic of the operator, and no post-drill restrictions are considered [49]. Well deviation is incorporated, and location of discharge point is assigned as open to atmosphere to seafloor (for subsea wellheads). During drilling of a well, several open-hole sections may be encountered as shown in Figure 11 by the 12 inch and the 8.25 inch sections [49]. The 12 inch section is open to an oil sand overlain by an aquifer which is overlain by a gas sand and the 8.25 inch section has two oil sands (Figure 11). The WCD estimate reported is the one that has the highest discharge of the two sections.

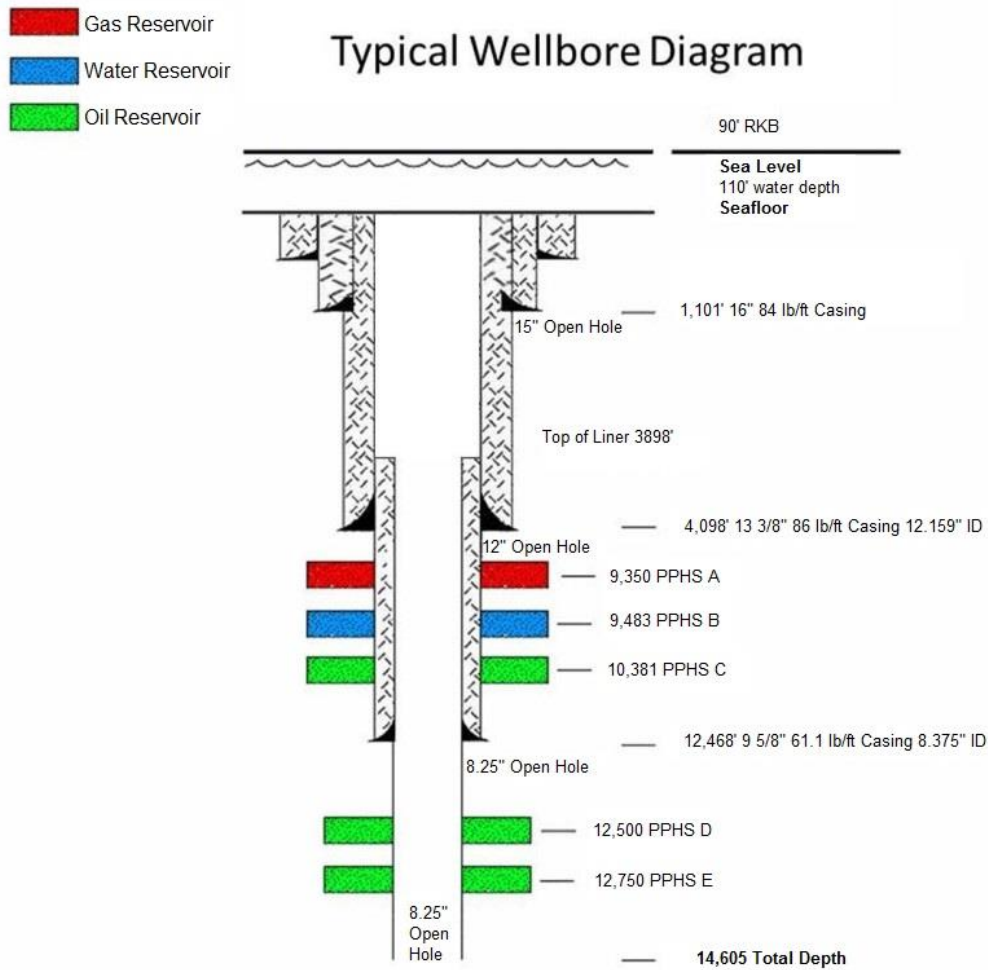


Figure 11. Figure showing typical wellbore configuration for 8.5" and 12" wellbores with stacked reservoir/non-reservoir rocks [49].

Once the wellbore configuration is set up, subsurface characterization is completed with analog or reservoir data of rock and fluid properties, drainage areas, drive mechanisms [49], current hydrocarbons in place, and reservoir pressures (this thesis). Regional or local geothermal gradients, open-hole roughness, downhole/casing equipment and their properties, and possibility for cross-flow are other input parameters considered in developing the WCD workflow and resultant models.

Finally, the IPRs from multiple reservoirs are generated, and the VLP from the wellbore is generated referenced to the top of the first reservoir in the open-hole section.

A forecasting model is then run to generate WCD volumes and rates for oil, gas and water over 60, 90 or 120 days. The forecasting time is based on the time that may be required for relief well and/or kill operations to be completed.

4.1 Governing Equations

The governing equations used in this research can be separated into reservoir performance and wellbore performance equations:

Reservoir performance:

- Darcy's law

Darcy's law describes the flow of a fluid through a permeable medium. This equation represents single phase flow for absolute permeability.

$$Q = -\frac{kA}{\mu} \frac{\partial p}{\partial x}$$

The negative sign is used to represent the flow from high pressure to low pressure.

- Material balance equation

The material balance equation is a volume balance relationship (mass balance for a particular density of fluids) and is given by:

$$\begin{aligned} N_p [B_o + (R_p - R_s) B_g] + W_p B_w - W_i B_w - G_i B_g \\ = N \left[(B_o - B_{oi}) + (R_{si} - R_s) B_g + (1 + m) B_{oi} \frac{(c_f + S_{wc} c_w)}{(1 - S_{wc})} \Delta P \right. \\ \left. + m B_{oi} \left(\frac{B_g}{B_{gi}} - 1 \right) \right] + W_e \end{aligned}$$

In this equation, the left-hand side (LHS) of the equation represents the production terms, and the right-hand side equation represents the reservoir/aquifer terms for

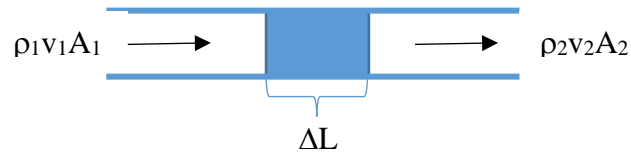
drive mechanisms like solution gas drive, water drive and compaction terms. This means that the RHS represents all the expansion and influx which is driven by the LHS production terms [13].

Wellbore performance:

The equations of conservation of mass, conservation of momentum and energy are the principles and bases to determine the change in pressure and temperature with distance that dictates the flow of fluids in pipes [39].

- **Mass conservation**

In a segment of pipe, conservation of mass means that the mass in minus mass out must be equal to mass accumulation.



$$\frac{\partial \rho}{\partial t} + \frac{\partial(\rho v)}{\partial L} = 0$$

For steady-state flow, mass accumulation does not occur, and ρv is constant.

Then, the above equation becomes:

$$\frac{\partial(\rho v)}{\partial L} = 0$$

- **Momentum conservation**

Newton's first law states that "every object persists in its state of rest or uniform motion in a straight line unless it is compelled to change that state by forces impressed on it" [40]. Applying this law to fluid flow in pipes means that the rate of

momentum out minus rate of momentum plus rate of momentum accumulation is equal to the forces on the fluids.

$$\frac{\partial(\rho v)}{\partial t} + \frac{\partial(\rho v^2)}{\partial L} = -\frac{\partial p}{\partial L} - \frac{\tau \pi d}{A} - \rho g \sin \theta$$

For steady-state flow, rate of accumulation is eliminated and the above equation becomes:

$$\frac{dp}{dL} = -\frac{\tau \pi d}{A} - \rho g \sin \theta - \rho v \frac{dv}{dL}$$

- Energy conservation

Conservation of energy in pipes means that in a segment of pipe, the energy in minus the energy out plus the heat energy transferred to or from the surroundings must be equal to the rate of energy accumulation.

$$\frac{\partial}{\partial t}(\rho e) = \frac{\partial}{\partial L} \left[\rho v \left(e + \frac{p}{\rho g_c J} \right) \right] + \frac{Q \pi d}{A}$$

And for steady-state flow, the above equation becomes:

$$\frac{d}{dL} \left[\rho v \left(e + \frac{p}{\rho g_c J} \right) \right] = -\frac{Q \pi d}{A}$$

Where,

$$e = \frac{gL \sin \theta}{g_c J} + \frac{v^2}{2g_c J} + u$$

Therefore,

$$\frac{d}{dL} \left[\rho v \left(e + \frac{p}{\rho g_c J} \right) \right] = \rho v \frac{\partial}{\partial L} \left(\frac{gL \sin \theta}{g_c J} + \frac{v^2}{2g_c J} + u + \frac{p}{\rho g_c J} \right) = -\frac{Q \pi d}{A}$$

Defining enthalpy, h, as: $h = u + \frac{p}{\rho g_c J}$, and,

$$\frac{\rho v g}{g_c J} \sin \theta + \frac{\rho v v}{g_c J} \frac{\partial v}{\partial L} + \rho v \frac{dh}{dL} = -\frac{Q \pi d}{A}$$

Then,

$$\frac{dh}{dL} = -\frac{Q\pi d}{\rho v A} - \frac{v}{g_c J} \frac{dv}{dL} - \frac{g \sin \theta}{g_c J}$$

CHAPTER 5. RESULTS – DEVELOPED WORKFLOW USING PRODUCTION MODELING TOOLS

5.1 Basis of Workflow

The workflow developed is adopted in the PETEX Integrated Production Modeling (IPM) software is used in this research to simulate worst-case discharge for an open wellbore. IPM is a production system with a modeling toolkit (GAP, PROSPER, MBAL, REVEAL, PVTP and RESOLVE) which can work together or separately. IPM optimizes, designs and models entire oil or gas production systems. In this thesis, the tools used are GAP, MBAL and PROSPER.

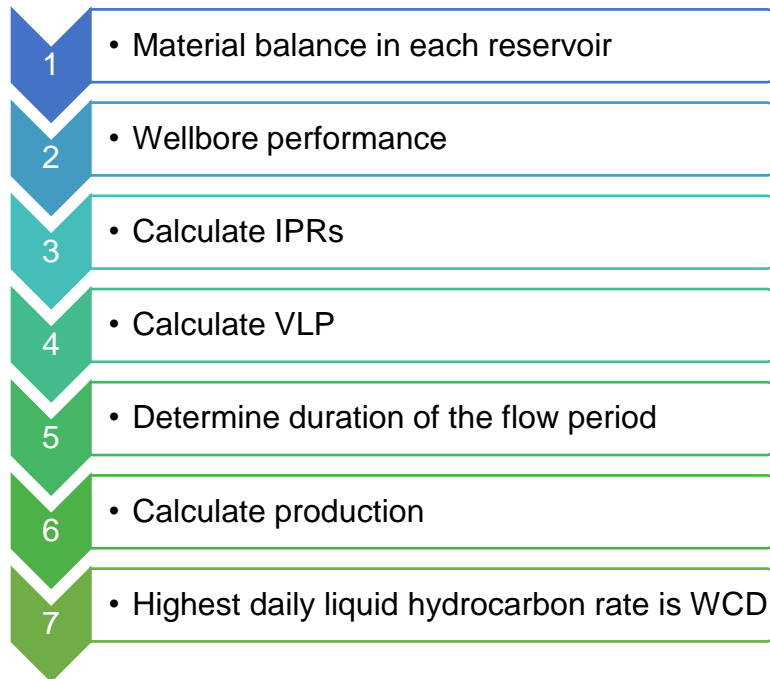
GAP is a multiphase flow simulator that is able to model and optimize production and injection networks [42]. In fact, linking PROSPER and MBAL to GAP, it is possible to achieve a full field production optimization and forecast. GAP is a steady state multiphase network optimizer well-known in the industry. The main objective of GAP is to capture the response of each item in a hydrocarbon field that affects the production.

PROSPER is a well performance, design and optimization program for modelling most types of well configurations [44]. One of the best advantage of PROSPER is that it has a variety of multiphase flow models, and it enables nodal analysis calculations for any type of well. PROSPER also shows the inflow/outflow response of the scenario chosen. Moreover, PROSPER can be linked directly to GAP.

MBAL is a material balance reservoir-modelling tool that help in the analysis of the reservoir, which in general is the material balance calculation [43]. MBAL provides a solid idea of the reservoir parameters in detail. One advantage is that it can be linked directly to GAP.

Although they are production tools, in this thesis they are used for modelling a WCD scenario quicker and easier than reservoir simulation tools.

Adopting the fundamental methodology outlined in Chapter 4 of this thesis, Integrated Production Modeling (IPM) tools are used to forecast production (in this case WCD) for a loss of control situation during drilling from an open hole section. IPM submodules used are MBAL for material balance, Prosper for IPR generation, GAP for VLP generation and forecasting. IPM, particularly GAP models have one reservoir from which multiple wells produce. In this study, to mimic a WCD scenario, one well is connected to multiple reservoirs different from the usual production scenario of one reservoir connected to multiple wells. As a result, a new WCD workflow is developed using IPM and outlined as below. The novelty of this workflow lies in the fact that material balance is coupled with IPR generation for all the sands that could potentially flow into the open hole section during a loss of control situation. This coupling enables dynamic update of pressures during forecasting of the WCD rates and volumes without employing a full scale reservoir simulation.



- 1) Material balance in each reservoir: Mathematically material balance means the mass conservation in a reservoir. Therefore, for calculation of material balance, it is necessary to characterize the reservoir with certain data such as PVT data - formation GOR, oil gravity, gas gravity, water salinity, reservoir composition(s)-, reservoir pressure, reservoir temperature, porosity, connate water saturation, reservoir permeability, rock compressibility. As part of material balance, aquifers are defined at this point.
- 2) Inflow Performance: The considerations that affect inflow performance are reservoir rock, fluid properties and reservoir geometry. The IPR is based on Darcy's model—, reservoir permeability, reservoir thickness, drainage area, Dietz shape factor, wellbore radius, mechanical skin, are required to compute the reservoir deliverability.
- 3) Outflow Performance: The consideration for outflow performance is the pressure changes, which are mainly caused by friction, acceleration and gravity. Moreover,

directional survey information is important in this calculation because of the drops in the well paths. Casing diameter, casing and open hole roughness, and geothermal gradient are also required inputs to generate the VLP.

- 4) Duration of flow period: The duration of the flow in the analysis mainly depends on the location of the well and the time that could take for the crew to drill a relief well.
- 5) Forecast production (in this case the WCD volume and rate): The cumulative production over the period chosen represents the potential spilled volume for WDC.

Although in SPE Technical Report [49] shows a typical workflow for WCD calculations, the singularity of the workflow developed above is that it goes beyond steady-state nodal analysis. It can be adapted in simple software/research codes like MS Excel and MATLAB. In this research, IPM tool is used.

The steps for the adoption of the workflow developed in this thesis and as applied to PETEX software is given in Appendix B.

CHAPTER 6. RESULTS - WORKFLOW VALIDATION WITH RESERVOIR SIMULATION

6.1 Base Case

The base case of this research is represented by a vertical well connected to four stacked layer sands, the first one represents oil layer sand, the second one represents water layer sand, the third one represents water layer sand, and the fourth one represents oil layer sand.

The workflow developed in this research and implemented in GAP was replicated with reservoir simulation using the same base case model (Figure 12) which had a stacked sequence of oil, water, water, and oil (OWWO henceforth) formations open to the mother bore. Reveal (from Petroleum Experts) was the simulator of choice. It is a robust near wellbore to reservoir scale simulator and has been benchmarked and validated by industry experts [2]. If the reservoir coupled nodal analysis workflow is to be recommended for future use, and implemented in more accessible tools like MS Excel – a reservoir simulation ‘validation’ is required.

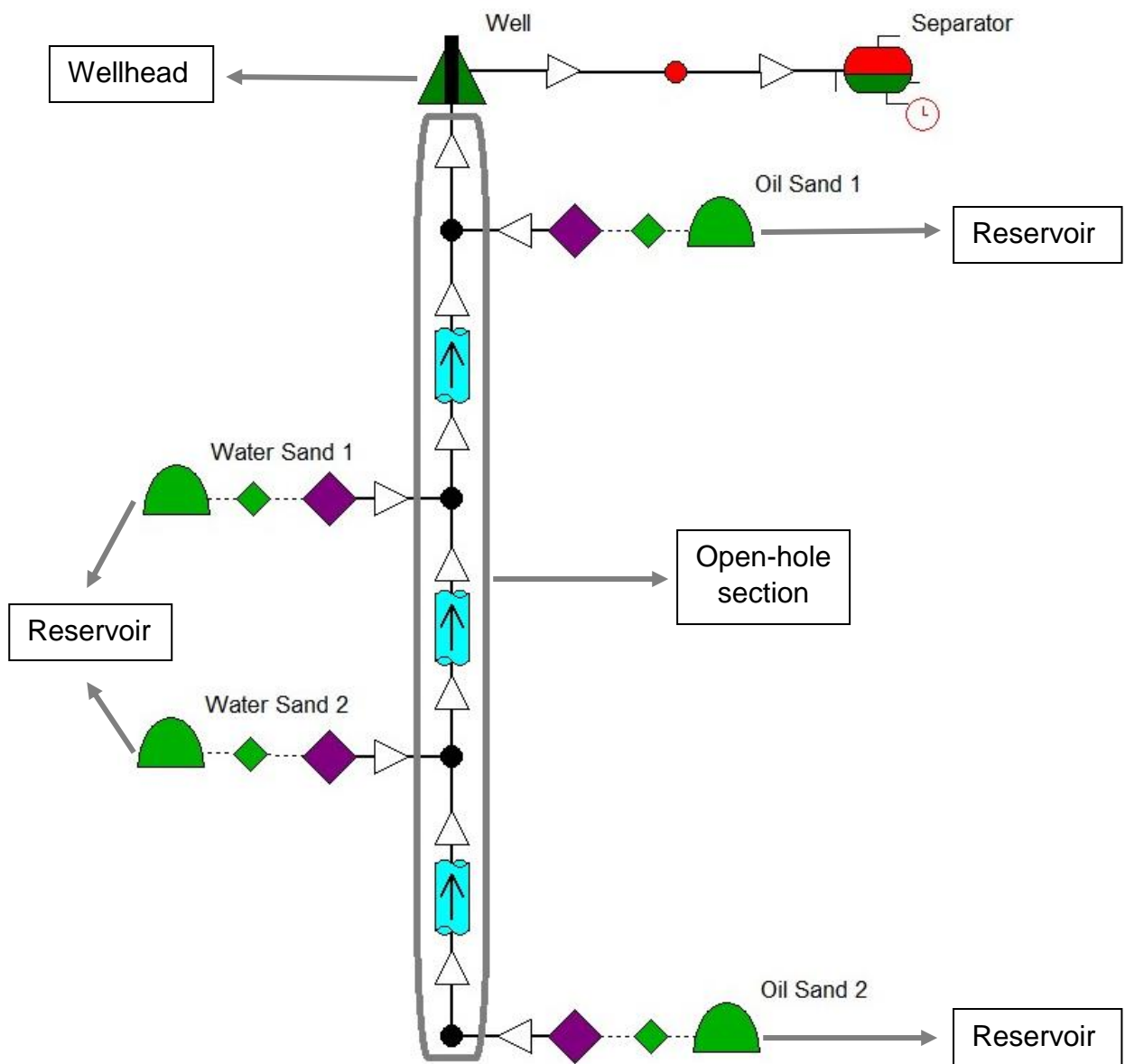


Figure 12. Example of a wellbore open to four sands.

Cumulative oil, gas and water rates are compared from GAP and REVEAL model (Figure 17) outputs for the OWWO scenario (Figures 12 and 17). Results show that for the fluid properties model and flow correlations used, the Hagedorn-Brown correlation gave the closest volumes (Figures 13 - oil, 14 - water, and 15 - gas). Different flow correlations were tested and the best option for the base case is Hagedorn-Brown (Table 2).

Table 2. Errors for BaseCase Model (OWWO Scenario) for Hagedorn and Brown Correlation.

FLOW CORRELATIONS	VOLUMES	GAP	REVEAL	ABSOLUTE %ERROR
BASE CASE - Hagedorn and Brown	Cumulative Oil Production (MMSTB)	0.917	0.758	17%
	Cumulative Water Production (MMSTB)	1.110	1.057	5%
	Cumulative Gas Production (MMscf)	390.810	394.135	1%
BASE CASE - Hagedorn and Brown - Water at the base	Cumulative Oil Production (MMSTB)	0.875	0.781	11%
	Cumulative Water Production (MMSTB)	1.108	1.074	3%
	Cumulative Gas Production (MMscf)	395.379	409.152	3%

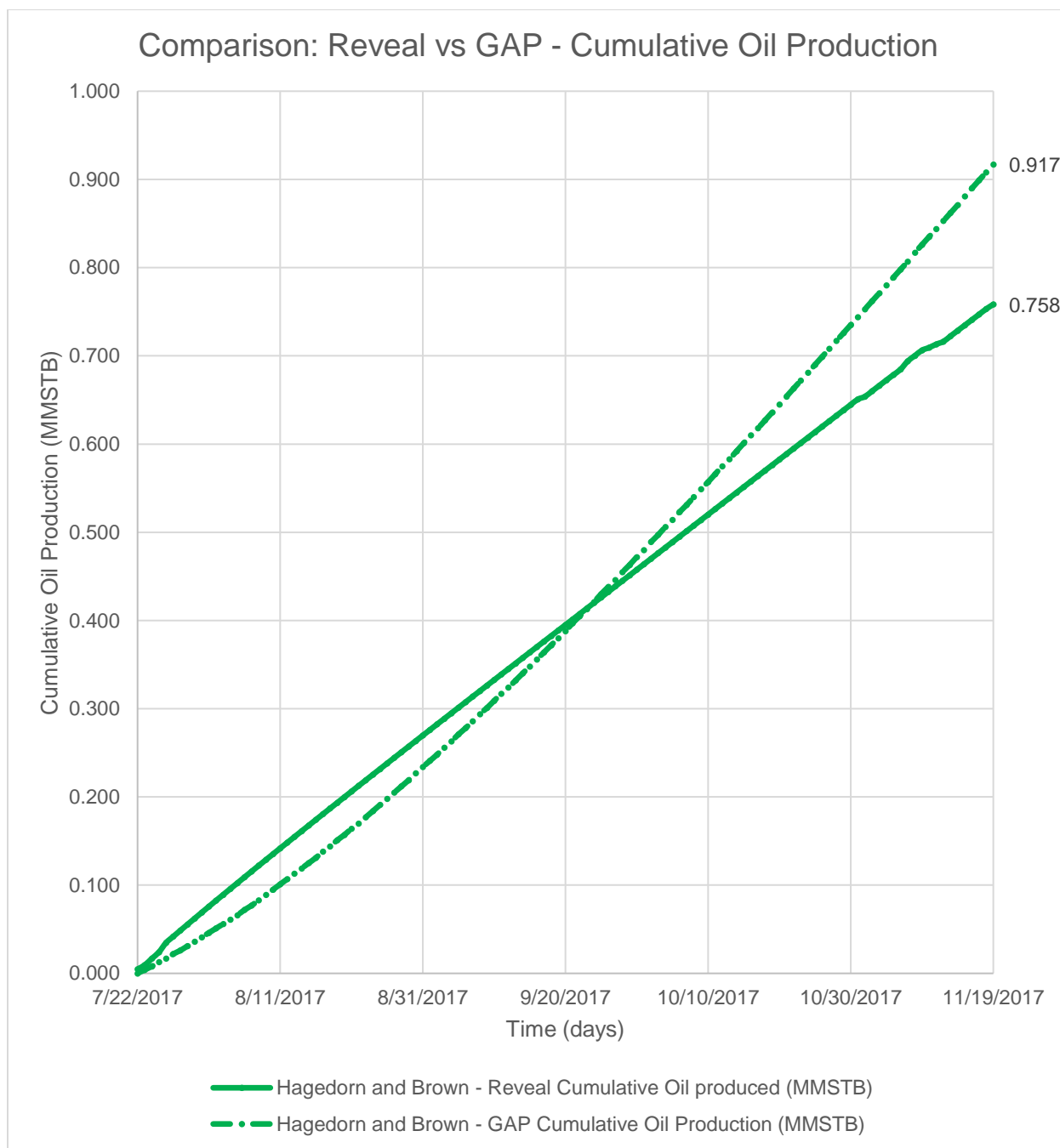


Figure 13. Cumulative Oil Production for GAP and Reveal Base Case Model (OWWO Scenario) – Hagedorn Brown

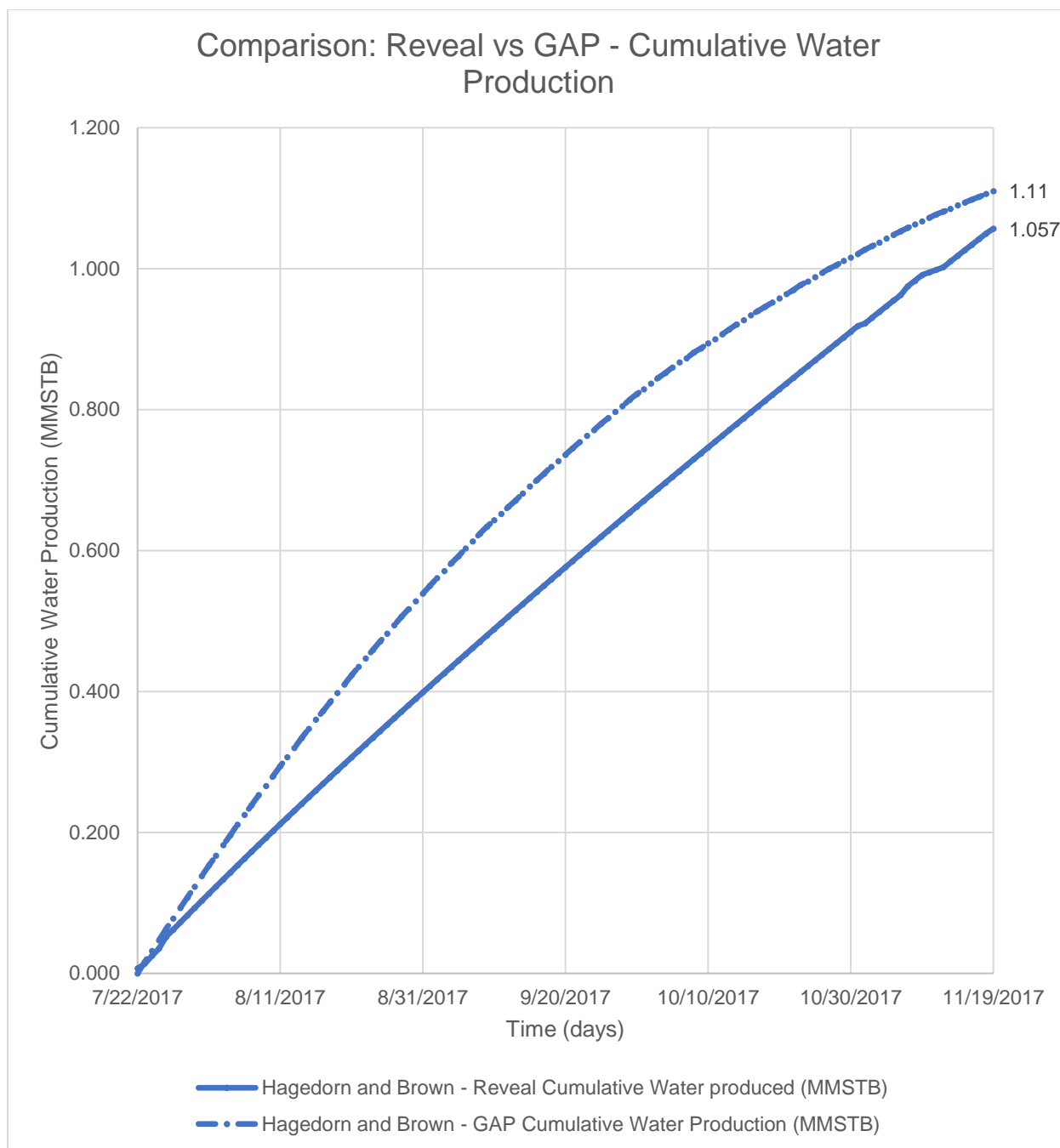


Figure 14. Cumulative Water Production for GAP and Reveal Base Case Model (OWWO Scenario) - Hagedorn Brown

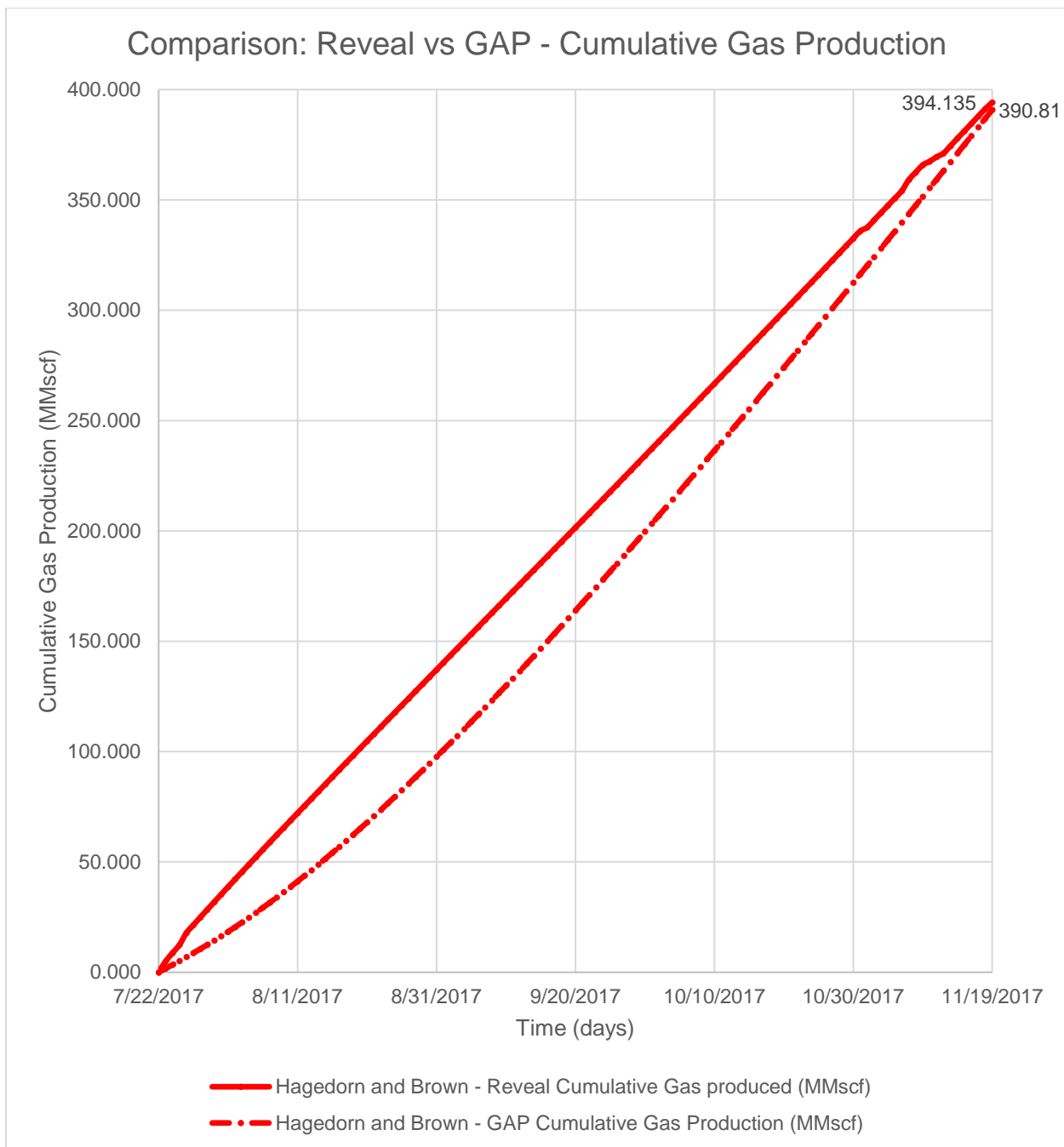


Figure 15. Cumulative Gas Production for GAP and Reveal Base Case Model (OWWO Scenario) - Hagedorn Brown

In the base-case model (OWWO scenario), both the oil sands had aquifers attached to the oil reservoirs. Carter-Tracy analytical models were used as aquifer models (material balance, drive mechanism).

Figure 16 shows the oil peak rates for oil only sequence of sands. The presence of water sands affects the timing and amount of peak rates if it is included.

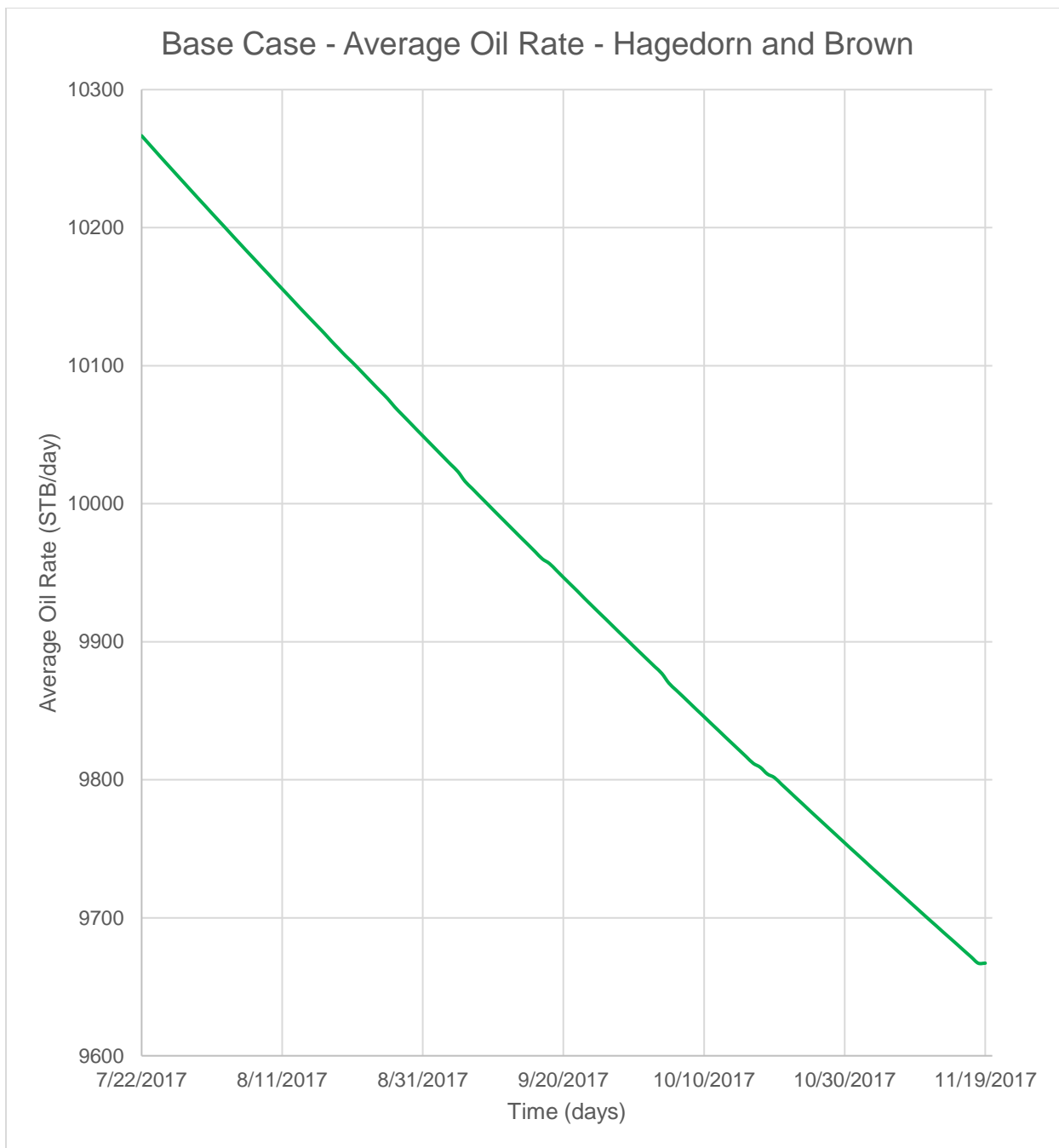


Figure 16. Average Oil Production for GAP Base Case Model (OWWO Scenario) - Hagedorn Brown

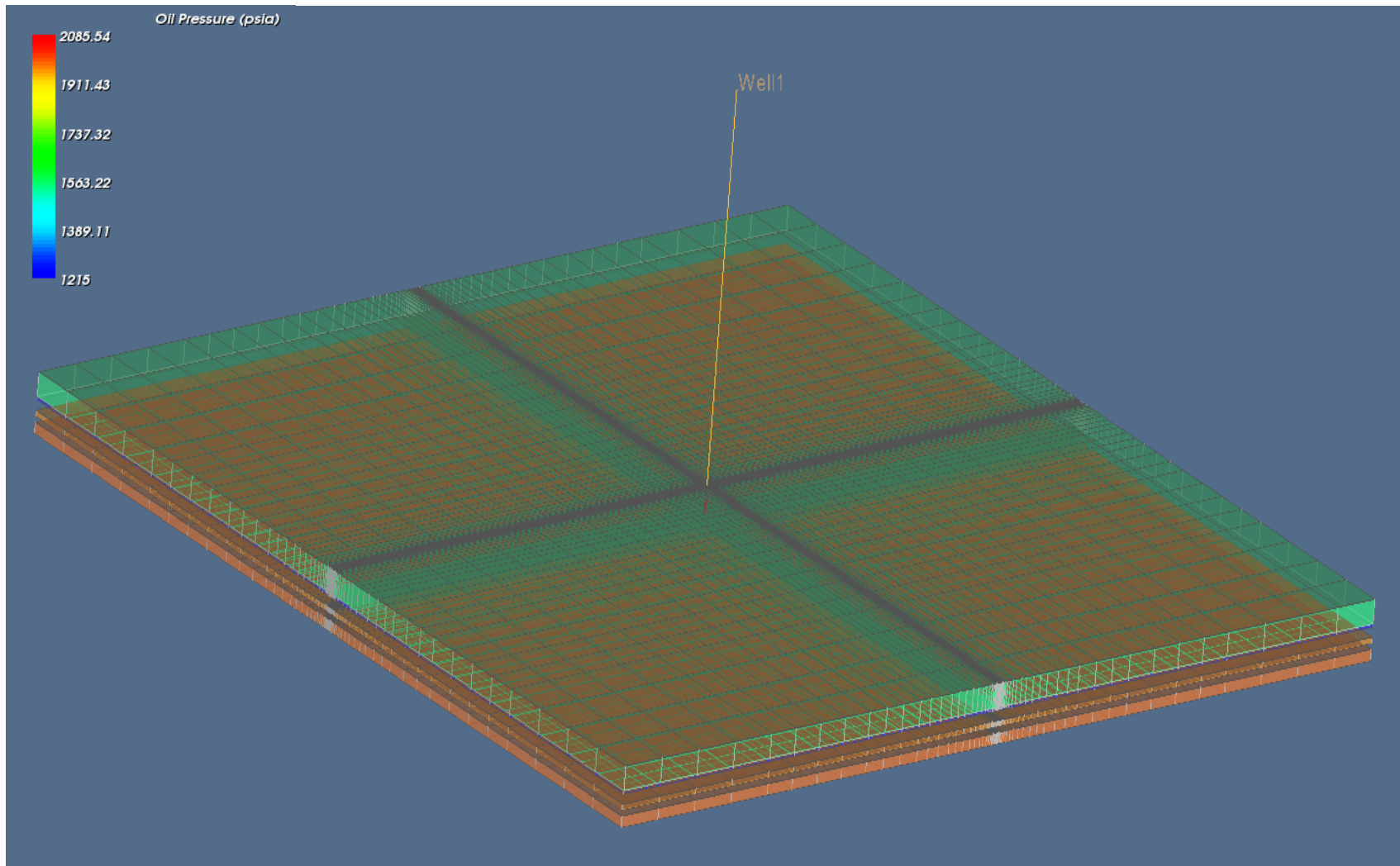


Figure 17. Reservoir simulation model for base case (OWWO scenario).

The similarity in WCD estimates from both the numerical simulation models (Reveal), and the integrated reservoir-nodal analysis workflow prove that the latter may be used as a quicker, simpler tool in place of reservoir simulation when the data/needs warrant their use, as mentioned earlier, for the fluid properties used.

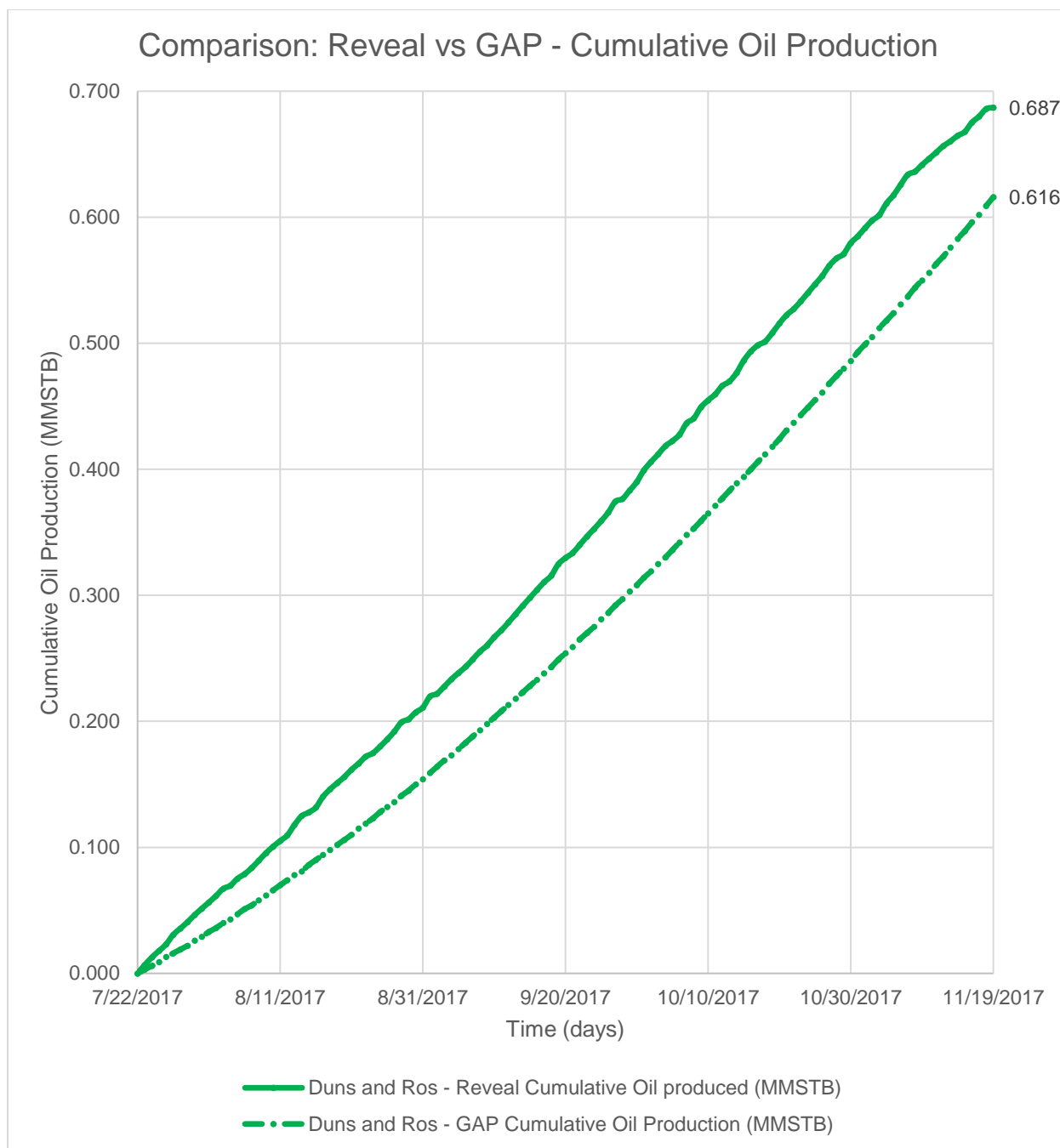


Figure 18. Cumulative Oil Production for GAP and Reveal Base Case Model (OWWO Scenario) – Duns and Ros Correlation

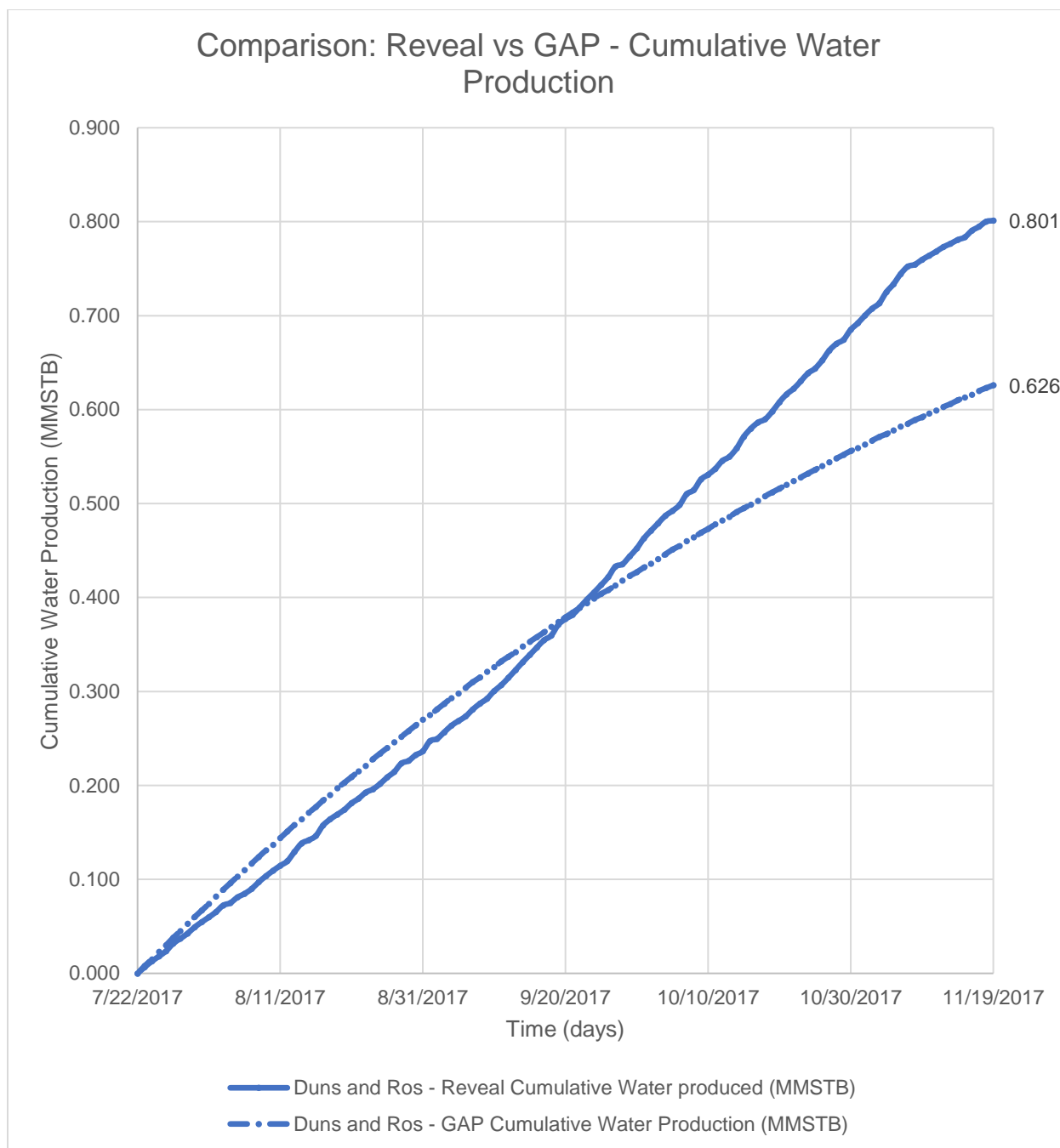


Figure 19. Cumulative Water Production for GAP and Reveal Base Case Model (OWWO Scenario) – Duns and Ros Correlation

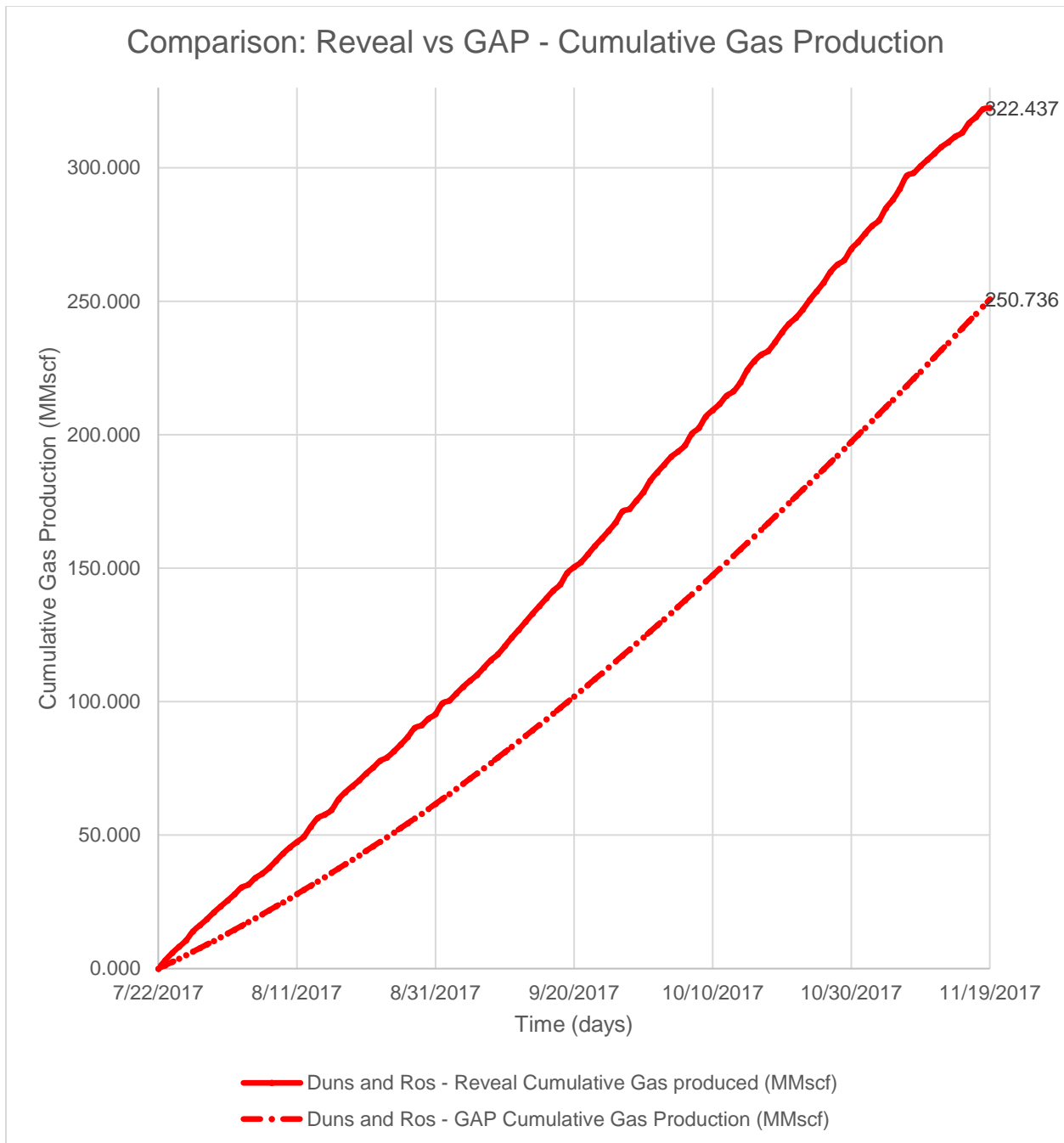


Figure 20. Cumulative Gas Production for GAP and Reveal Base Case Model (OWWO Scenario) – Duns and Ros Correlation

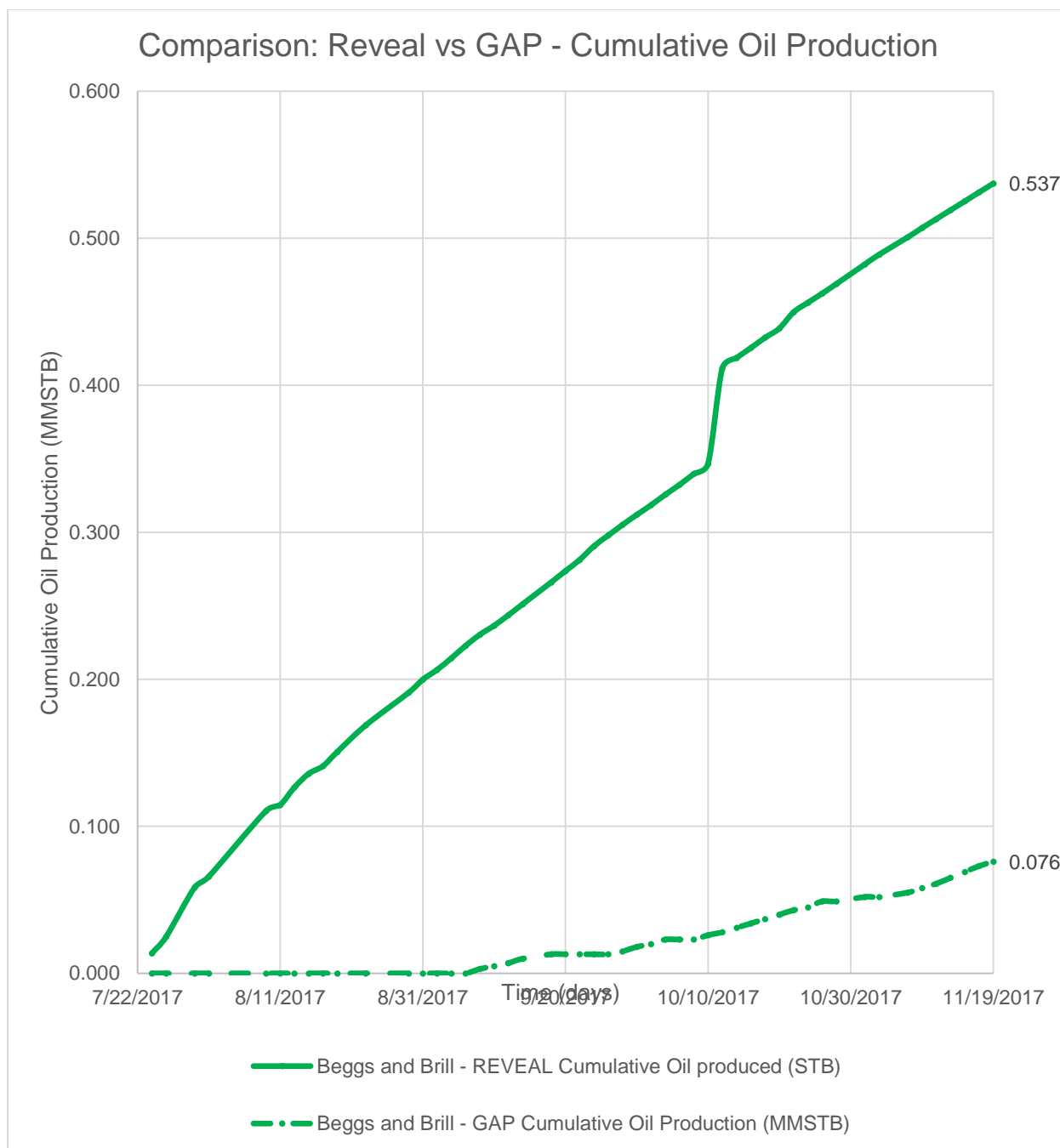


Figure 21. Cumulative Oil Production for GAP and Reveal Base Case Model (OWWO Scenario) – Beggs and Brill Correlation

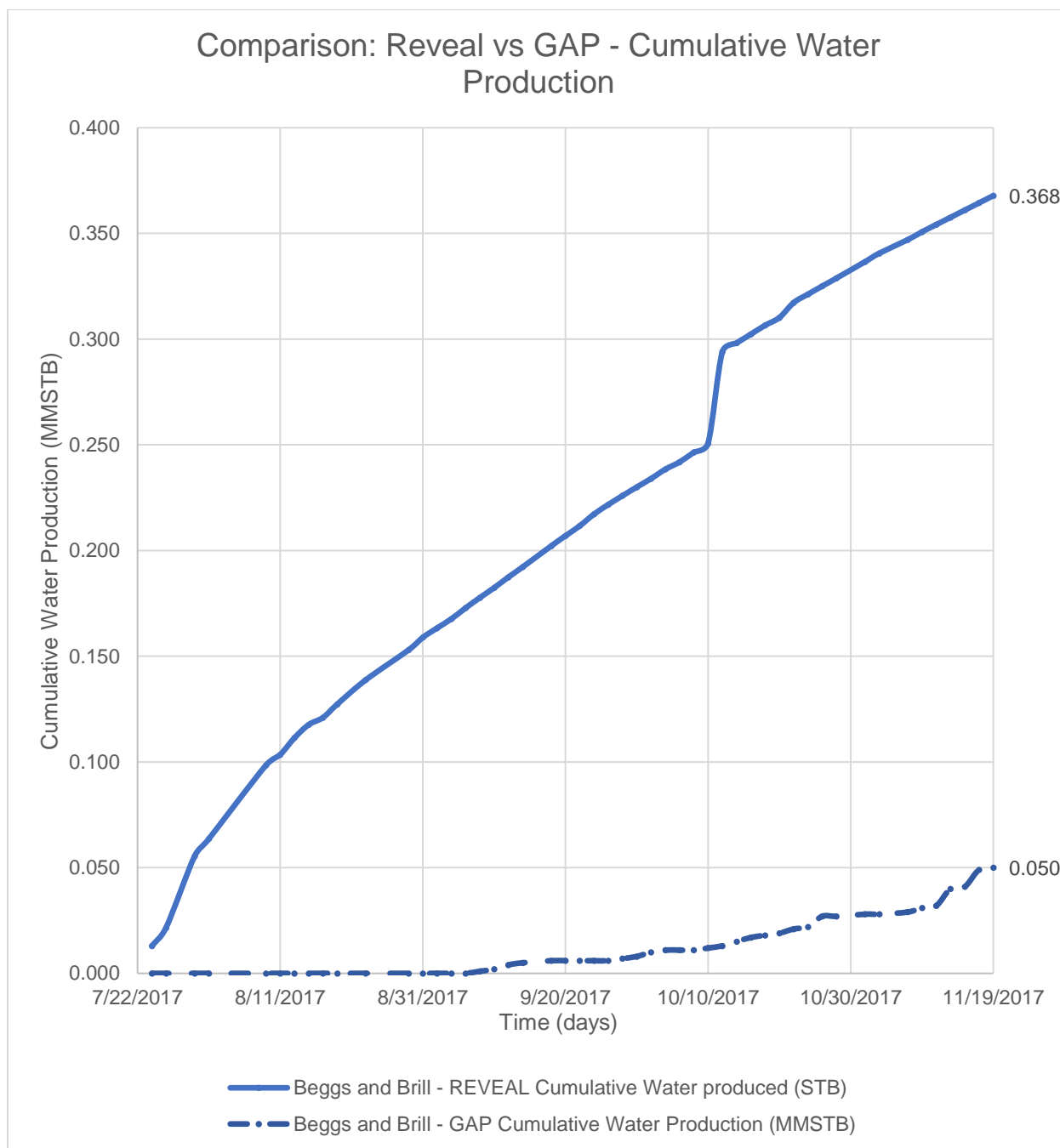


Figure 22. Cumulative Water Production for GAP and Reveal Base Case Model (OWWO Scenario) – Beggs and Brill Correlation

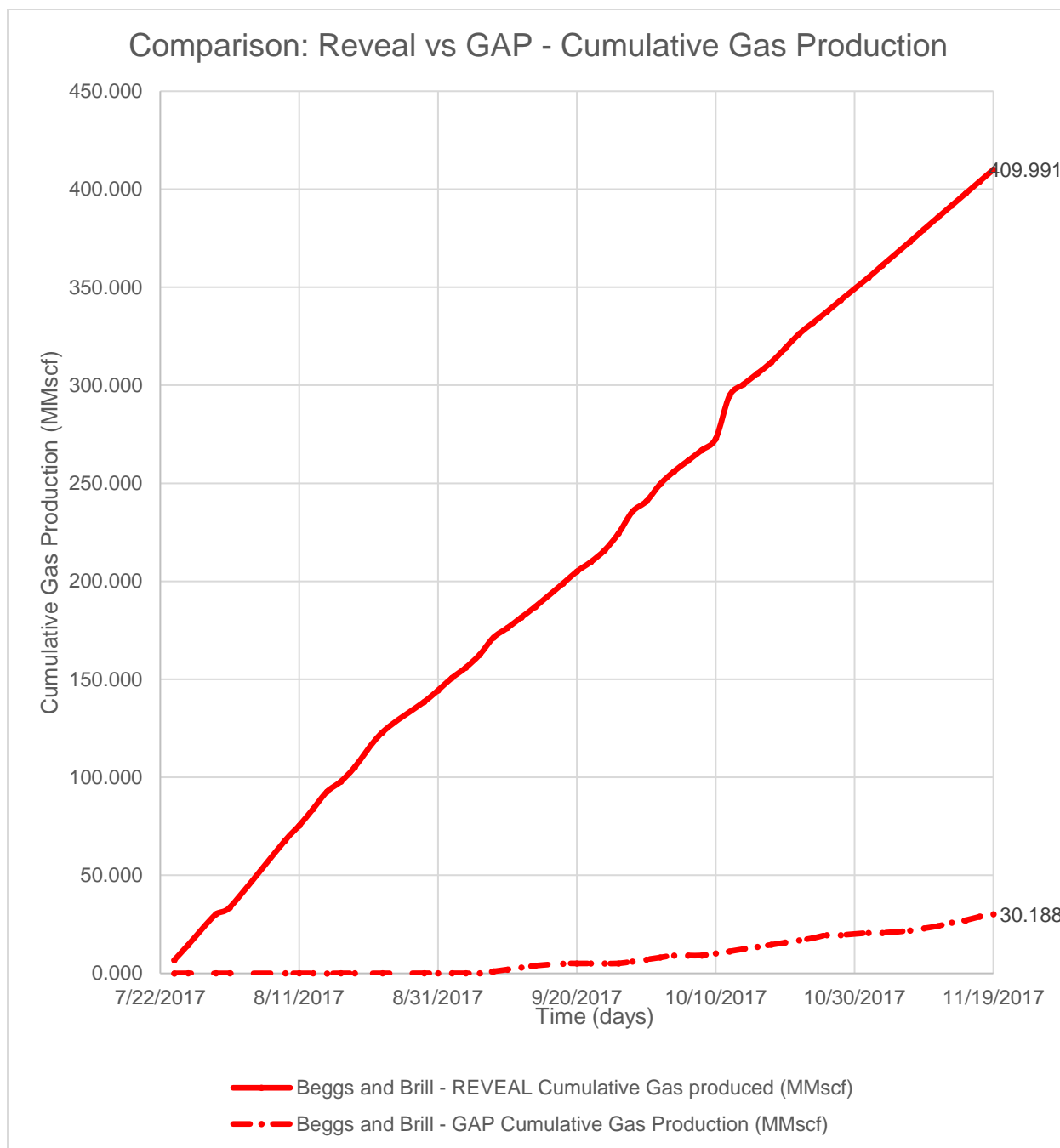


Figure 23. Cumulative Gas Production for GAP and Reveal Base Case Model (OWWO Scenario) – Beggs and Brill Correlation

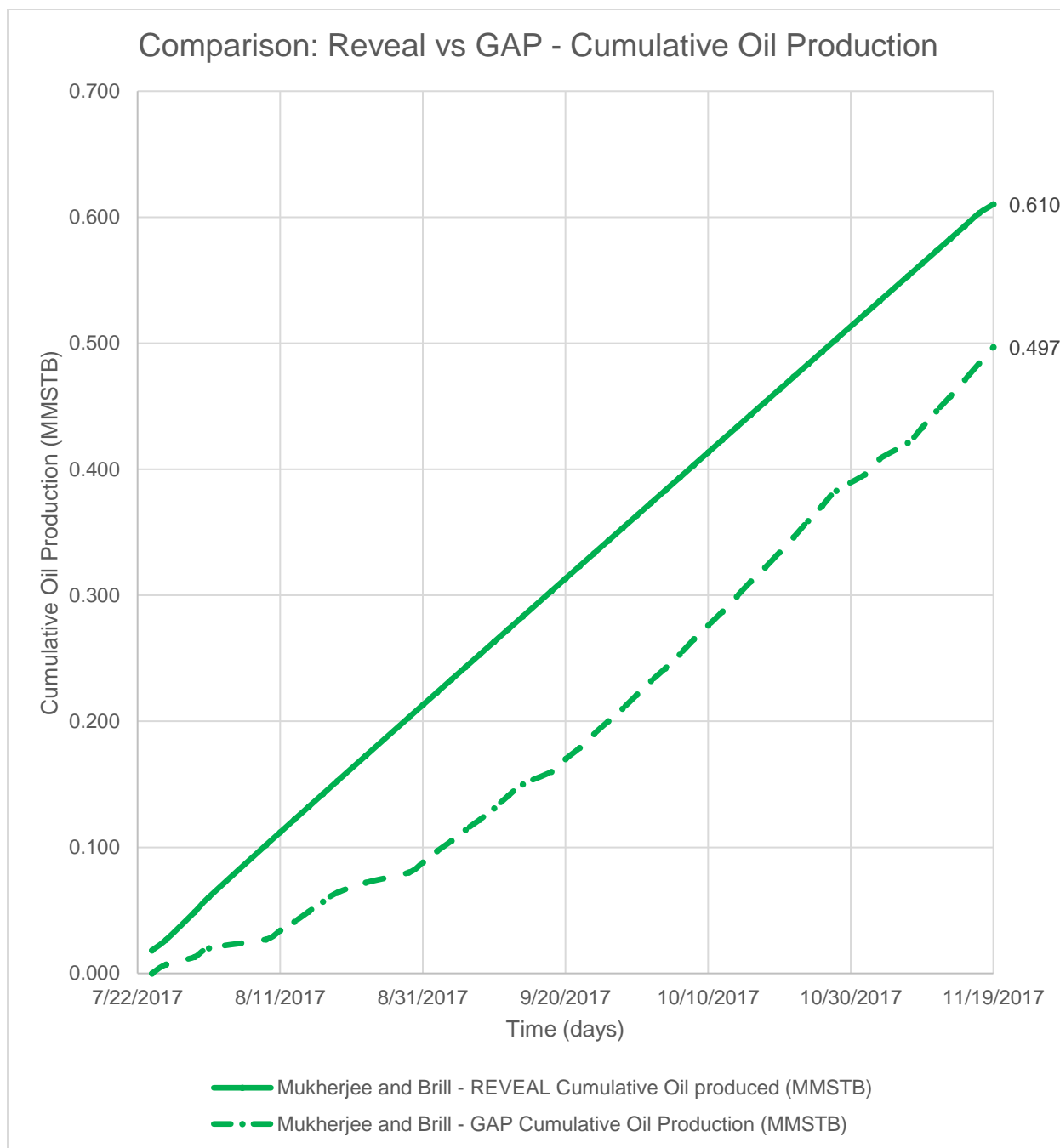


Figure 24. Cumulative Oil Production for GAP and Reveal Base Case Model (OWWO Scenario) – Mukherjee Brill Correlation

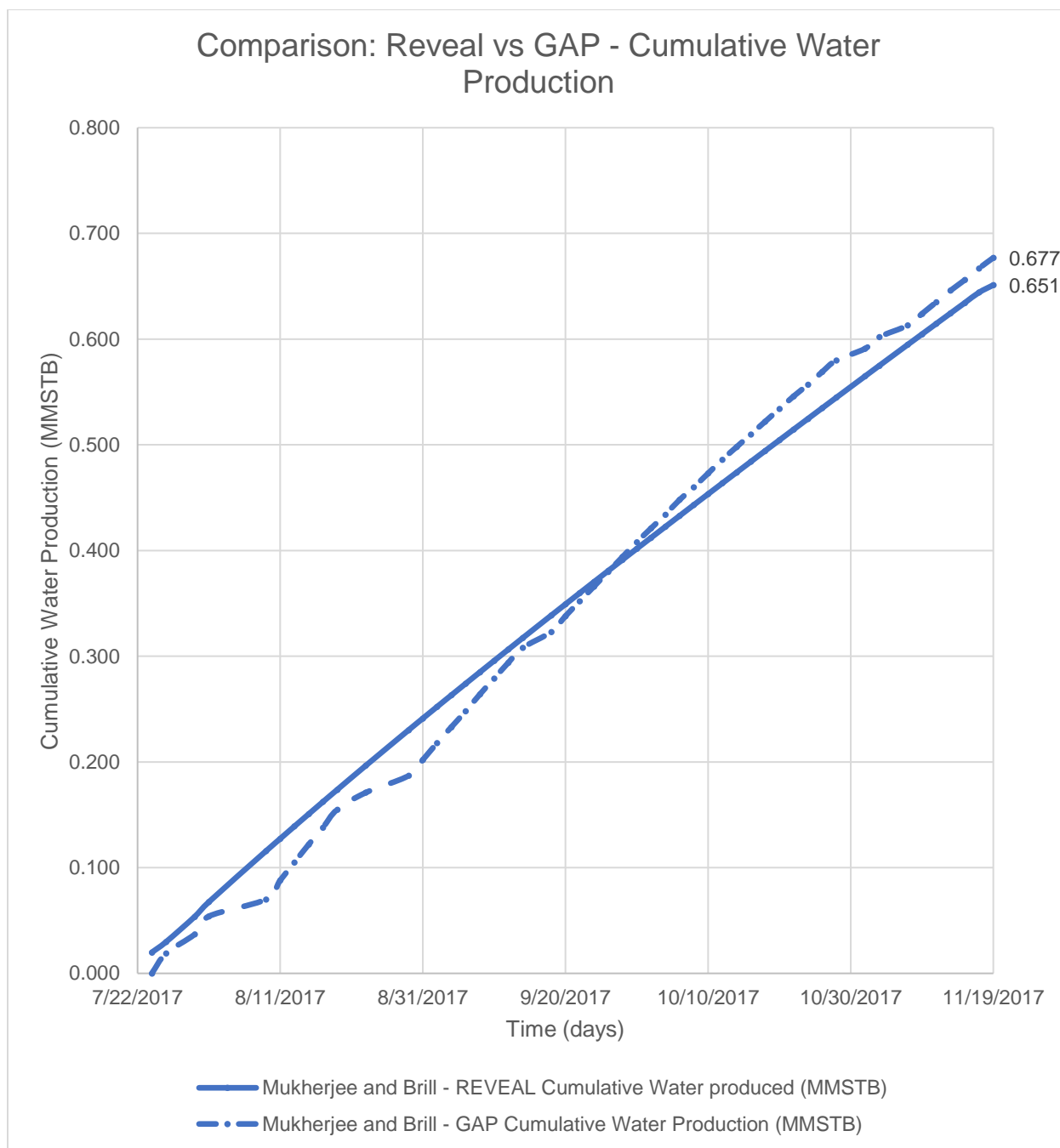


Figure 25. Cumulative Water Production for GAP and Reveal Base Case Model (OWWO Scenario) – Mukherjee Brill Correlation

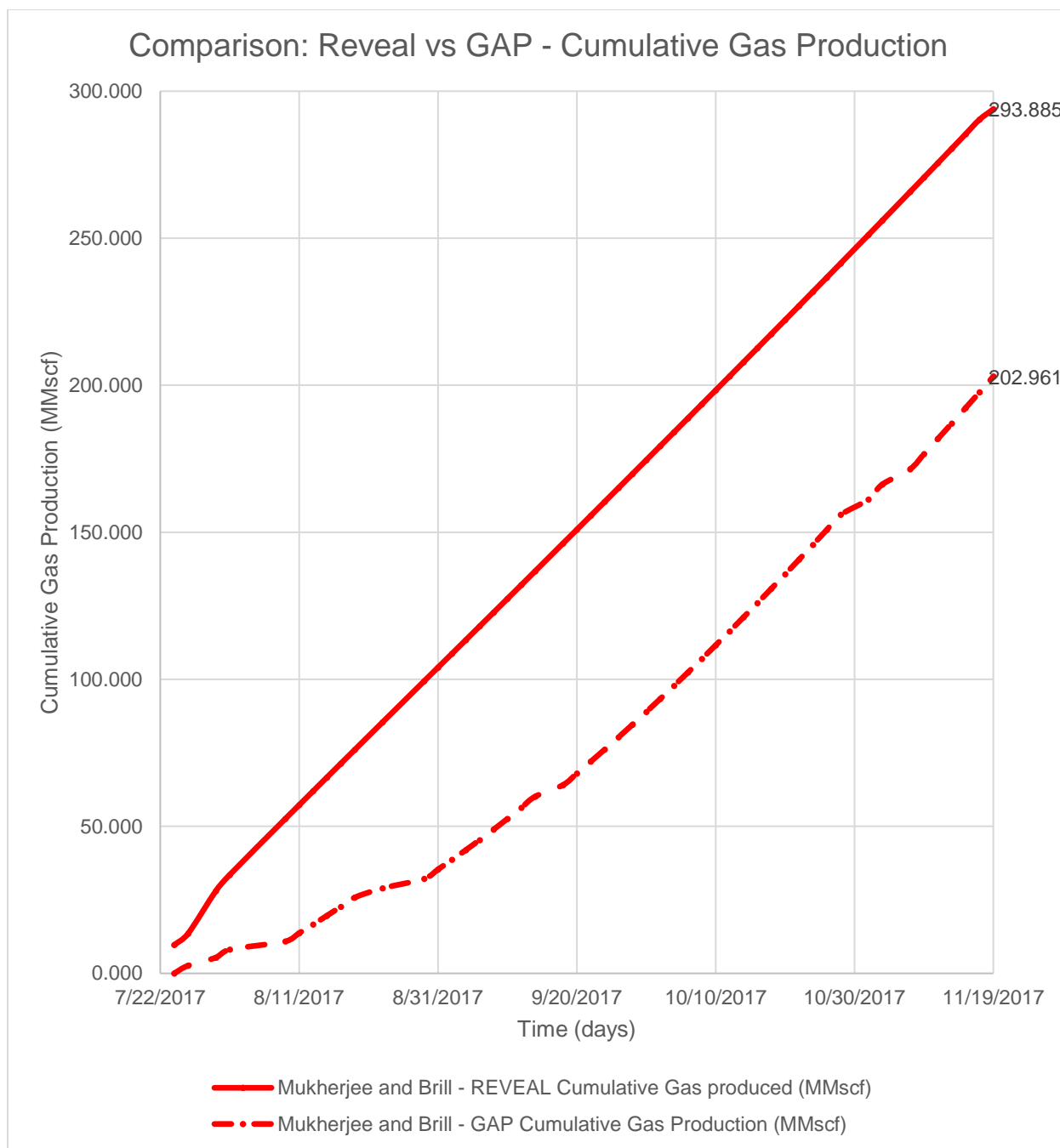


Figure 26. Cumulative Gas Production for GAP and Reveal Base Case Model (OWWO Scenario) – Mukherjee Brill Correlation

Each of the reservoirs and aquifers contributed to the WCD volumes and rates as shown in Figure 27 where all the formations show declining pressures.

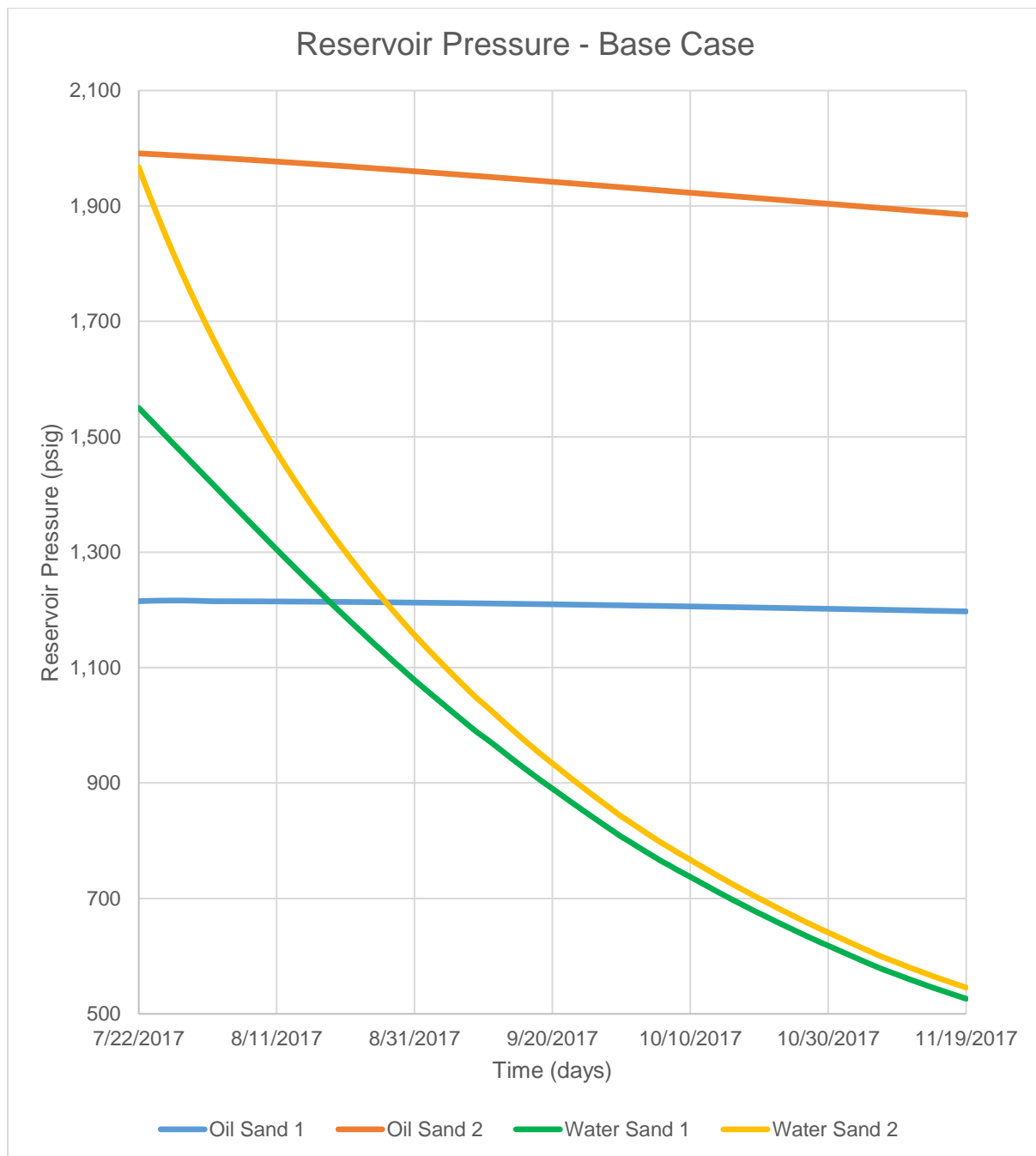


Figure 27. Reservoir pressure for base case.

6.2 Sensitivities

With the base-case model (generated from the integrated reservoir-wellbore nodal analysis workflow) validated with a reservoir simulation model, different sensitivity tests were then performed to assess their influence on WCD rates and volumes.

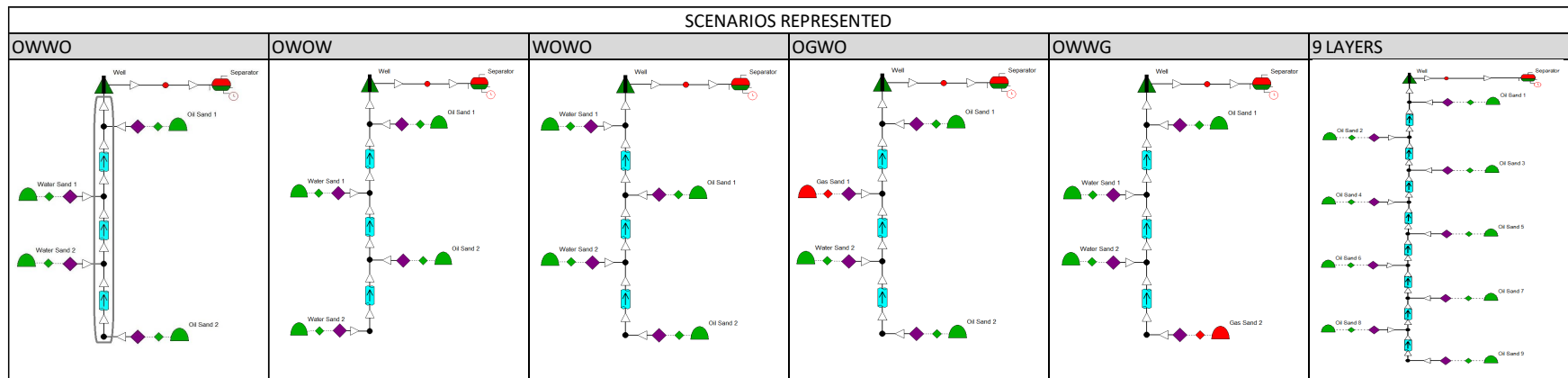
Sensitivity tests were performed on the following parameters:

- Impact of the stacking geology patterns;
- Vertical location of water sands;
- Rock compressibility;
- Well deviation.

6.2.1 Geology

Difference in stacking patterns of oil, gas and water sands may impact their flow into the wellbore and their lift to the surface, primarily as a result of differing gas-liquid ratios (GLR). Five different reservoir-aquifer stratigraphic stacking were tested other than base case model represented by OWWO – (Figure 12). The scenarios represented were water-oil-water-oil (WOWO) sands (Figure 29), oil-water-oil-water (OWOW) (Figure 28), oil-gas-water-oil (OGWO) (Figure 30), oil-water-water-gas (OWWG) (Figure 31), and a 9 layers multi-stacked system (Figure 33). All of these cases are representative of offshore Gulf of Mexico stratigraphy (Figures 7 and 8, chapter 2), and they are better describe in Table 3.

Table 3. Scenarios represented.



The geology affected the WCD volumes and rates as the GLR changed based on the fluids-in-place volumes, pressure differentials, and the number of sands open to wellbore. Comparative results between those from base case (OWWO) model, and sensitivity studies (examples, OWWG and OGWO) demonstrate that fact as shown in Figures (32, 35, 36 and 37). Table 4 shows those results.

Table 4. Comparative results between OWWO, OGWO and OWWG.

GEOLOGY SEQUENCE	VOLUMES	GAP RESULTS
OWWO	Cumulative Oil Production (MMSTB)	0.917
	Cumulative Water Production (MMSTB)	1.110
	Cumulative Gas Production (MMscf)	390.810
OGWO	Cumulative Oil Production (MMSTB)	1.145
	Cumulative Water Production (MMSTB)	0.294
	Cumulative Gas Production (MMscf)	1342.177
OWWG	Cumulative Oil Production (MMSTB)	0.159
	Cumulative Water Production (MMSTB)	0.417
	Cumulative Gas Production (MMscf)	1101.096

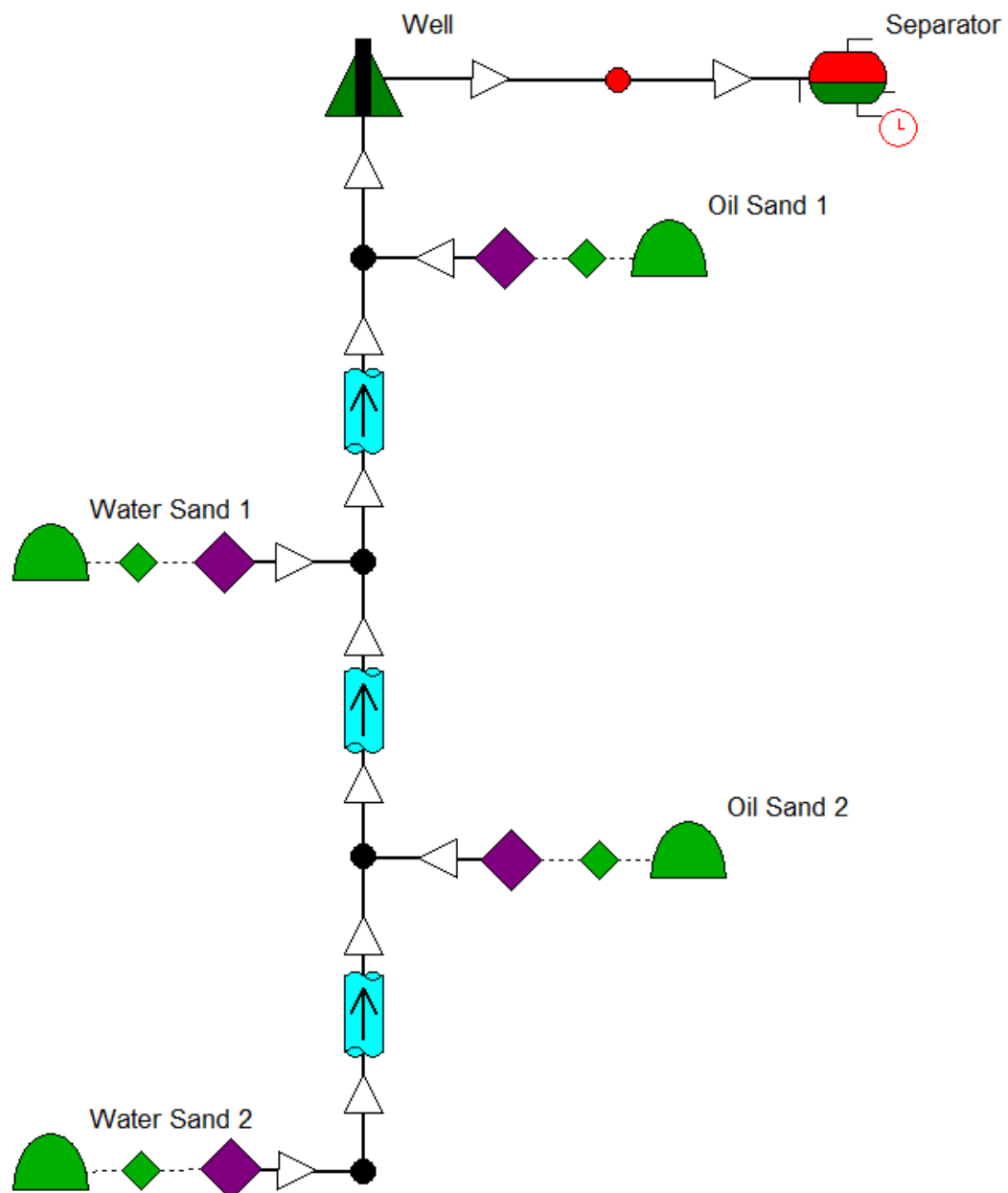


Figure 28. Oil, water, oil, water (OWOW) sands.

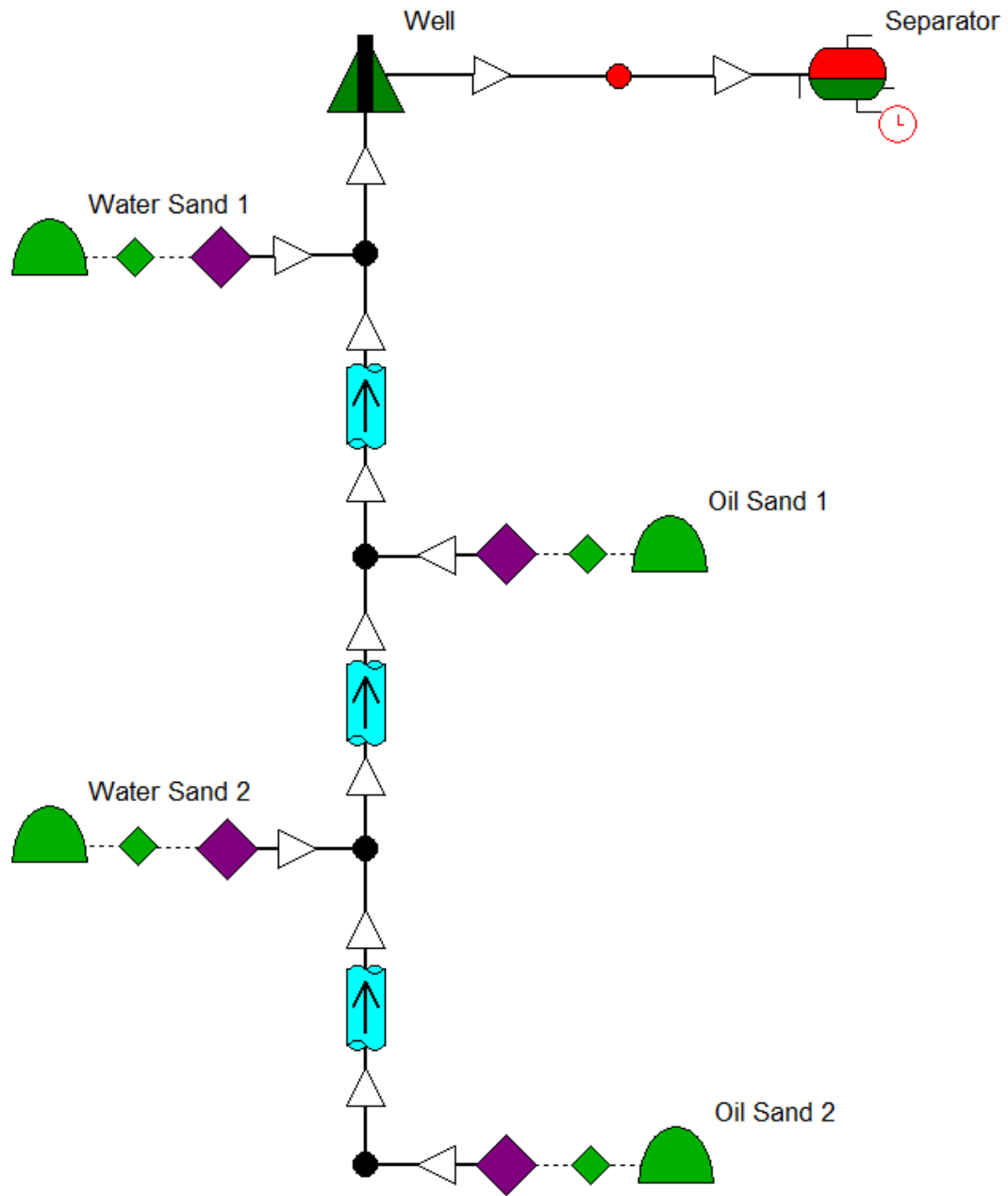


Figure 29. Water, oil, water, oil (WOWO) sands.

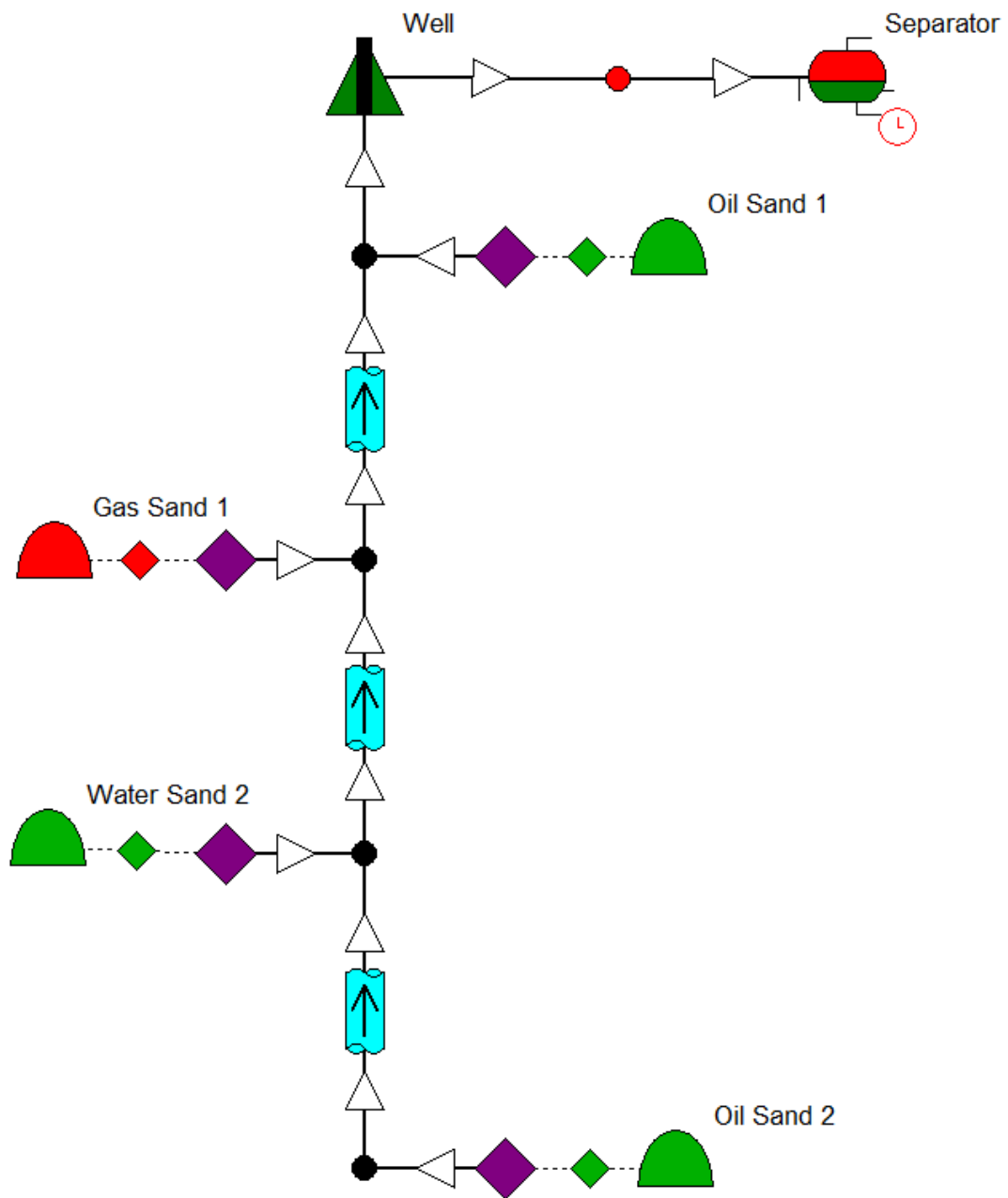


Figure 30. Oil, gas, water, oil (OGWO) sands.

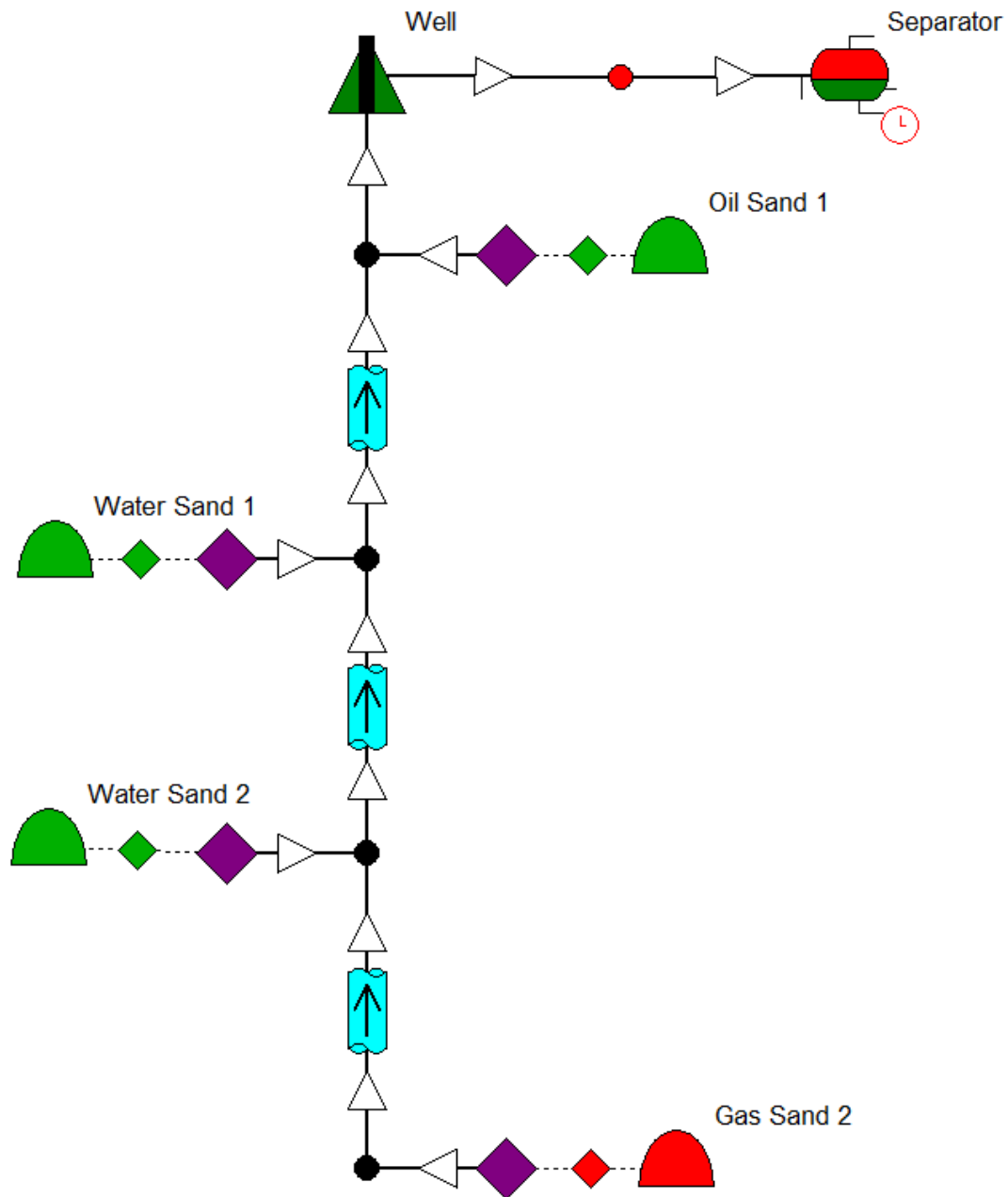


Figure 31. Oil, water, water, gas (OWWG) sands.

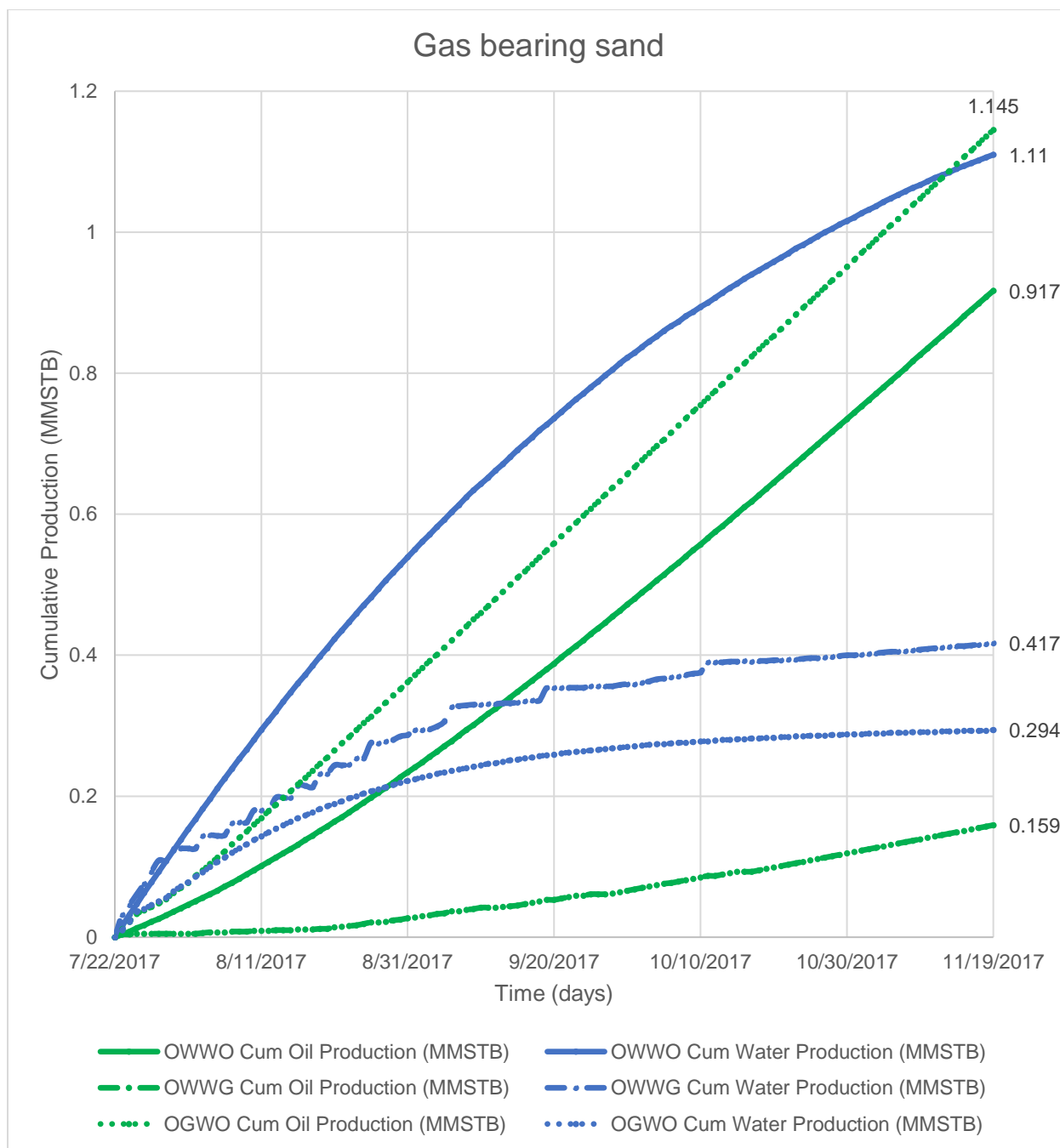


Figure 32. Water and gas bearing sand.

Comparative results from the different stratigraphic sequencing show that the WCD volumes and rates were different for the different kinds of fluids encountered in the reservoirs open to wellbore which changes the GLR and thus the WCD volumes. It was quite remarkable to note the increase in cumulative oil introduced by the gas formation due to natural gas-lift induced by the gas flowing the gas formations.

A complicated nine-sand stacking pattern was also tested to determine if the reservoir coupled nodal analysis could handle complex stratigraphy. The forecasting simulation ran without convergence error and all sands contributed to WCD volumes as shown in the individual responses from each of the reservoirs in the stratigraphic sequence (Figure 34).

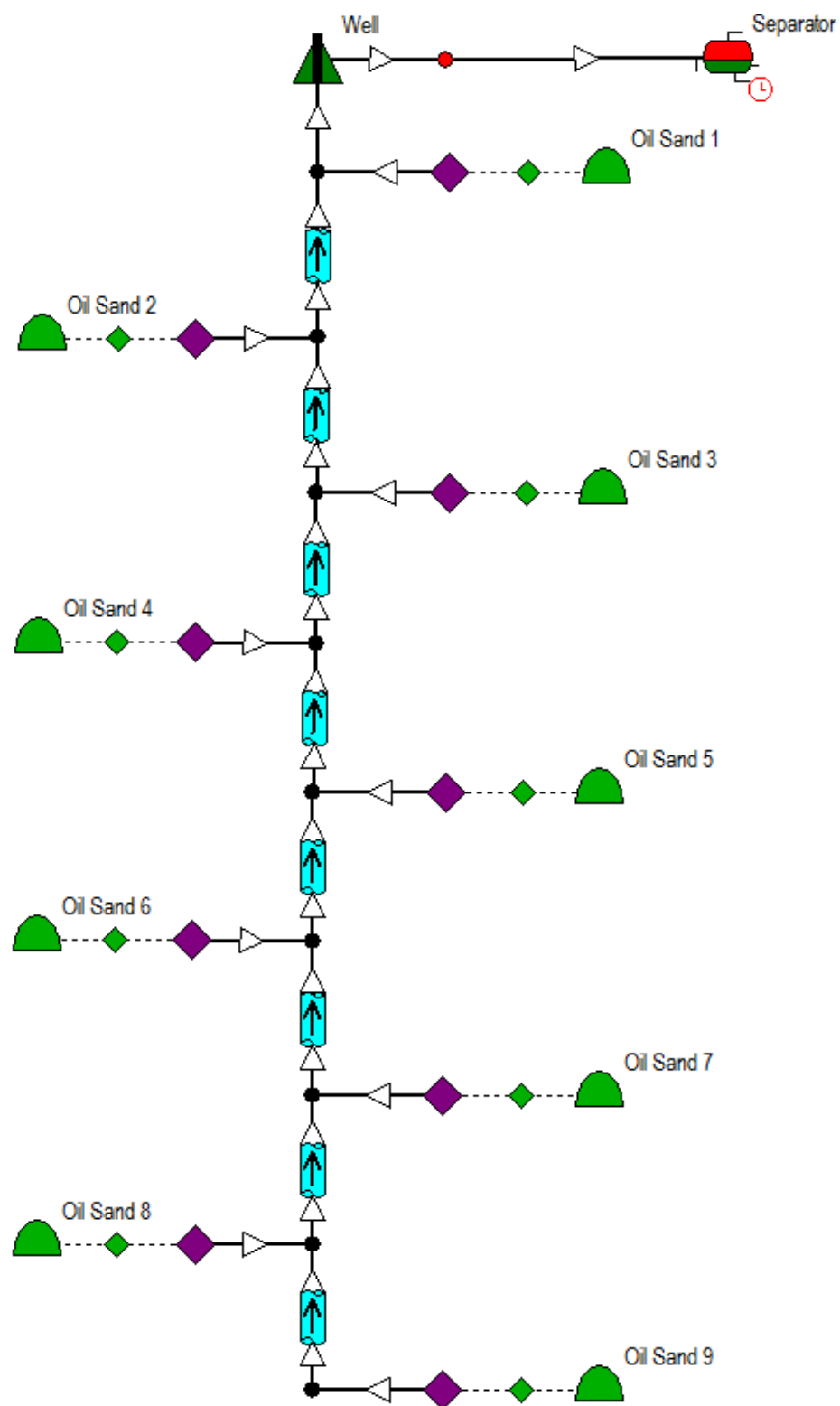


Figure 33. Nine oil layer sands.

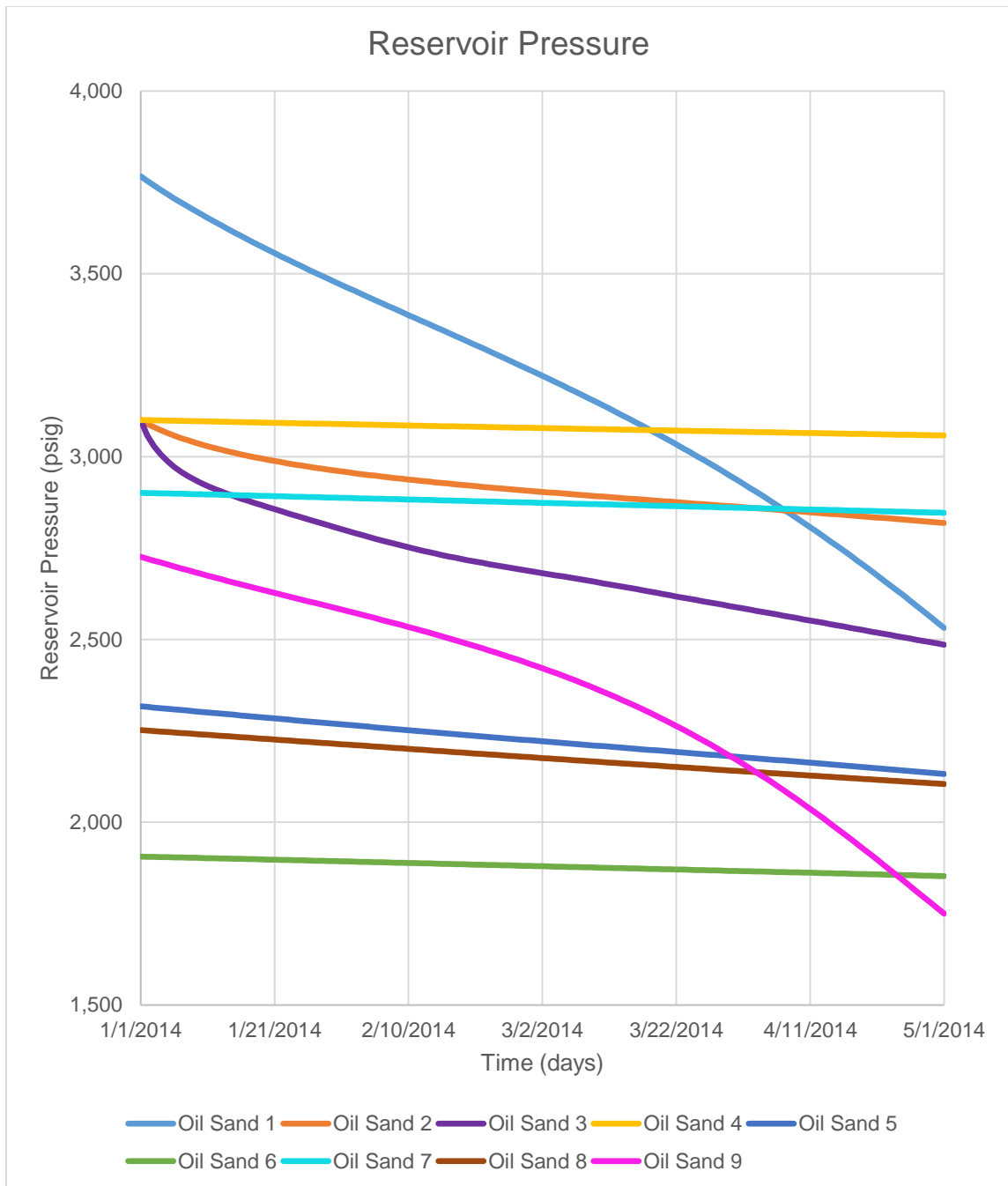


Figure 34. Reservoir pressure for nine layers case.

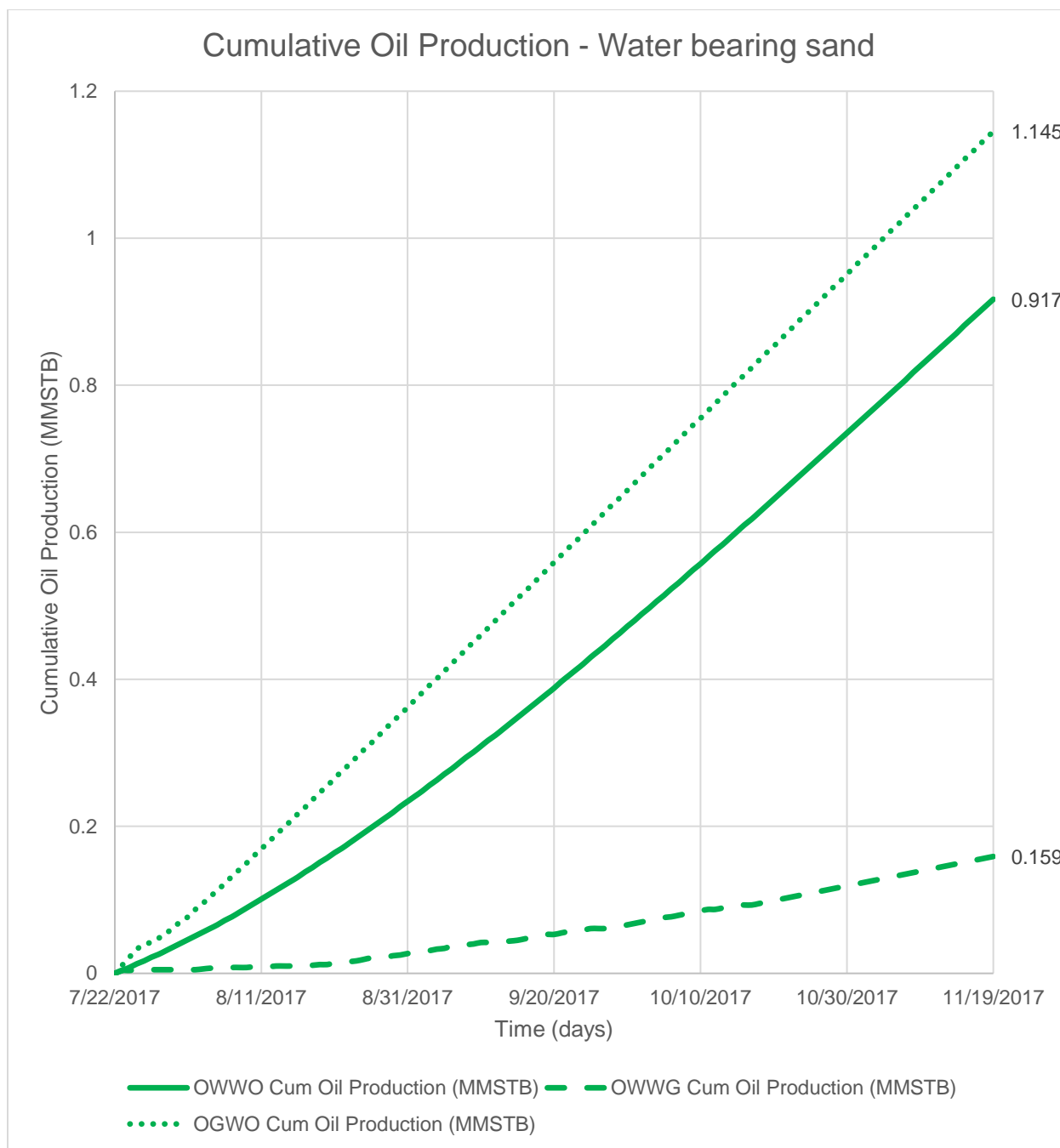


Figure 35. Comparison of cumulative oil production for different stacking patterns of oil, water and gas reservoirs.

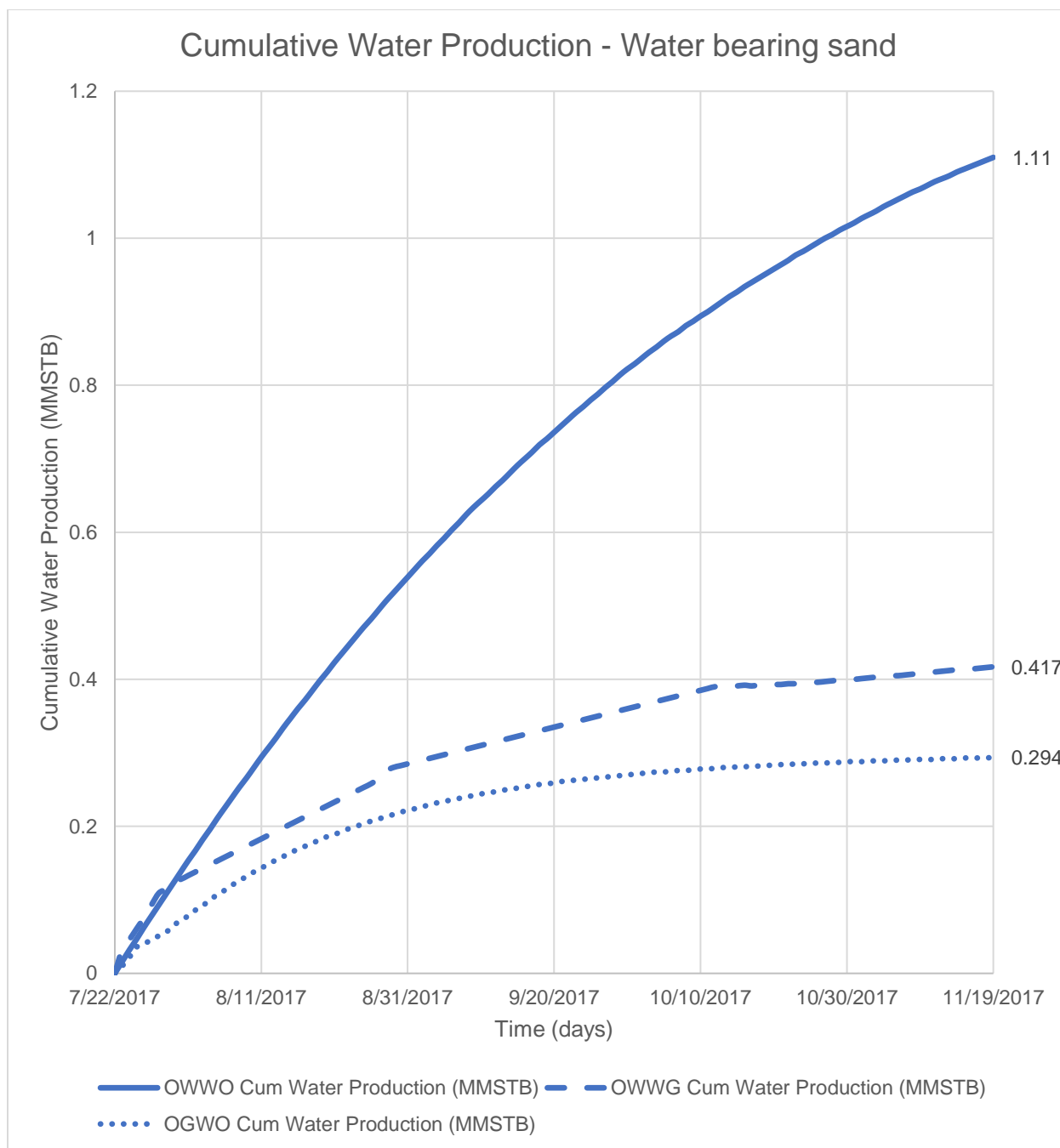


Figure 36. Comparison of cumulative water production for different stacking patterns of oil, water and gas reservoirs.

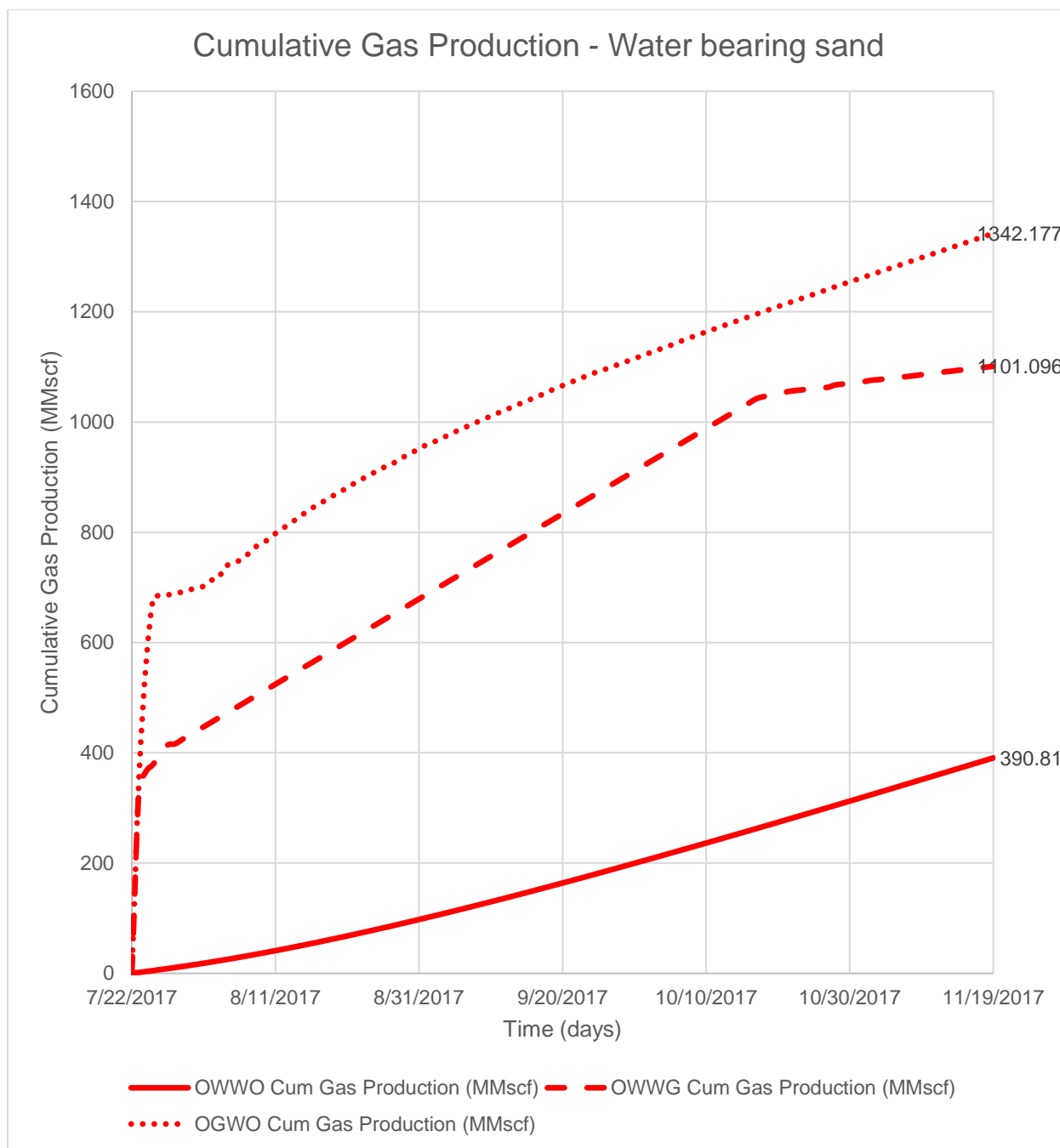


Figure 37. Comparison of cumulative gas production for different stacking patterns of oil, water and gas reservoirs.

6.2.2 Vertical location of water sands

A sensitivity test was performed on the impact of including a water sand if it lay at the bottom of the open-hole versus if it lay up-hole (Figure 28 versus Figure 29). Another was performed to assess the impact if the water sand was the first formation in the open-hole section. Results indicate that while water sands at the bottom of the open-hole section can be ignored for WCD oil volumes (8% error – Table 5), water sands at the top of the open-hole sections must be included as ignoring them resulted in nearly 99% error in WCD oil volumes.

Table 5. Errors for water sands at top and bottom of open-hole sections in variation for base-case model.

		GAP - Water at the base	GAP - Water at the base disable	ABSOLUTE % ERROR
BASE CASE - Hagedorn and Brown - Water at the base	Cumulative Oil Production (MMSTB)	0.875	0.952	8%
	Cumulative Water Production (MMSTB)	1.102	0.907	21%
	Cumulative Gas Production (MMscf)	375.332	411.839	9%
		GAP - Water at the top	GAP - Water at the top disable	ABSOLUTE % ERROR
BASE CASE - Hagedorn and Brown - Water at the top	Cumulative Oil Production (MMSTB)	2.32	1.166	99%
	Cumulative Water Production (MMSTB)	1.007	0.321	214%
	Cumulative Gas Production (MMscf)	15.622	4.042	286%

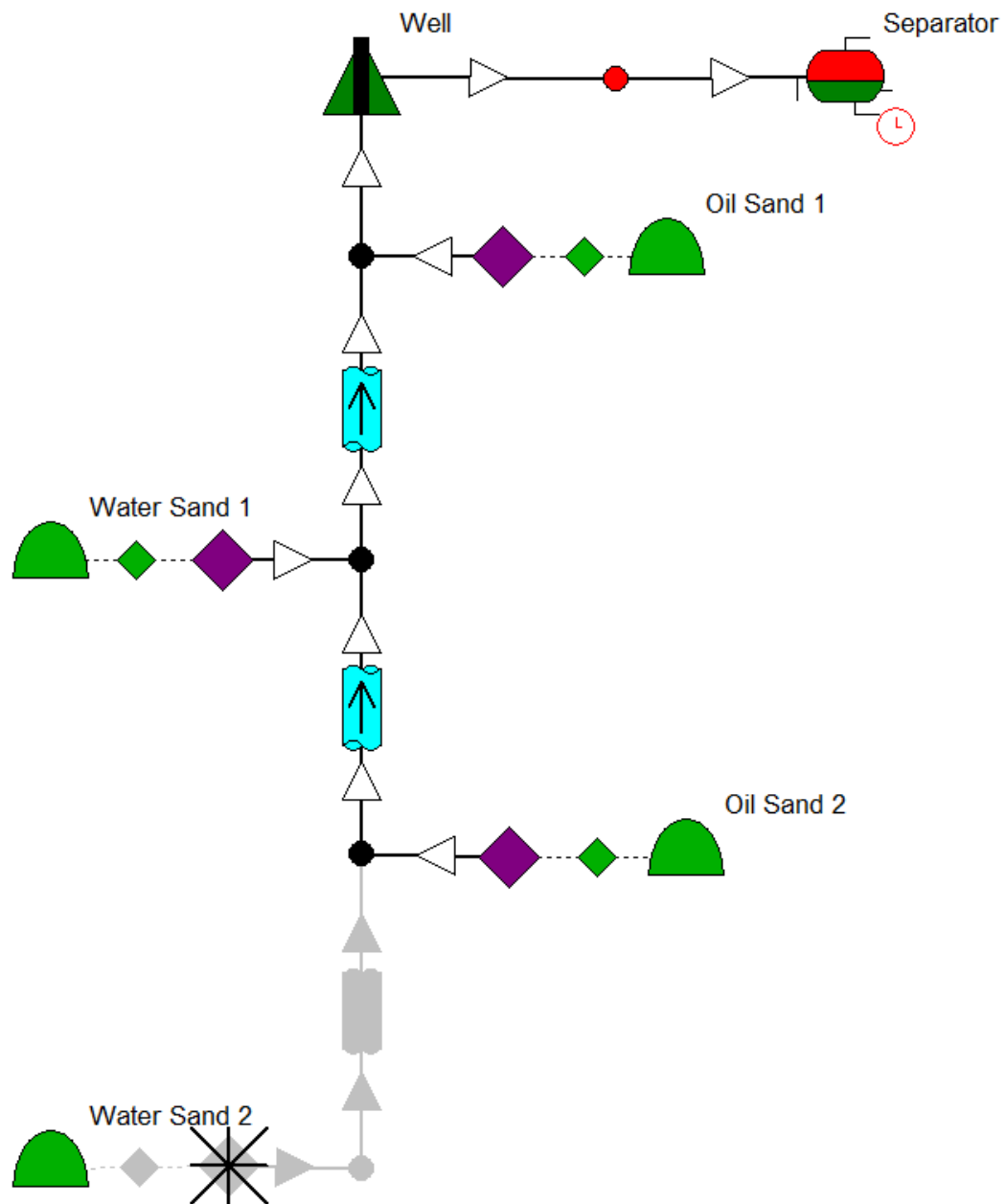


Figure 38. Oil, water, oil sands. Bottom water is disabled.

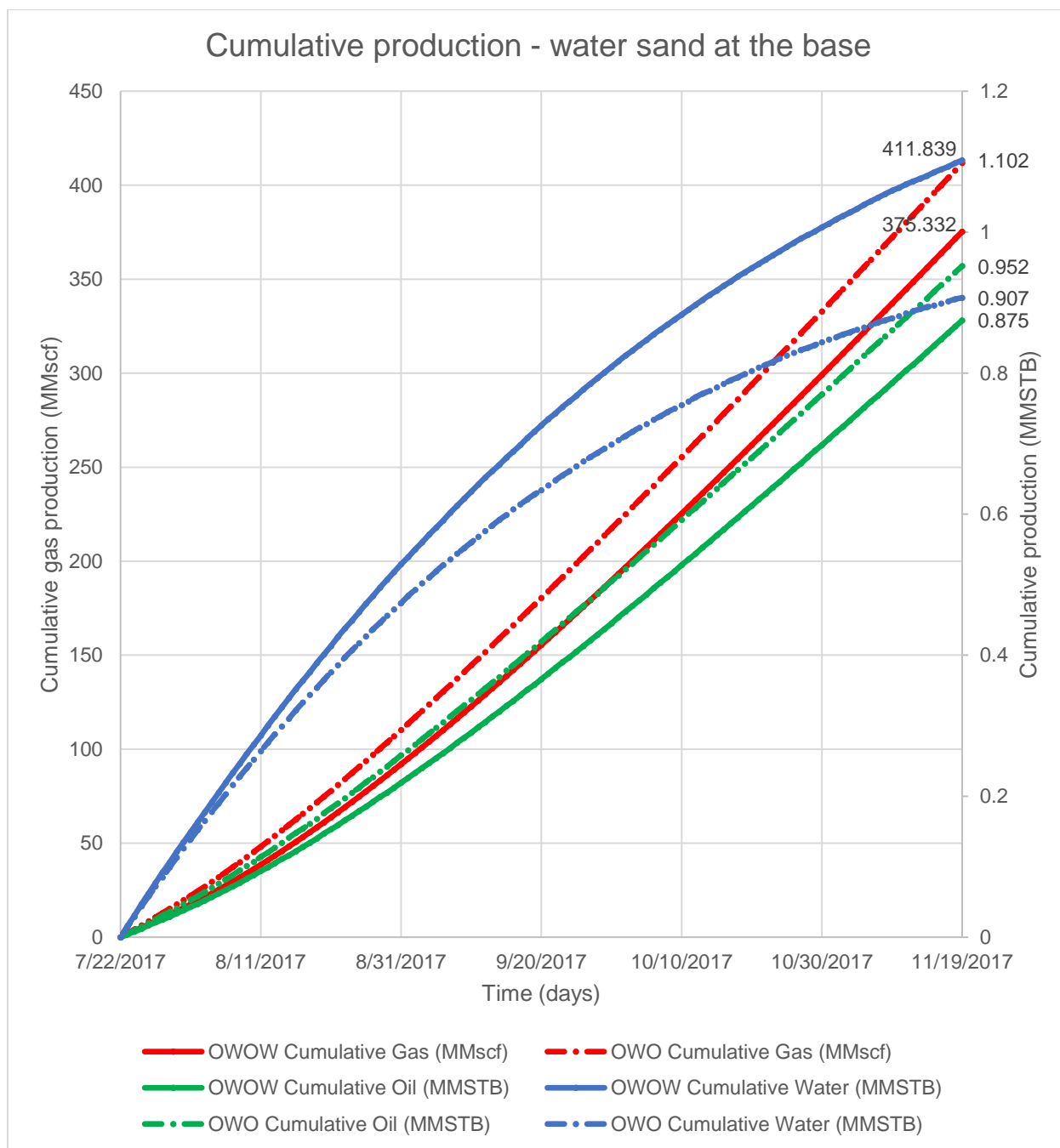


Figure 39. Scenario with water sand at the base.

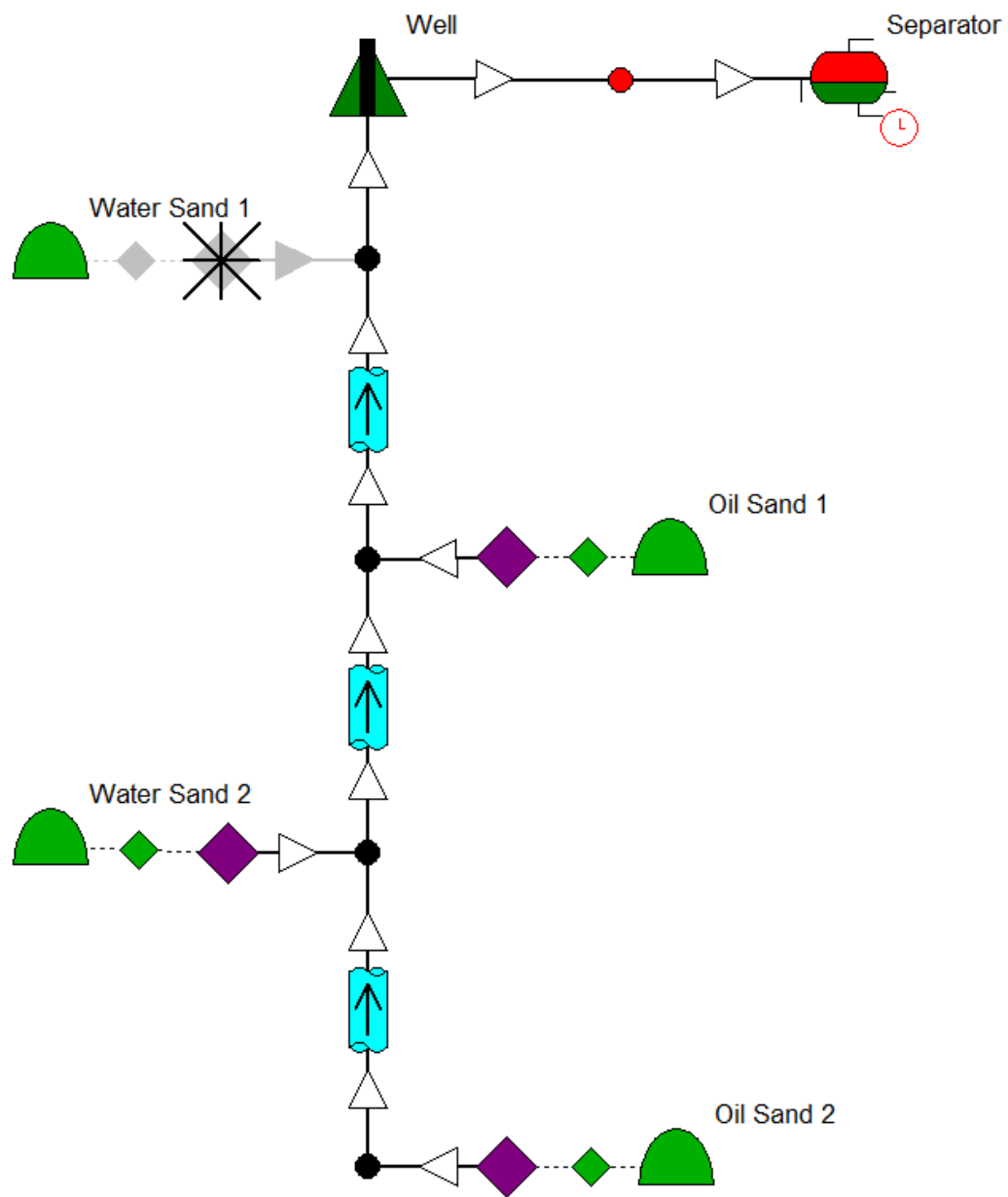


Figure 40. Oil, water, oil. Water sand at top disabled.

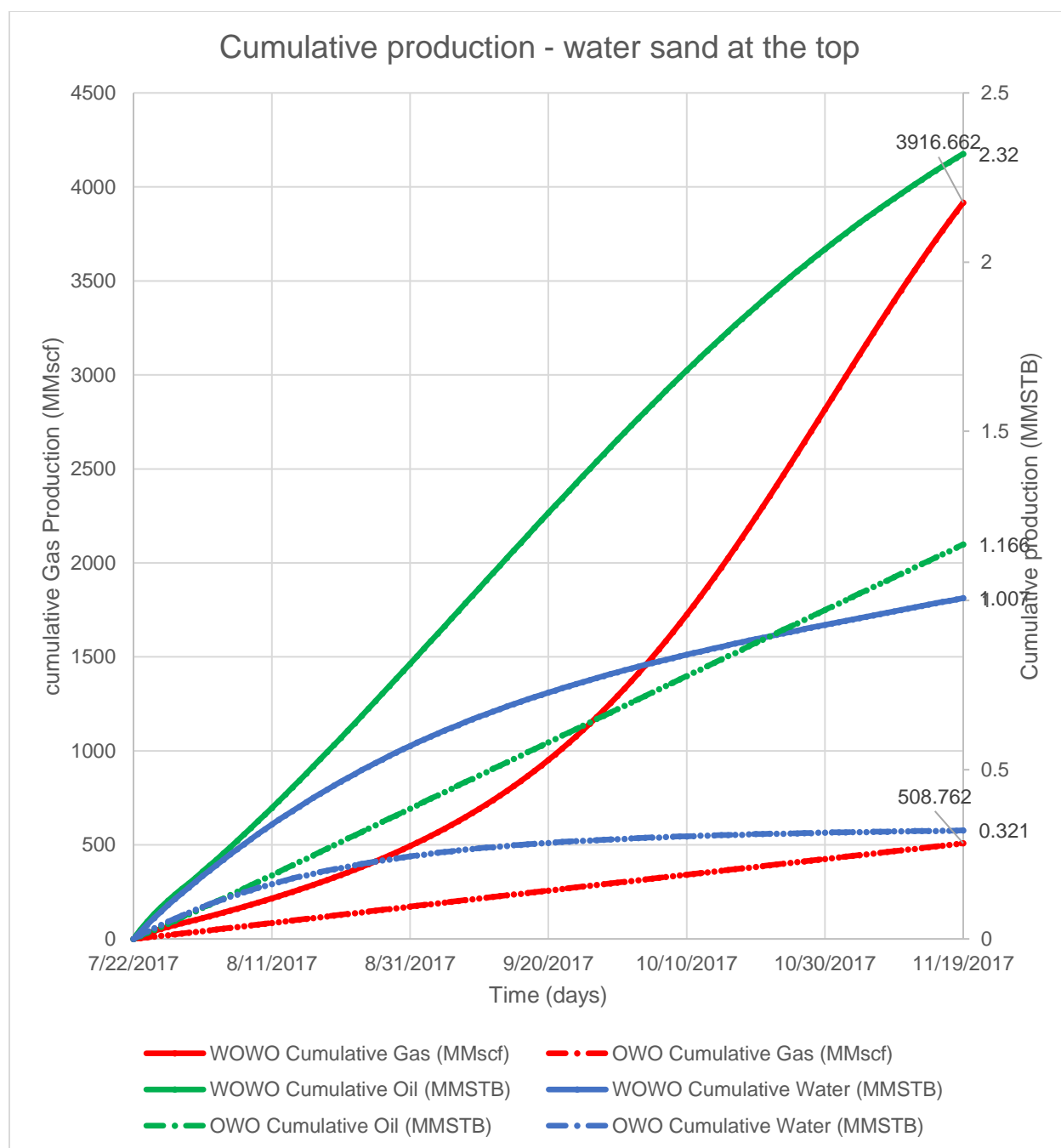


Figure 41. Scenario with water sand at the top.

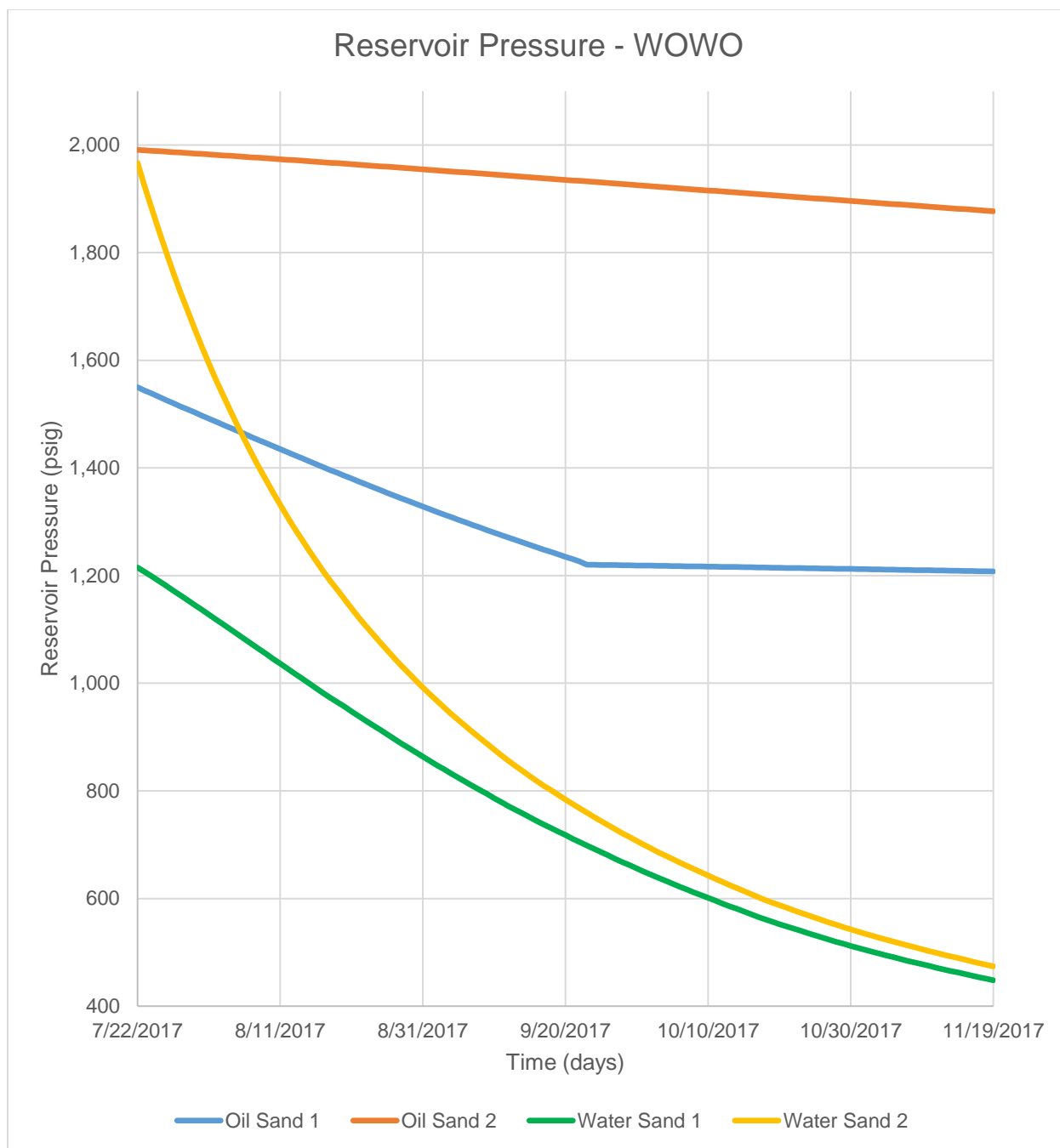


Figure 42. Reservoir pressure for scenario with water sand at the top.

The margin of error between calculations when the water sand at the top is active and when it is disabled is more than 50% (50% for oil, 87% for gas and 68% for water). This means that when a water layer is in the top of the sequence, it must be taken into account for calculations because it affects WCD calculations.

Additionally, the WCD volumes for oil and gas were determined if water sands were not included in the models. The oil and water cumulative volumes for OWWO (base case), OW-O (one of the water sands not included), and O-O (neither water sand included) were compared (Figure 38-41), and results show that for the base-case geologic sequence, inclusion of water decreased the WCD cumulative oil volume.

The best practices provided by BOEM suggest to include water sands when it is at the top of the sequence, and when it is at the base of the sequence it can be ignored. This research proved that, within the same geology sequence, the vertical location of water sands affects the WCD results.

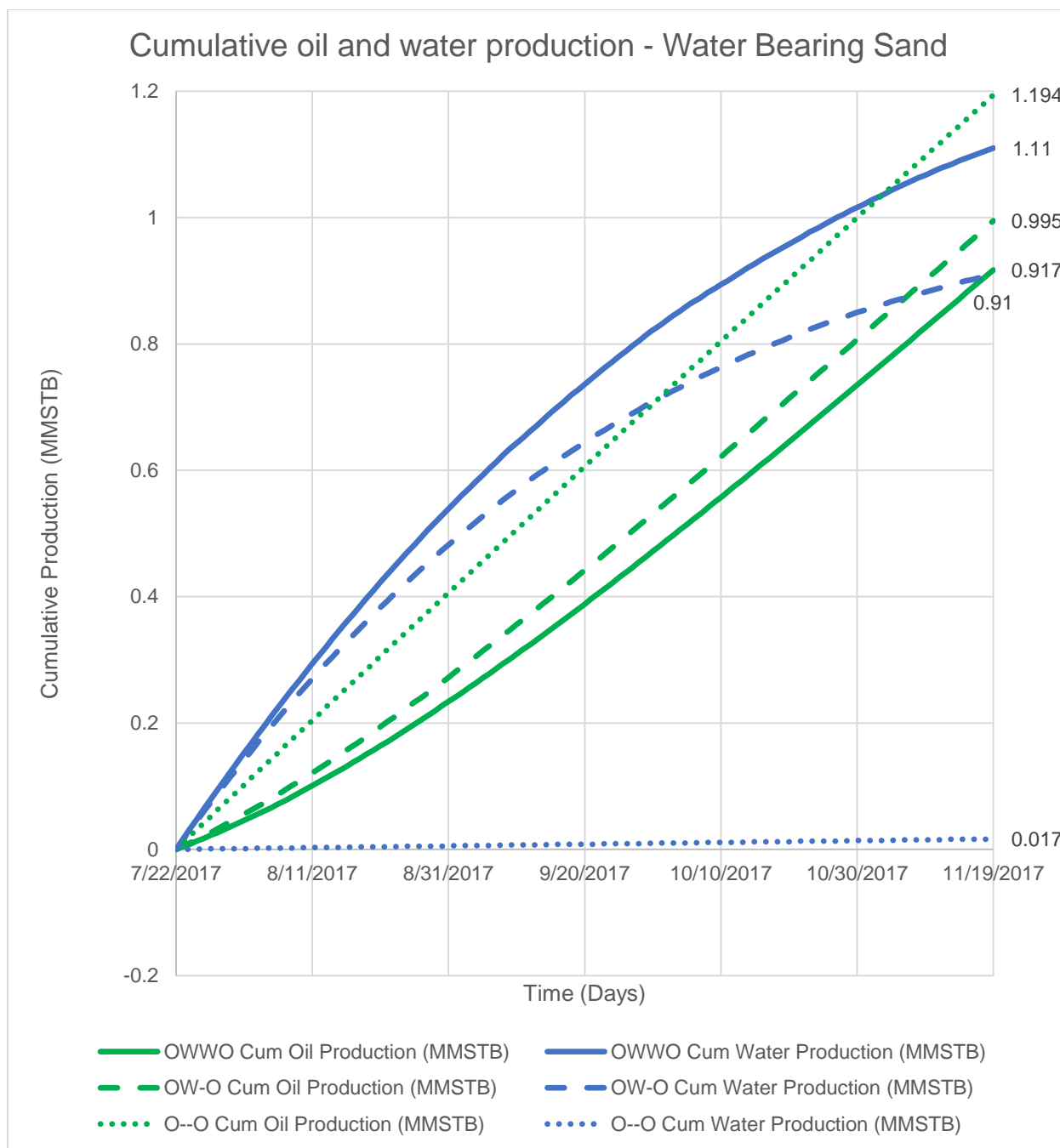


Figure 43. Cumulative oil and water production when water bearing sand (OWWO).

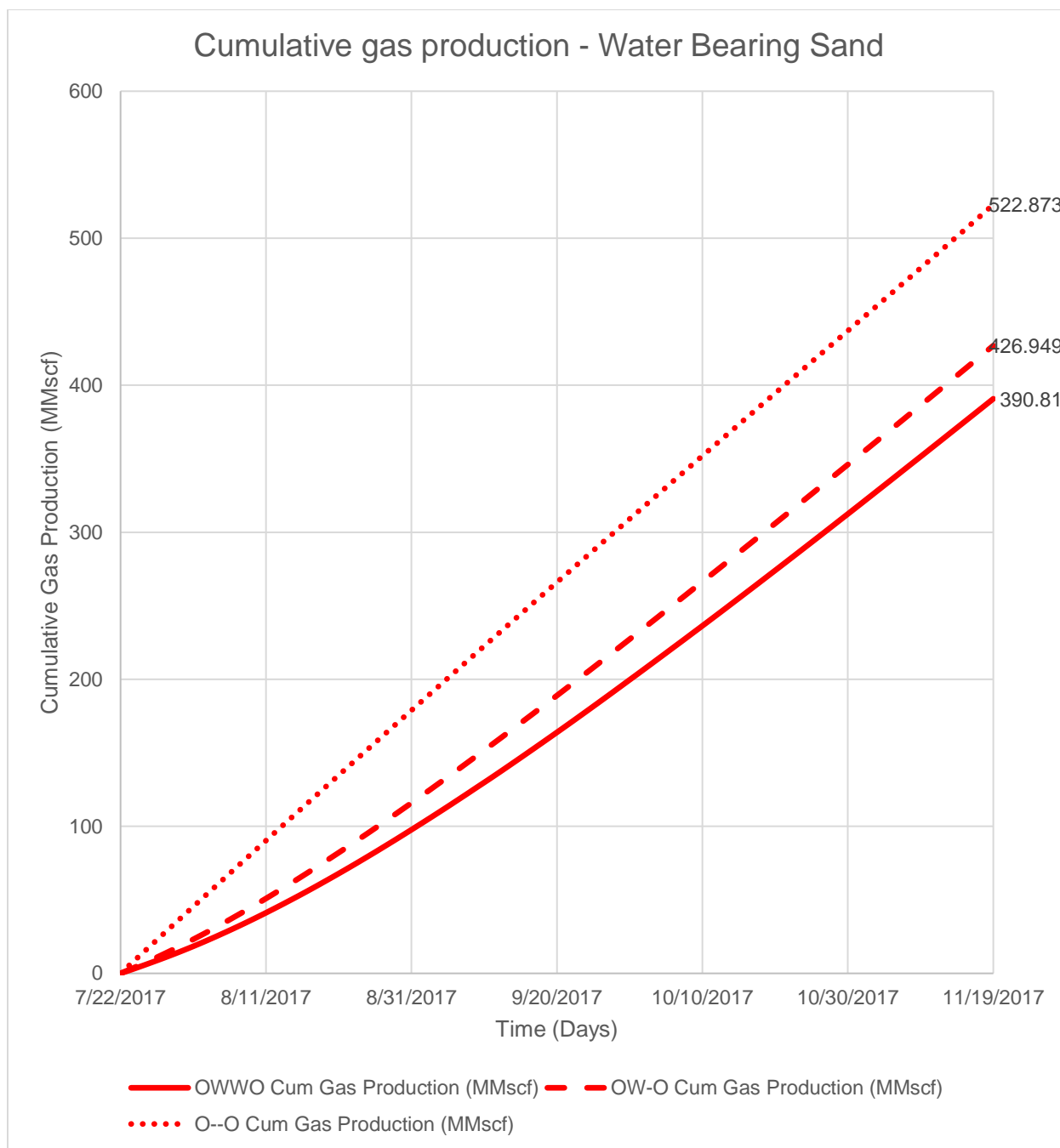


Figure 44. Cumulative gas production when water bearing sand (OWWO).

6.2.3 Rock compressibility

Higher rock compressibility should result in higher production (in this case discharge), making the WCD scenario “worse”. Given that Gulf of Mexico has over pressured, highly compressible formations, a sensitivity test was run on the impact of worst case discharge rates and volumes in a stacked sequence. Results indicate that if only oil reservoirs are considered in the modeling, then higher compressibility leads to higher cumulative WCD volumes. Range tested was from 3×10^{-7} 1/psi to 3×10^{-5} 1/psi (Figure 45).

Interestingly however, when we changed the compressibility values of all the layers in the base case model (OWWO), we observed the inverse of what would be expected, that is cumulative oil volumes were less if compressibility values were higher, and vice versa as shown in Table 4, and Figures 46 and 48. This is a curious result (Figures 46 and 48) and can only be explained by the presence of the aquifers (water sands). The water flowing into the wellbore decreases the GLR, and inhibits the oil rate and thus cumulative volume of oil in the WCD estimate. It is thus clear that in a geologic setting that has compressible sands and aquifers, different stratigraphic sequences, and volumes in place of fluids will influence the WCD volumes. Figure 45 shows the cumulative water volume to be following the natural order of high volume with high compressibility, as one would expect.

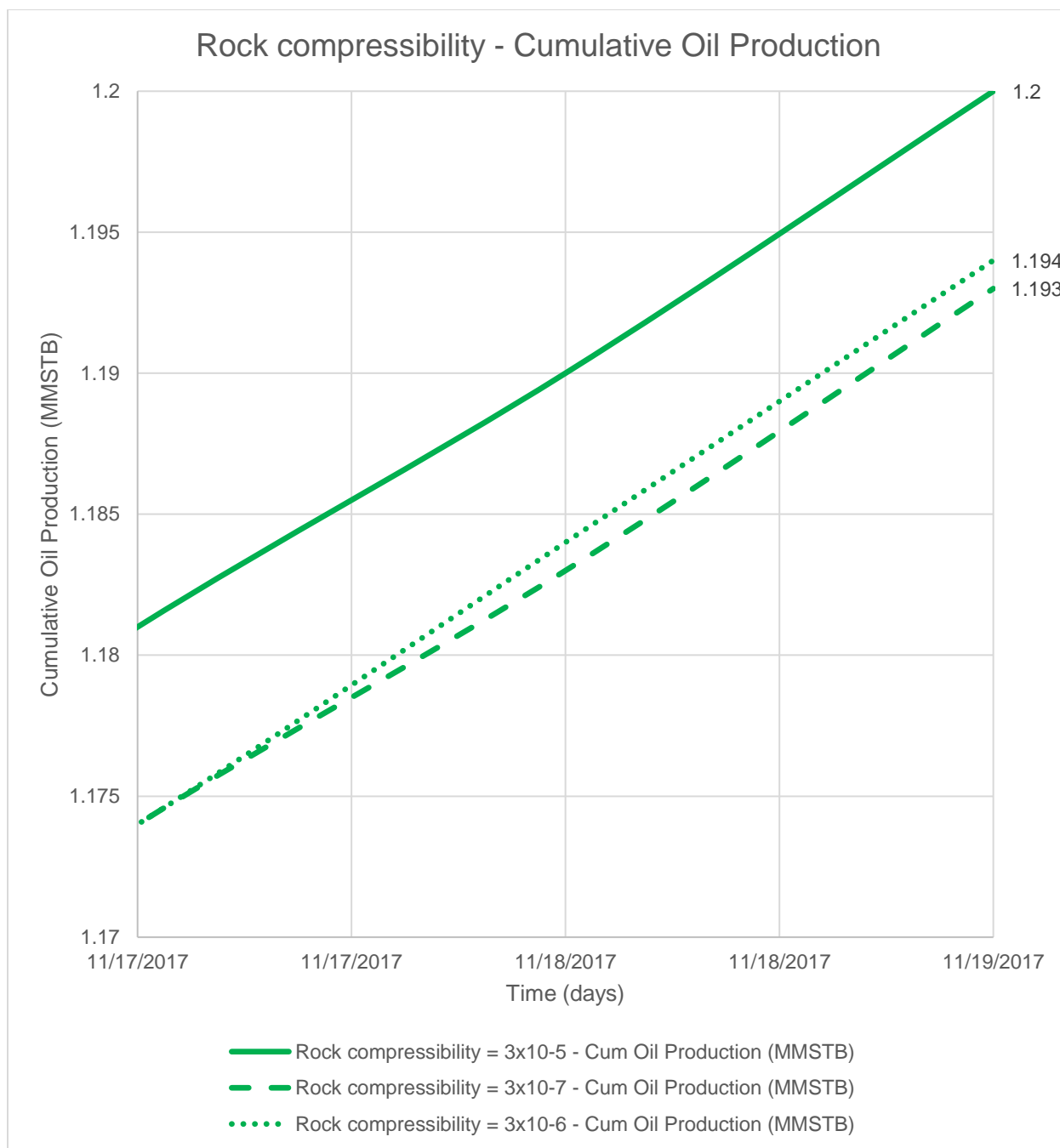


Figure 45. WCD cumulative oil volumes for different compressibility when only oil sands are considered.

Table 6. Cumulative Oil, Water and Gas Productions for Different Compressibility Scenarios.

		Rock compressibility 3x10⁻⁵ (1/psi)	Rock compressibility 3x10⁻⁶ 1/psi)	Rock compressibility 3x10⁻⁷ 1/psi)
BASE CASE - Hagedorn and Brown - Rock compressibility	Cumulative Oil Production (MMSTB)	0.599	0.927	1.04
	Cumulative Water Production (MMSTB)	1.718	1.083	0.684
	Cumulative Gas Production (MMscf)	243.115	395.272	448.446

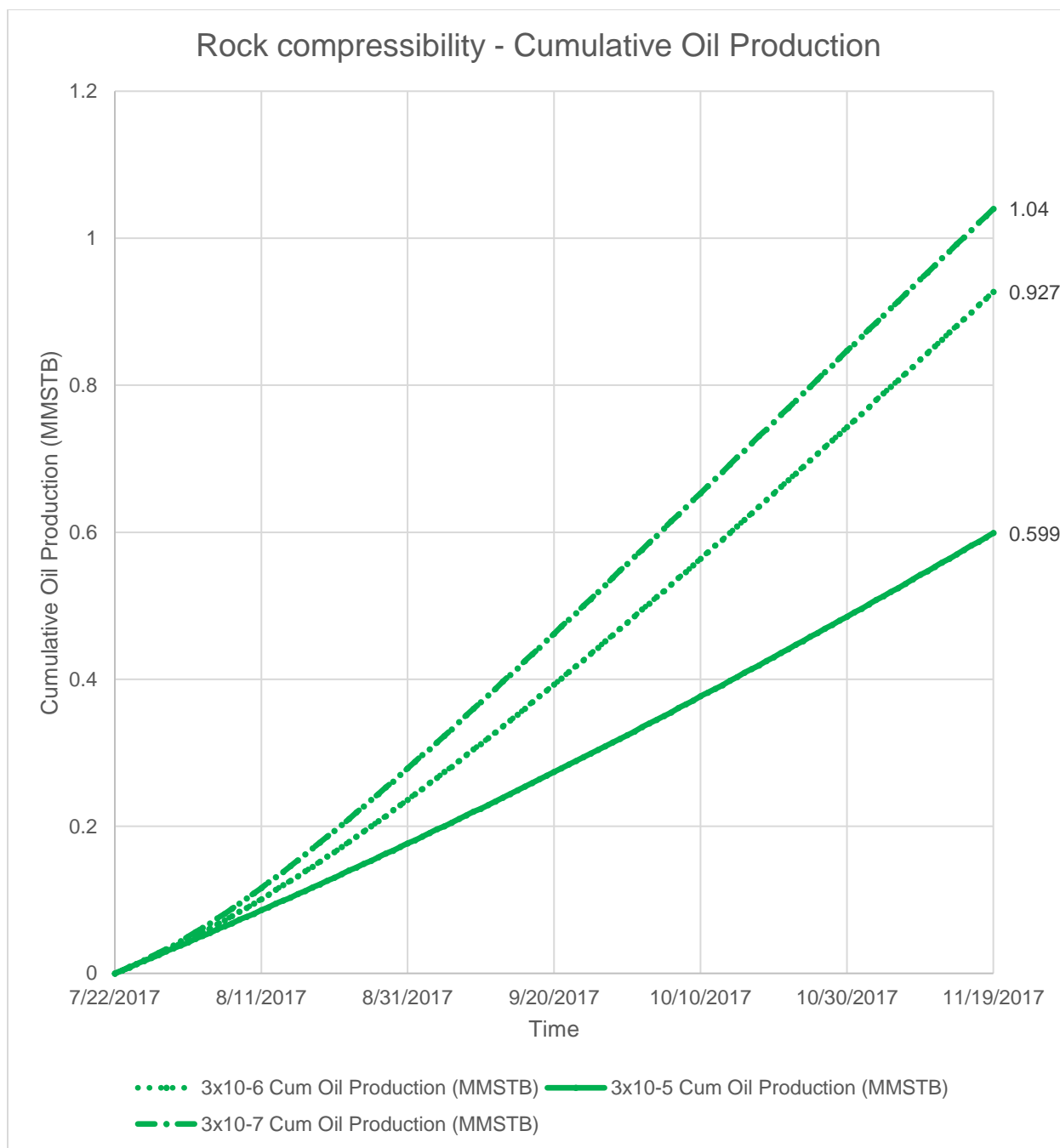


Figure 46. Cumulative oil production, rock compressibility comparison.

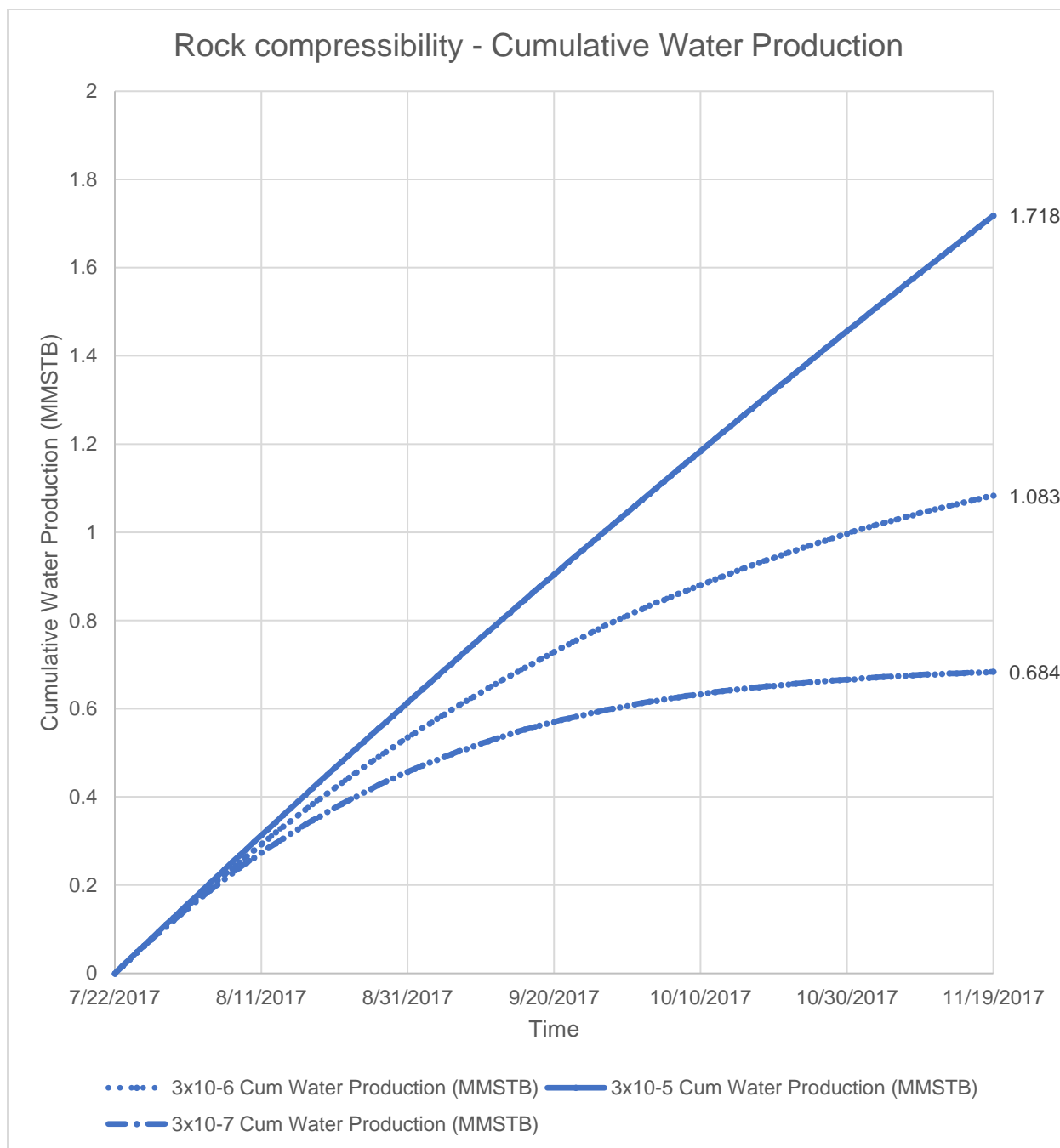


Figure 47. Cumulative water production, rock compressibility comparison.

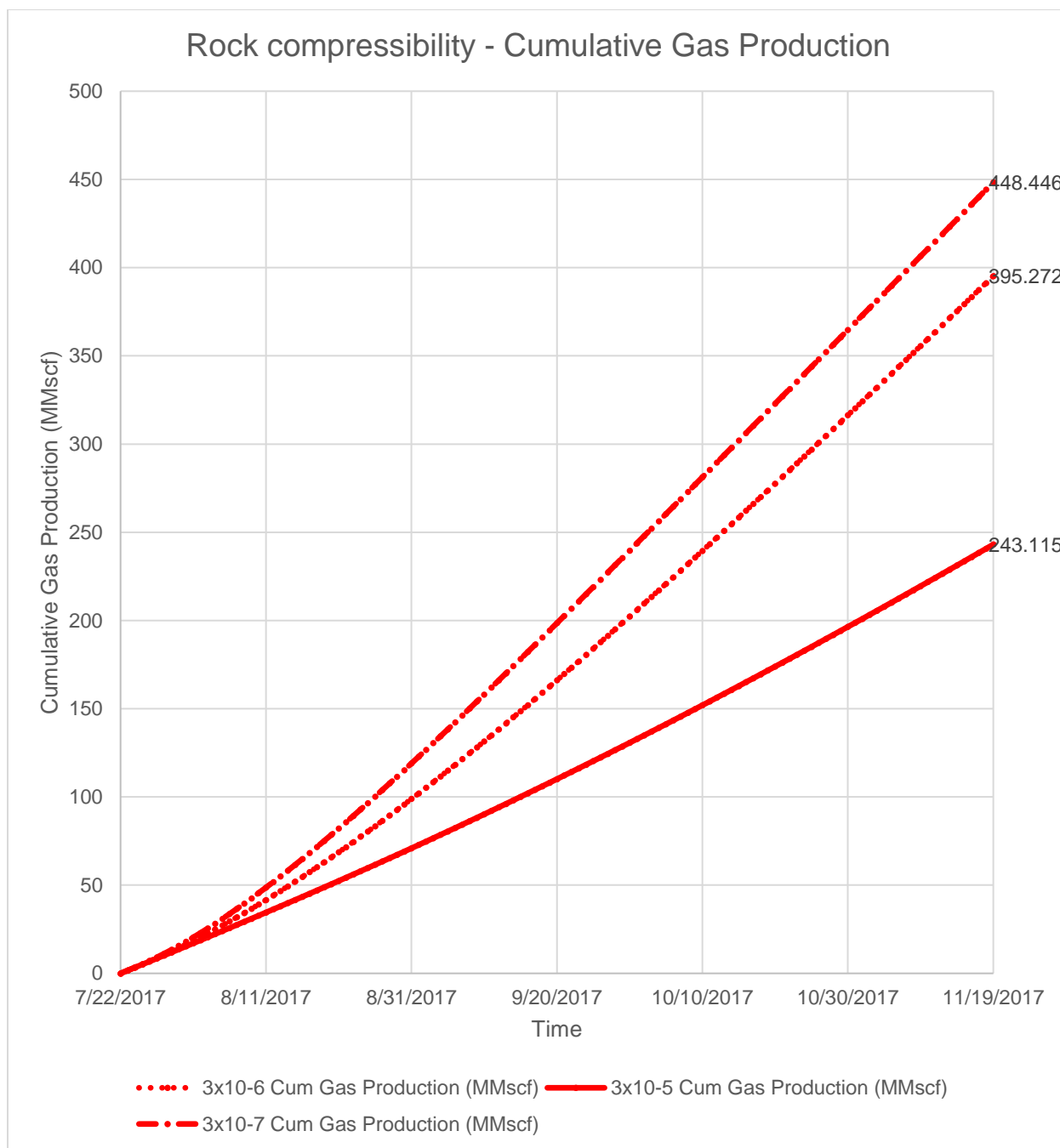


Figure 48. Cumulative gas production, rock compressibility comparison.

6.2.4 Well Deviation

The impact of a deviated well was tested and as expected, the Beggs and Brill correlation gave an improved result. This result was expected because Beggs and Brill is a flow correlation designed for inclined wells. Therefore, the difference in results (cumulative oil production) between Hagedorn Brown and Beggs and Brill in a vertical well is 0.848 MMSTB, while in a deviated well this difference reduces to 0.579 MMSTB. This is an improvement in WCD scenario, because it shows a real possible scenario with a possible correct flow correlation.

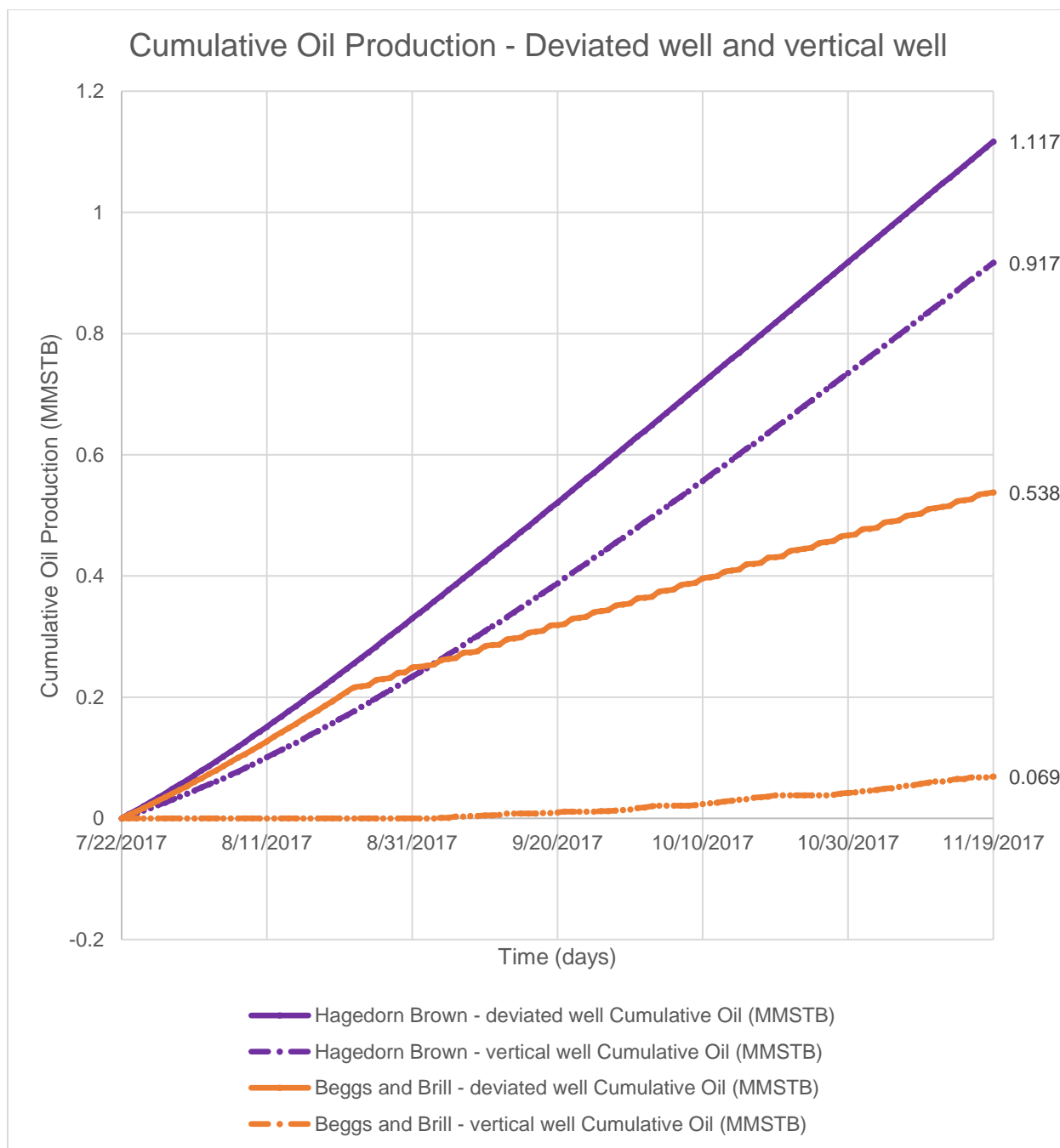


Figure 49. Cumulative oil production; comparison between deviated well and vertical well.

CHAPTER 7. CONCLUSIONS AND RECOMMENDATIONS

In this study, a new reservoir-coupled nodal analysis workflow for worst case discharge calculations is developed, then implemented in the PETEX software GAP and then tested against reservoir simulation models from REVEAL. The worst case scenario will be the one with the highest amount of oil spilled in the case of a blowout. This integrated reservoir-wellbore nodal analysis workflow can be used by operators and regulators to estimate WCD rates and volumes, and taken a step further and implemented in easier to access software like MS Excel. This is a recommended future work for this application/research.

Second, several sensitivity tests are conducted with the input parameters one of which is the geologic stacking pattern. Rarely in a production modeling scenario, are both reservoirs and non-reservoirs considered. Through this study we not only include them, but go further in changing their sequencing (as in GoM geology) to determine the impact on WCD volumes and rates for several oil, water, gas configurations. The importance of their coupling using material balance in contrast to traditional steady-state nodal analysis workflows is demonstrated through the variable output from the different scenarios modeled using the new workflow. Results show that with difference in stacking patterns, and reservoir types, WCD estimates differed. Additionally, it was observed that incorporating an aquifer (water sand) at the bottom of the stack is not relevant, but excluding a water sand at the top of the stack is inadmissible for an accurate WCD volume estimate.

Third, rock parameters such as rock compressibility affect WCD volumes – higher the compressibility, higher the WCD volumes. This, however, happened to hold true only

when considering oil formations in the WCD modeling, and ignoring the sandwiched aquifers and water sands. When the water sands were included (with high compressibility as well), then the WCD models for the base case showed an increase in oil volume with decreasing compressibility. This occurred due to the resultant decrease in GLR which reduced the lift of oil through the wellbore. Thus, we learnt that ignoring a highly compressible formation, as is common in the GoM [46], will lead to erroneous estimates of WCD, but ignoring a combination of aquifer and rock compressibility could significantly affect results.

Wellbore parameters like well-deviation were also found to affect the WCD volumes.

Future studies should include implementing the workflow developed here in easier to access software like MSExcel, and testing more parameters like rate dependent skin, and transient effects to assess their impact of WCD estimates.

REFERENCES

- [1] Ahmed, T. (2006). Reservoir engineering handbook. *Elsevier*.
- [2] Amudo, C., Walters, S., O'Reilly, D. I., Clough, M., Beinke, J. P., & Sawiris, R. S. (2011, January). Best Practices and Lessons Learned in the Construction and Maintenance of a Complex Gas Asset Integrated Production Model (IPM). *SPE Asia Pacific Oil and Gas Conference and Exhibition. Society of Petroleum Engineers*.
- [3] Baldwin, M. F. (1970). The Santa Barbara Oil Spill. *U Colo. L. Rev.* 42, pp. 33-76.
- [4] Bartlit, F. H., Grimsley, S. C. and Sambhav, S. N. (2011). Macondo: The Gulf Oil Disaster. *Chief Counsel's Report, National Commission on the BP Deepwater Horizon Oil Spill and Offshore Drilling*.
- [5] Beggs, D. H., and Brill, J. P. (1973). A Study of Two-Phase Flow in Inclined Pipes. *Journal of Petroleum technology*, 25(05), pp. 607-617.
- [6] BP. (2010). *Deepwater horizon accident investigation report*.
- [7] Brown, A. R. (2010). Interpretation of three-dimensional seismic data. Tulsa, Oklahoma. *The American Association of Petroleum Geologists and the Society of Exploration Geophysicists*, 7th edition, pp.164 and 176.
- [8] Buchholz, K., Krieger, A., Rowe, J., Etkin, D. S., McCay, D. F., Schroder Gearon, M., Grennan, M., & Turner, J. (2016). Worst Case Discharge Analysis (Volume I): Oil Spill Response Plan (OSRP) Equipment Capabilities Review, BPA No. E14PB00072. *US Department of the Interior Bureau of Safety and Environmental Enforcement (BSEE)*.
- [9] Bureau of Ocean Energy Management (BOEM), Gulf of Mexico OCS Region. (2017). Catastrophic Spill Event Analysis: High-Volume, Extended-Duration Oil Spill Resulting from Loss of Well Control on the Gulf of Mexico Outer Continental Shelf. *U.S. Department of the Interior, Bureau of Energy Management*.
- [10] Carter, R. D., and Tracy, G. W. (1960). An Improved Method for Calculating Water Influx.
- [11] Clarke, K. C., and Hemphill, J. J. (2002). The Santa Barbara oil spill: A retrospective. *Yearbook of the Association of Pacific Coast Geographers*, 64(1), pp. 157-162.
- [12] Covello, V., and Sandman, P. M. (2001). Risk communication: evolution and revolution. *Solutions to an Environment in Peril*, pp. 164-178.
- [13] Craft, B. C., Hawkins, M. F., Terry, R. E., and Rogers, J. B. (2013). Applied petroleum reservoir engineering. *Pearson Education*.
- [14] CTES, LC. (1998). Multiphase Flow Models Range of Applicability.

- [15] Doveton, J. H., and Watney, W. L. (2003). Geo-Engineering through Internet Informatics (GEMINI). *National Petroleum Technology Office, Tulsa, OK (US)*.
- [16] Duns Jr, H., and Ros, N. C. J. (1963). Vertical flow of gas and liquid mixtures in wells. *6th World Petroleum Congress*.
- [17] Economides, M. J., Hill, A. D., Ehlig-Economides, C., and Zhu, D. (2013). Petroleum Production Systems. *Prentice Hall*.
- [18] Etkin, D.S. (2001). Analysis of Oil Spill Trends in the US and Worldwide. *Proceedings of the International Oil Spill Conference*, pp. 1291-1300.
- [19] Fetkovich, M. (1973). The isochronal testing of oil wells. *Fall Meeting of the Society of Petroleum Engineers of AIME. Society of Petroleum Engineers*.
- [20] Fingas, M. (2016). Oil spill science and technology. *Gulf professional publishing*.
- [21] Forrest, J., Marcucci, E., and Scott, P. (2007). Geothermal gradients and subsurface temperatures in northern Gulf of Mexico: Search and discovery article no. 30048.
- [22] Foster, M., Charters, A. C. and Neushul, M. (1971). The Santa Barbara oil spill Part 1: Initial quantities and distribution of pollutant crude oil. *Environmental Pollution (1970) 2(2)*, pp. 97-113.
- [23] Gallice, F., and Wiggins, M. L. (1999). A comparison of two-phase inflow performance relationships. *SPE Mid-Continent Operations Symposium. Society of Petroleum Engineers*.
- [24] Galloway, W. E. (2008). Depositional evolution of the Gulf of Mexico sedimentary basin. *Sedimentary basins of the world, 5*, pp.505-549.
- [25] Grace, R. D. (1994). Advanced Blowout and Well Control. *Gulf Publishing Company*.
- [26] Guo, B., Lyons, W. and Ghalambor, A. (2007). Petroleum production engineering, a computer-assisted approach. *Gulf Professional Publishing*.
- [27] Hagedorn, A. R., and Brown, K. E. (1965). Experimental Study of Pressure Gradients Occurring During Continuous Two-Phase Flow in Small-Diameter Vertical Conduits. *Journal of Petroleum Technology 17(04)*, pp. 475-484.
- [28] Harlow, W. F., Brantley, B. C., and Harlow, R. M. (2011). BP initial image repair strategies after the Deepwater Horizon spill. *Public Relations Review, 37(1)*, pp. 80-83.
- [29] Hoffman, A. J., and Devereaux Jennings, P. (2011). The BP oil spill as a cultural anomaly? Institutional context, conflict, and change. *Journal of Management Inquiry 20(2)*, pp. 100-112.

- [30] Jaeger, C. C., Webler, T., Rosa, E. A., and Renn, O. (2013). Risk, uncertainty and rational action. *Routledge*.
- [31] Ji, Z., Johnson, W. R., Li, Z., Green, R. E., O'Reilly, S.E., and Gravois, M. P. (2012). Oil Spill Risk Analysis: Gulf of Mexico Outer Continental Shelf (OCS) Lease Sales, Central and Western Planning Areas, 2012-2017, and Gulfwide OCS Program, 2012-2051. *U.S. Department of the Interior, Bureau of Energy Management*.
- [32] Jones, L. G., Blount, E. M., and Glaze, O. H. (1976). Use of short term multiple rate flow tests to predict performance of wells having turbulence. *SPE Annual Fall Technical Conference and Exhibition. Society of Petroleum Engineers*.
- [33] Jones, P.H. (1970) Geothermal resources of the northern Gulf of Mexico basin. *Geothermics*, 2, pp. 14-26.
- [34] Klins, M. A., and Majcher, M. W. (1992). Inflow performance relationships for damaged or improved wells producing under solution-gas drive. *Journal of Petroleum Technology*, 44(12), pp.1-357.
- [35] Liu, Y., Weisberg, R. H., Hu, C., and Zheng, L. (2011). Tracking the Deepwater Horizon oil spill: A modeling perspective. *Eos, Transactions American Geophysical Union*, 92(6), pp. 45-46.
- [36] McNutt, M., Camilli, R., Guthrie, G., Hsieh, P., Labson, V., Lehr, B., Maclay, D., Ratzel, A., and Sogge, M. (2011). Assessment of flow rate estimates for the Deepwater Horizon/Macondo well oil spill. Flow rate technical group report to the National Incident Command, Interagency Solutions Group. *U.S. Department of the Interior*.
- [37] Michel, J., Owens, E. H., Zengel, S., Graham, A., Nixon, Z., Allard, T., Holton, W., Doug Reimer, P., Lamarche, A., White, M., Rutherford, N., Childs, C., Mauseth, G., Challenger, G., and Taylor, E. (2013). Extent and degree of shoreline oiling: Deepwater Horizon oil spill, Gulf of Mexico, USA. *PloS one*, 8(6), e65087.
- [38] Mukherjee, H., and Brill, J. P. (1985). Pressure drop correlations for inclined two-phase flow. *Journal of energy resources technology*, 107(4), pp. 549-554.
- [39] Mukherjee, H., and Brill, J. P. (1999). Multiphase Flow in Wells. *SPE*.
- [40] National Aeronautics and Space Administration. (2015). *Newton's First Law*. NASA website.
- [41] Orkiszewski, J. (1967). Predicting Two-Phase Pressure Drops in Vertical Pipes. *Journal of Petroleum Technology*, 19(06), pp. 829-838.
- [42] Petroleum Experts Integrated Production Modeling. (2016). Version 10.0. GAP User Manual 2016.

- [43] Petroleum Experts Integrated Production Modeling. (2016). Version 13.0. MBAL User Manual 2016.
- [44] Petroleum Experts Integrated Production Modeling. (2016). Version 14.0. PROSPER User Manual 2016.
- [45] Petroleum Experts (2008). IPM: Engineering Software Development. *Product brochure*.
- [46] Poston, S. W., and Chen, H. Y. (1989). Case history studies: abnormal pressured gas reservoirs. *SPE Production Operations Symposium. Society of Petroleum Engineers*.
- [47] Schlumberger. (1998). Schlumberger Oilfield Glossary.
- [48] Shoham, O. (2006). Mechanistic modeling of gas-liquid two-phase flow in pipes. *SPE Books*.
- [49] SPE Technical Report (2015). Calculation of Worst-Case Discharge (WCD). *Society of Petroleum Engineers*.
- [50] US Department of the Interior, Bureau of Ocean Energy Management, Regulation, and Enforcement. (2015). NTL No. 2015-N01, Information Requirements for Exploration Plans, Development and Production Plans, and Development Operations Coordination Documents on the OCS for Worst Case Discharge and Blowout Scenarios.
- [51] Vogel, J. V. (1968). Inflow performance relationships for solution-gas drive wells. *Journal of petroleum technology*, 20(01), pp.83-92.
- [52] Waltrich, P. J., Capovilla, M. S., Lee, W., Zulqarnain, M., Hughes, R., Tyagi, M., Williams, W. et al. (2017). Experimental Evaluation of Wellbore Flow Models Applied to Worst-Case-Discharge Calculations. *SPE Health, Safety, Security, Environment, & Social Responsibility Conference-North America*. Society of Petroleum Engineers.
- [53] Wiggins, M. L., Russell, J. E., and Jennings, J. W. (1996). Analytical development of vogel-type inflow performance relationships. *SPE Journal*, 1(04), pp.355-362.
- [54] Wilhelm, O., and Ewing, M. (1972). Geology and history of the Gulf of Mexico. *Geological Society of America Bulletin*, 83(3), pp.575-600.

APPENDIX A. ROCK COMPRESSIBILITY AND AQUIFER INFLUX

The method used for analyzing and predicting reservoir behavior in this research is material balance, which is based on the principle of mass conservation. Although the material balance equation is zero dimensional, this approach is very useful in many tasks, such as quantifying different parameters of a reservoir, determining the presence of an aquifer, estimating the depth of the gas/oil, water/oil, gas/water contacts [43].

As explained in the purpose of this thesis, a central goal is to perform sensitivity studies on the effect of rock compressibility and aquifer presence on inflow-performance and WCD rates. So, it is important to clarify those terms in this paper.

According to Geertsma (1957), it is important to distinguish between three types of compressibility in rocks: rock-matrix compressibility, rock-bulk compressibility and pore compressibility. However, the rock and bulk compressibility can be neglected since they are too small in contrast with pore compressibility. Therefore, commonly pore compressibility represents the formation compressibility (c_f), and it describes the total compressibility of the formation [1].

$$c_f = c_p = \frac{1}{\phi} \frac{\partial \phi}{\partial p} = \frac{-1}{V_p} \frac{dV_p}{dp}$$

For further understanding, rock compressibility is going to be considered as formation compressibility, which was defined above.

Aquifers are water-bearing rocks that bound all the peripheries of many reservoirs or just a portion of them [13]. Sometimes, aquifers can be neglected because its pore volume is insufficient compared with the pore volume of the petroleum reservoir, or because of the low aquifer permeability would require a very large pressure differential

that doesn't actually occur. However, some aquifers are huge enough and the rock permeability is sufficient that water encroachment occurs [1].

In MBAL software, it is possible to choose between different mathematical water influx models; some of them are: pot aquifer, Schilthuis' steady-state, Hurst steady state, Hurst-Van Everdingen, Fetkovich's method, Carter-Tracy [30]. In this paper, the matter is focused in one aquifer model:

- Carter-Tracy

The main difference between Carter-Tracy and the Hurst-Van Everdingen is that this last one delivers the exact solutions to the diffusivity equation using the principle of superposition, which involves tedious calculations, while Carter-Tracy model assumes constant water influx rates during finite time interval and it does not require superposition [10].

Mathematically, the water influx equation is:

$$W_e(t_{Dj}) = W_e(t_{Di}) + \sum_{n=i}^{j-1} a_n(t_{D_{n+1}} - t_{Dn}) \quad (1)$$

Where $i = j - 1$.

Assuming that water influx is approximated by series of constant rates intervals:

$$a_{j-1} = \frac{B_1 \Delta P(t_{Dj}) - W_e(t_{D_{j-1}}) P'(t_{Dj})}{P(t_{Dj}) - t_{D_{j-1}} P'(t_{Dj})} \quad (2)$$

Substituting Eq. (2) into Eq. (1), and letting $i = j - 1$,

$$W_e(t_{Dj}) = W_e(t_{D_{j-1}}) + \left[\frac{B_1 \Delta P(t_{Dj}) - W_e(t_{D_{j-1}}) P'(t_{Dj})}{P(t_{Dj}) - t_{D_{j-1}} P'(t_{Dj})} \right] * (t_{Dj} - t_{D_{j-1}}) \quad (3)$$

Where $B_1 = 1.119 \phi_a c_t r_e^2 h f$

$$f = \frac{\theta}{360}$$

$$t_D = 6.328 * 10^{-3} \frac{k_a t}{\varphi \mu_w c_t r_e^2}$$

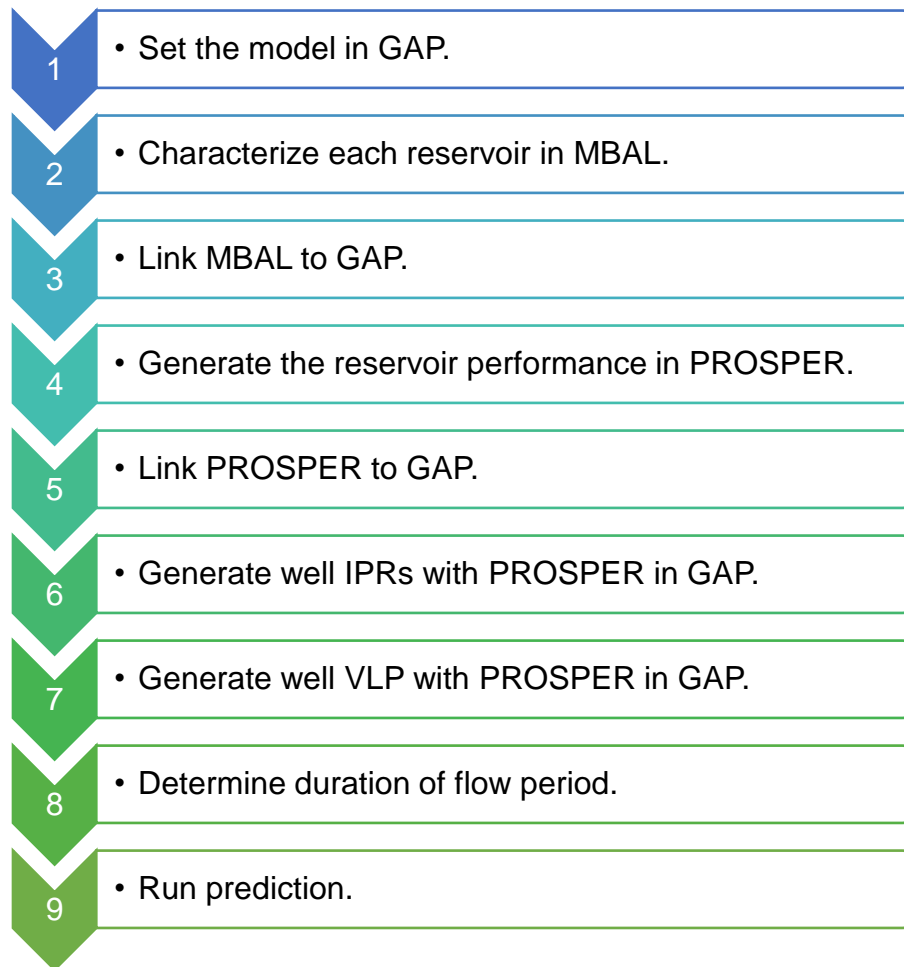
$$c_t = c_w + c_{fa}$$

$$\Delta P\left(t_{Dj}\right)=p(0)-p\left(t_{Dj}\right)$$


APPENDIX B. WORKFLOW ADOPTED IN INTEGRATED PRODUCTION MODELING SOFTWARE

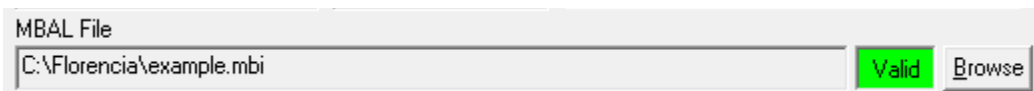
WCD nodal-coupled-material balance workflow in PETEX:

Steps:



- 1) Set the model in GAP: the first step is to create/model our scenario in GAP, using tanks –which represent reservoirs, wells, joints –which represents network nodes, inflow –given by IPR, separator – which are set to atmospheric or sea-floor pressures to simulate pressure drops during blowouts, and pipes that represent the wellbore.


- 2) Characterize each reservoir in MBAL: Create a file in MBAL for each layer of the stacked scenario. In 'tool' option, it is necessary to choose "Material Balance" since it is the tool used for evaluating hydrocarbons in place. Choosing the reservoir fluid is the next step, followed by inputting the PVT data, such as formation GOR, oil gravity, gas gravity, water salinity. In MBAL it is also necessary to input reservoir parameters such as reservoir pressure, temperature, porosity, connate water saturation, reservoir permeability, rock compressibility. If one or more layers have water encroachment, the water influx model is chosen in MBAL.
- 3) Link MBAL to GAP: To link MBAL () to GAP, we should upload the MBAL file that contains the model corresponding to each layer.



MBAL File

C:\Florencia\example.mbi

Valid Browse

- 4) Generate the reservoir performance in PROSPER: Each purple diamond , represents the prosper file which will contain the data for generating IPRs curves. So, the information in there must correspond to the reservoir (MBAL tank) it is linked to. In the PROSPER file, the data needed are: fluid type; PVT data; IPR data, which includes reservoir model – Darcy's model in this case–, reservoir pressure, temperature, water cut, total GOR, reservoir permeability, reservoir thickness, drainage area, Dietz shape factor, wellbore radius, mechanical skin.

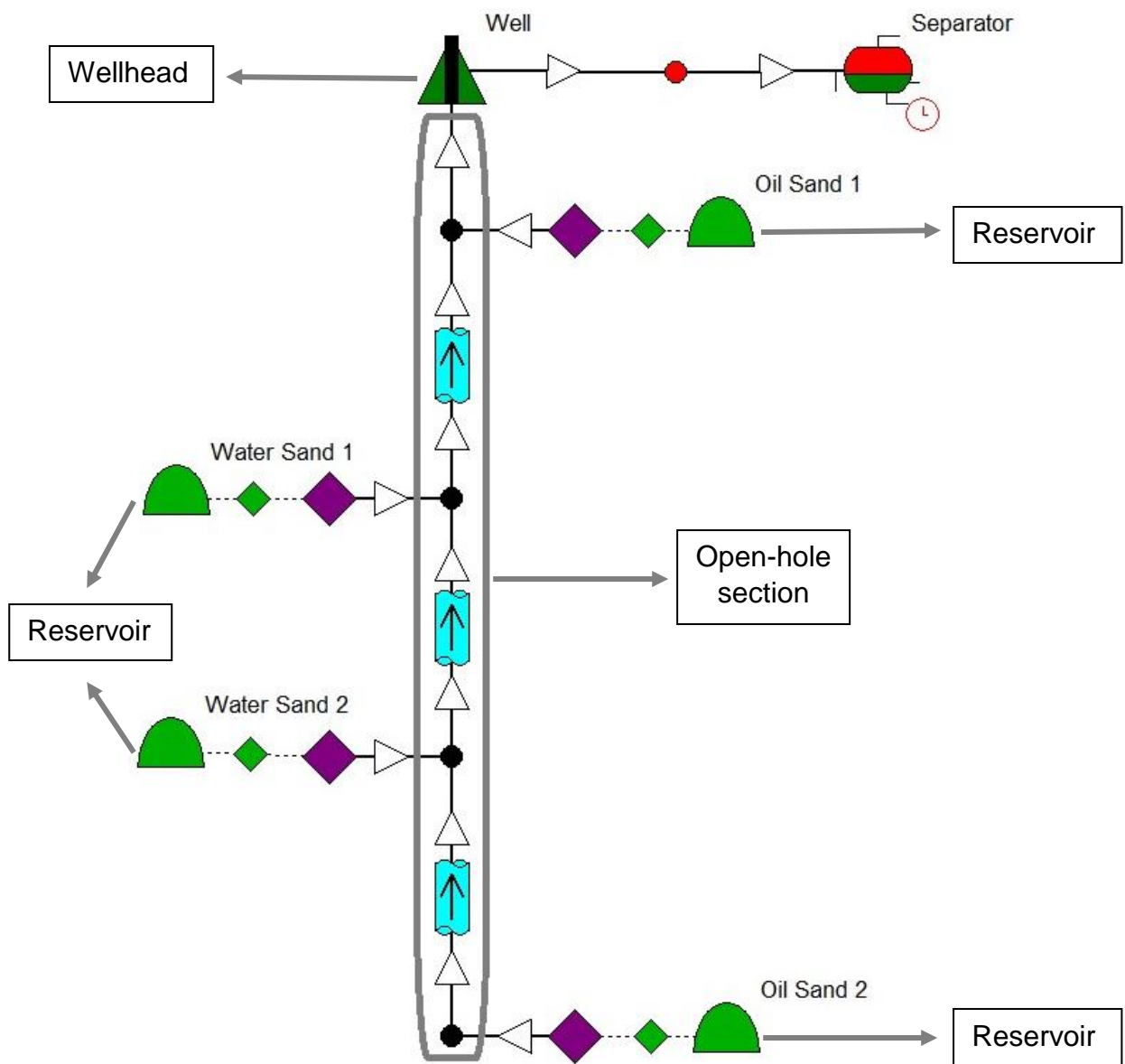
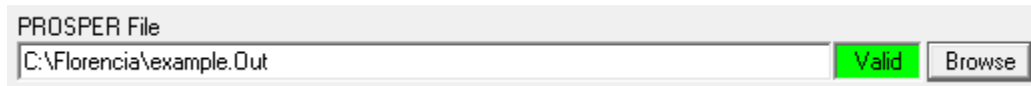


Figure 50. Example of a wellbore open to four sands.

- 5) Link PROSPER to GAP: Similar as in step 3, to link PROSPER to GAP, the PROSPER file needs to be uploaded as well as linked to MBAL tank it receives pressure support from.



PROSPER File
C:\Florenia\example.Out Valid Browse

- 6) Generate well IPRs with PROSPER in GAP: To generate the IPRs curves, click Generate, and then Generate Well IPRs with PROSPER.
- 7) Generate well VLPs with PROSPER in GAP: To generate the VLPs curves, click Generate, and then Generate Well VLPs with PROSPER. In the mother wellbore (▲) a different Prosper file is necessary which incorporates the data for generating the wellbore VLP curve. Furthermore, the wellbore deviation; downhole equipment data, such as casing diameter, casing roughness; geothermal gradient; average heat capacities are input data only for the Prosper file representing the wellbore. In VLP (analysis summary), it is possible to choose the VLP correlation, and a VLP curve is then generated
- 8) Determine duration of flow period: At this point, it is necessary to consult with the drilling team to determine the flow period which for WCD estimates represents the time needed for relief well.
- 9) Run prediction: The model is already set up, so once the flow period is determined from step 8, a forecasting model is run. This step may require some time-step adjustments depending on convergence of solution. WCD volumes, and rates are thus determined.

The model thus generated is shown in Figure 50.

The durations of flow period used for calculation of total spill volume in this study are 60 days (representative of GoM shallow waters – up to 500 feet), 90 days (for deep-water) and 120 days.

Flow rate decline provides an estimate of the expected production decline and any potential changes in the ratio of fluids produced. Therefore, calculations of production rates of oil, production rates of gas and production rates of water are necessary.

VITA

Florencia Anahi Vasquez Cordoba was born in 1991, in Salta, Argentina. She worked as contractual administrator in Buenos Aires after receiving her bachelor's degree in industrial engineering from Universidad Catolica de Salta. She worked in a natural gas pipelines project in an international company, where her interest in oil and gas industry grew. Therefore, she decided to enter the Department of Petroleum Engineering at Louisiana State University to pursue graduate education. She is currently a candidate for MS in Petroleum Engineering, who plans to graduate in August 2018.